Prevention and therapy of type 2 diabetes by selective modulation of the human peroxisome proliferator-activated receptor gamma (PPARγ)

Dissertation zur Erlangung des akademischen Grades des Doktors der Naturwissenschaften (Dr. rer. nat.)

eingereicht im Fachbereich Biologie, Chemie, Pharmazie der Freien Universität Berlin

vorgelegt von

Dipl.- Biochem. Christopher Weidner
aus Berlin

Juni 2011

Die Dissertation wurde in der Zeit von Januar 2008 bis Juni 2011 im Max-Planck-Institut für molekulare Genetik in Berlin in der Arbeitsgruppe Nutrigenomics and Gene Regulation unter der Leitung von Dr. Sascha Sauer angefertigt.

1. Gutachter: Dr. Sascha Sauer
Max-Planck-Institut für molekulare Genetik
2. Gutachter: Prof. Dr. Markus Wahl
Freie Universität Berlin

Disputation am: 29.09.2011

Acknowledgements

I am deeply grateful to my advisor Dr. Sascha Sauer for giving me the opportunity to freely develop my research study on PPARγ, for supporting me with inspiring discussions, encouragement and guidance, and for reviewing this thesis. I also thank Prof. Dr. Markus Wahl for reviewing this work.

I like to express my gratitude to my colleagues for their technical support, scientific discussions and daily encouragements. My special thanks are to Anja Freiwald and Radmila Feldmann.

For their commendable technical assistance during the animal studies I am very grateful to Katharina Hansen, Ulf Schröder and Dr. Ludger Hartmann.

I am thankful to Prof. Dr. Frank C. Schroeder for essential chemical synthesis of the amorfrutins, to Jens C. de Groot and Dr. Konrad Büssow for excellent crystallography of the PPARy-amorfrutin complex, and to Dr. Matthias Baumann for pharmacological experiments.

I am further grateful to Prof. Dr. Annette Schürmann and Prof. Dr. Andreas F. Pfeiffer for fruitful discussions.

My special thanks are to my dear wife Nicole and to my cute sons Jonathan and Theodor for their encouragement, sympathy, and love.

This work was supported by the German Federal Ministry of Education and Research (BMBF) and the Max Planck Society.

Contents

1 Introduction

1.1 The diabetic epidemic – a challenge for the 21st century

30 million, 135 million, 217 million - the worldwide prevalence of diabetes in 1985, 1995 and 2005 reached an alarming epidemic state and is estimated to shoot up to 366 million people in 2030 (*1*). This disease is not restricted to modern Western Societies - it is a worldwide growing public health burden with 80% of diabetics who live in low and middle income countries (*2*). Most people suffering from diabetes are from India (51 million), China (43 million) and the USA (27 million), (*3*). Strikingly, the relative prevalence is highest for countries in Middle East and Caribbean regions (10% each, **Figure 1**).

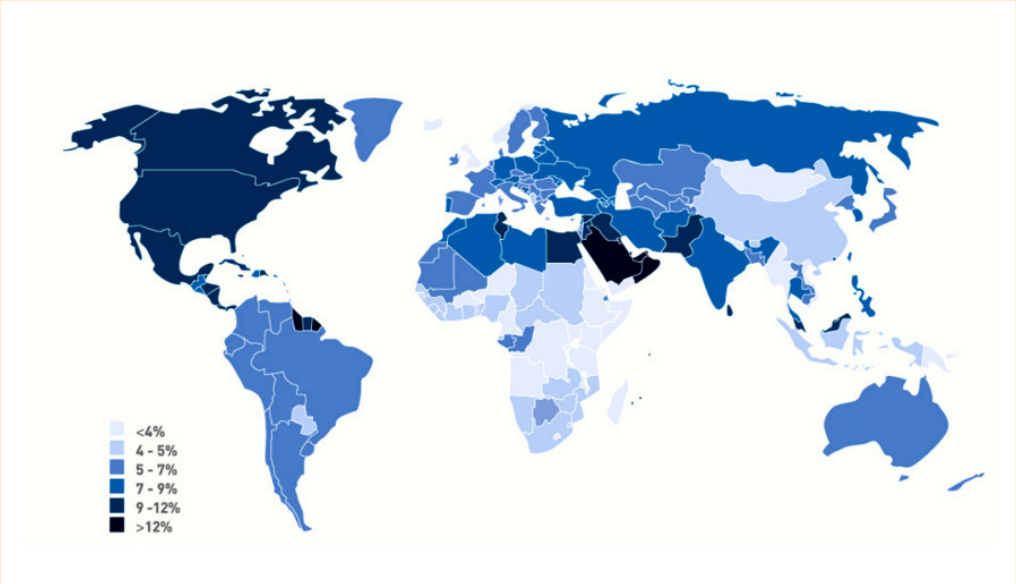

Figure 1. Global prevalence (%) of diabetes (20-79 years) in 2010 *(3)*.

Most of these patients are affected by the non-insulin-dependent form of diabetes (type 2 diabetes), which is characterized by an impairment of the body for insulin action (insulin resistance) and a depletion of insulin-producing pancreatic β-cells (relative insulin deficiency) (*4*). In general, pancreatic islet β-cells are capable of counteracting decreased insulin sensitivity by increased insulin release (*5*), but eventually this reciprocal response is disordered at the progression of type 2

diabetes mellitus, including elevated concentrations of blood glucose. Chronic hyperglycemia leads to dysfunction of various organs, especially the blood vessels (atherosclerosis), kidneys (nephropathy), eyes (retinopathy) and nerves (neuropathy). About 50% of diabetics die of cardiovascular diseases such as stroke. Diabetes is a leading cause of kidney failure, resulting in 20% mortality rate provoked by renal failure. Diabetic neuropathy affects about 50% of people having diabetes and can be accompanied by e.g. pain, foot ulcers and gastrointestinal symptoms. Ten percent develop severe visual impairment such as blindness (*2*). Other comorbidities like depression further dramatically decrease the quality of life (*6*). In summary, diabetes and its complications are considered the major cause of death in many countries, constituting 7% of global mortality. It entails a huge impact on the public health systems. Twelve percent of the public healthcare expenditure in 2010 were attributed to type 2 diabetes (*1, 3*). Therefore, the high prevalence and rapid increase in diabetes is a global challenge for the 21st century.

1.2 Going hand in hand: Insulin resistance, obesity and inflammation

1.2.1 Evolutionary considerations

As proposed by Neels thrifty genotype theory in 1962 (*7*), genes rendering susceptible to obesity may have conferred an evolutionary advantage in times of famine through efficient energy storage. In the last thousands of years the genetic adaptation could not keep up with the environmental and dietary alterations accompanied by substantial progress in agriculture, industrialisation and automation. As a result, the inherited ‘hunter-gather’ genotype can be denoted as ill-suited under high-caloric and sedentary conditions.

During the past decades, it became obvious that obesity and diabetes are also causatively linked to inflammation. However, metabolic overload-derived inflammation is distinctive from classical inflammation. The former is modest, chronic and unresolved over time (*8*). From an evolutionary perspective, mankind

was not only confronted with famines, but also with infectious diseases, additionally leading to selection of strong immune responses. Under certain conditions, the coordinated regulation of immunity and metabolism may be beneficial from a physiological perspective. Immune responses require redistribution of energy. A host strategy could be to minimize anabolic processes (e.g. by insulin resistance) to withhold structural components of the pathologic invader (*9*). But as optimised metabolic efficiency, immune responses that are too sensitive could be disadvantageous in times of caloric excess. The evolution of fat tissue, liver and immune cells emphasizes the association between inflammation and metabolic diseases. Whereas these tissues are separated in mammals, they all are organized in one functional unit, the fat body, in ancestral organisms such as *Drosophila* (*9*).

1.2.2 Insulin resistance

Insulin is a very potent anabolic hormone that regulates various metabolic and developmental processes (**Figure 2**). Insulin resistance is a pathophysiological state characterised by impaired insulin signalling and precedes the manifestation of type 2 diabetes. Without action of insulin blood glucose is not properly absorbed and hepatic glucose production is not inhibited. Hyperglycemia is of central pathophysiological importance. Different biochemical mechanisms have been postulated for hyperglycemia-induced tissue damage, including glycation of tissue proteins, elevated polyol pathway and hexosamine pathway flux as well as activation of protein kinase C (PKC) (*10*). Consistently, all these mechanisms lead to overproduction of reactive oxygen species (ROS) (*10*).

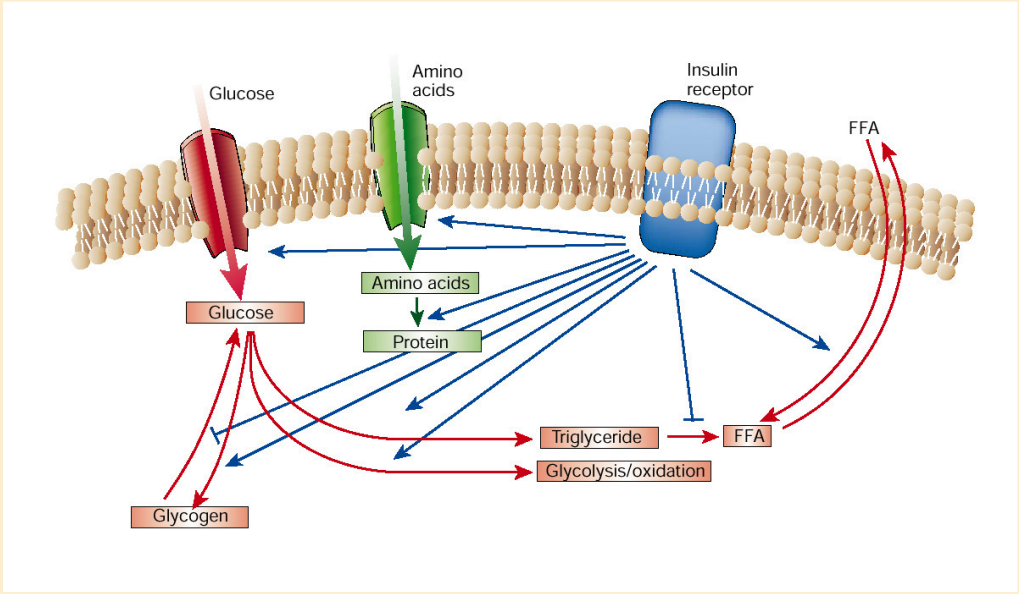

Figure 2. Regulation of metabolism by insulin. Insulin regulates the homeostasis of carbohydrates, proteins and fats. Insulin, released from pancreas after postprandial blood glucose elevation, stimulates the uptake of glucose, amino acids and free fatty acids (FFA) in different cell types. It promotes the storage of substrates in liver, muscle and fat by activating glycogenesis, lipogenesis, glycolysis and protein synthesis, and inhibition of glycogenolysis, proteinolysis and lipolysis. Red arrows indicate metabolic processes, blue arrows indicate regulation by insulin. Adopted from ref. *(11)*.

The risk of developing type 2 diabetes is correlated to obesity, physical sedentariness, nutrition, and genetic predisposition amongst others (*3, 4, 11, 12*) (*13*). The concurrent epidemic of obesity indicates the causal connection to the formation of diabetes, as about 90 % of people with type 2 diabetes are obese or overweight (*14*). This correlation was already described with the term ‘diabesity’ in 1980 by Ethan A. H. Sims (*15*).

1.2.3 Obesity

Obesity is characterized by excessive fat accumulation in adipose tissue. By definition, overweight and obesity are existent with a body mass index (BMI) greater than 25 or 30 kg/m², respectively (*16*). The number of overweight and obese people has reached more than 1 billion worldwide. Again, this metabolic

disorder is not restricted to Western societies but increasingly affects people in newly industrializing countries (*14*). Although most of diabetic people are obese or overweight, the reverse is not true. The rationale is the distribution of body fat. Visceral (abdominal) obesity, but not peripheral obesity, is associated with insulin resistance and cardiovascular diseases (*17, 18*). This is also reflected by the recommendation of the US National Institutes of Health (*19*) to measure waist circumference rather than BMI. Intra-abdominal adipocytes are closer to essential organs such as liver and pancreas, and are primarily involved in secretion of proteins and peptides responsible for metabolism (*20*). Furthermore, compared to peripheral fat tissue, visceral fat is less sensitive to the anti-lipolytic effect of insulin (*21*) accompanied by higher concentration of detrimental free fatty acids.

1.2.4 The connection between diabetes, obesity and inflammation

Several mechanisms for the link between insulin resistance and obesity are obvious. The prevalent lipotoxicity or lipid overload hypothesis assumes an accumulation of fat in muscle, liver and pancreas cells, when adipose tissue cannot store excessive fat properly. Then, elevated intracellular lipids result in an accumulation of metabolites such as fatty acyl-coenzyme A, diacylglycerol (DAG) and ceramides. These metabolites lead to inhibition of insulin-signalling via activation of protein kinase C (PKC) (*22, 23*) and serine/threonine kinase cascades including inhibitor kappa B kinase (IKK) and JUN N-terminal kinase (JNK). Consequently, glucose utilization is reduced (**Figure 3, left**).

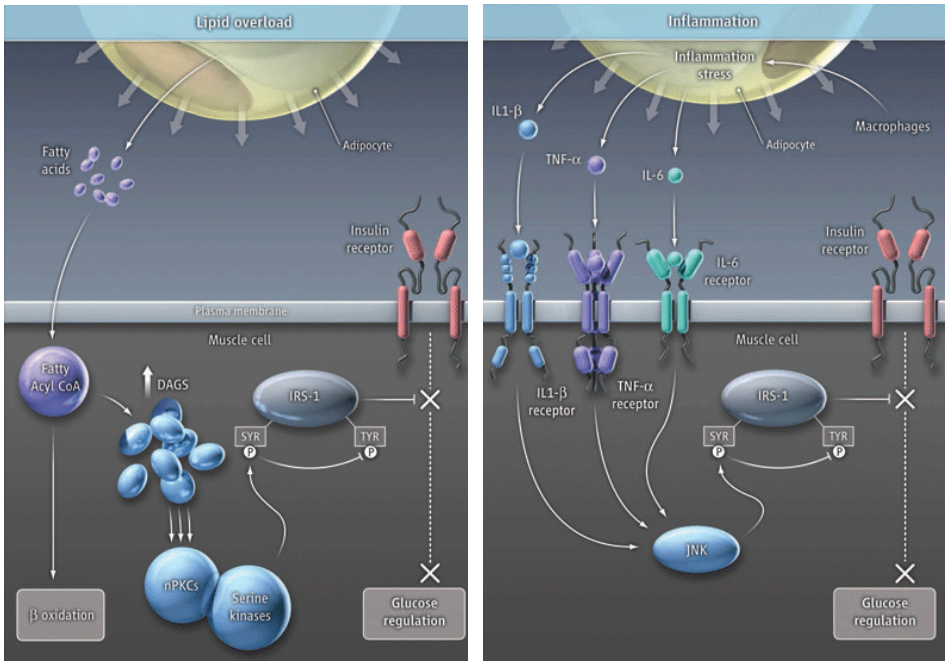

Figure 3. Lipid overload **(left)** and macrophage attraction hypothesis **(right)** linking obesity with low-grade inflammation and insulin resistance. **(Left)** Enlarged adipocytes secrete a huge amount of fatty acids that accumulate in form of diacylglycerols (DAGS) in the muscle tissue. DAGS activate a panel of stress-sensitive protein kinases C (nPKCs) leading to inhibition of insulin signalling through serine phosphorylation of insulin receptor substrate 1 (IRS-1). **(Right)** Enlarged adipocytes accumulate macrophages, resulting in secretion of pro-inflammatory cytokines. In the muscle cell these molecules activate the JUN N-terminal kinase (JNK) that inhibits insulin signalling through serine phosphorylation of insulin receptor substrate 1 (IRS-1). Adopted from ref. (*188*).

Besides, Randle et al. proposed a competition of fatty acids with glucose for oxidation resulting in the inhibition of activity of the pyruvate dehydrogenase, phosphofructokinase and hexokinase II and thus to diminished glucose import into the cell (*24*). Additionally, recent studies revealed that the endoplasmatic reticulum (ER), the organelle responsible for protein folding and maturation, mainly contributes to the obesity-related progression of insulin resistance. Nutrient excess leads to an accumulation of newly synthesized, unfolded proteins in the ER, which thereon activates the unfolded protein response (UPR) (*25*).

Three branches mediate the UPR, including PERK (PKR-like eukaryotic initiation factor 2α kinase), IRE1 (inositol requiring enzyme 1), and ATF6 (activating transcription factor-6). Finally, the UPR triggers an activation of JNK, IKK, NF-κB (nuclear factor of kappa light polypeptide gene enhancer in B-cells) and an increase in reactive oxygen species leading to inflammatory conditions (*26*). It further was postulated that nutrient overload and pathogens activate the eIF2α kinase PKR (double-stranded RNA-activated protein kinase), which thereon triggers the assembly of the metabolic inflammasome (metaflammasome). Thus, insulin signalling is impaired (*27*).

The adipose tissue has a pivotal role in storage of detrimental body fat. Inhibition of white adipose tissue development in transgenic mice leads to an accumulation of fat in internal organs such as the liver, and consequently to lipoatrophic diabetes (*28*). Reversely, transplantation of adipose tissue restores the metabolic phenotype (*29*). Concordantly, expansion of the adipose tissue by overexpression of adiponectin increases insulin sensitivity although the mice become morbidly obese (*30*). These and further studies underscore the importance of the adipose tissue as a compartment of body fat storage.

Besides, adipose tissue does not only store triglycerides, but functions as endocrine organ that secretes many proteins and peptides (adipokines) involved in metabolism and immunity (*31, 32*). This includes adiponectin, leptin, resistin, tumor necrosis factor α (TNFα) and monocyte chemotactic protein-1 (MCP-1) (*33*). Adipokines not only modulate glucose and lipid metabolism directly, but additionally have important immune functions (*34*). Impressively, more than 100 molecules involved in immunity are expressed in adipocytes (*34*). Furthermore, adipocytes themselves are responsive to immunomodulating molecules, since they express various receptors such as the toll-like receptor (TLR) family, interleukin 6 (IL-6) receptor and TNFα receptor (*34*).

The association between insulin resistance and inflammation was already observed in 1978 in studies of sepsis (*35*), and was meanwhile verified in many infectious or inflammatory disorders (*36-38*). On the other side, in obese

individuals the inflammatory cytokine TNFα is overexpressed in adipose tissue (*39*) and is one of the major risk factors in obesity-related insulin resistance (*40*). The reverse could be shown by inducing insulin resistance in fat cells by TNFα treatment (*39*). Further, obese mice lacking TNFα or its receptors are protected from insulin resistance (*39*). TNFα could be shown to inhibit the insulin pathway by changing important phosphorylation states of insulin receptor, IRS and protein phosphatase-1 (*41, 42*).

Additional immunomodulating adipokines were shown to impair insulin sensitivity. The chemokine MCP-1 is overexpressed in obese mice and induces insulin resistance in adipocytes (*43*). In several studies markers of the acute-phase response, IL-6 (*44*) and C-reactive protein (CRP) (*45*), were increased in diabetic patients. Reduction of IKKβ expression leads to improved insulin sensitivity in vivo (*46*). Concordantly, it was shown that IKKβ-inhibiting salicylates, which are used to treat inflammatory diseases, also reduce blood glucose in the clinical usage (*47*). JNK1, another key mediator of inflammatory responses, is linked to insulin sensitivity. JNK1 is overexpressed in obese mice and knocking it out protects from insulin resistance and adiposity (*48*). The pro-inflammatory cytokine interleukin 1 (IL-1) has been found in pancreatic β-cells from diabetic patients. In a clinical trial drugs that block IL-1 were able to improve glycemia and β-cell secretory function (*49*).

Mice lacking the gene for the pathogen-sensing toll-like receptor 4 (TLR4), which in general is expressed in adipose tissue, are protected against obesity provoked by a saturated fatty acid rich diet (*50*). This observation confirms a ‘mistaken identity theory’ (*8*) - the system considers abundant nutrients as pathological molecules and immune-response pathways become activated (e.g. through TLR4). Consequently, key genes in inflammation-signalling pathways are causatively linked to insulin responsiveness and adiposity.

Immunohistochemical and expression analysis of adipose tissue from obese and insulin resistant mice revealed, that obesity is accompanied by macrophage

infiltration into the fat tissue. This recruitment leads to activation of inflammatory pathways (*51, 52*).

Secretion of pro-inflammatory molecules by adipocytes and immune cells increases macrophage attraction and activation, synergistically stimulating inflammatory activity of the other (*53*). This crosstalk is especially based on free fatty acids, MCP-1, TNFα, IL1-β and IL-6 and leads to a vicious cycle of inflammation resulting in insulin resistance (**Figure 3, right, pg. 12**) (*54*).

Hence, type 2 diabetes and obesity are considered as chronic low-grade inflammation. This 'metaflammation' is present in metabolic active tissues like adipose tissue, liver, muscle, pancreas and also brain (*8*). Noteworthy, it recently was shown that adiposity-induced insulin resistance in mice could be improved by immunotherapy (*55*). However, from a therapeutic perspective, the preferential target of treatment should focus on the nutritional overload, since inhibition of inflammation alone may not restrain the high caloric diet-induced risk of tissue damage.

1.2.5 The role of pathogens

Metabolic inflammation that underlies diabetes and obesity may also involve a role of pathogens. Indeed, it could be shown that adipocytes can be a direct target for parasites and viruses that contribute to metabolic abnormalities (*56, 57*). Especially the intestinal microbiota, composed of hundreds of billions of prokaryotics and eukaryotics belonging to 40,000 different species (*58*), has an important role in maintaining physiologic functions of the host. The gut microbiota extends the metabolic abilities of the host by producing essential vitamins including vitamin K, vitamin B12 and folic acid, and further by modulating intestinal bile acid metabolism (*59*). Additionally, the gut microbiota can improve the digestion and absorption of ingested nutrients and modulate the host energy metabolism by food-derived signalling molecules like short-chain fatty acids and glucagon-like peptides (*60*). Besides, high-fat feeding leads to

increased migration of bacterial membrane-derived lipopolysaccharides (LPS) into the blood (*61, 62*), which contributes to systemic insulin resistance (*63, 64*). Consistently, germ-free mice are protected against high-fat diet-induced obesity (DIO) and glucose intolerance (*65, 66*). Further evidence for a causative role of the microbiota comes from a recent study that has shown the transferability of the diabetic phenotype by intestinal microbiota inoculation (*67*). The link between human health and gut microbiota will gain deeper insight by progress in metagenomic research, e.g. by he Human Microbiome Project (HMB) (*68*).

1.3 Nuclear receptors

The nuclear receptor (NR) superfamily comprises a group of ligand-induced transcription factors that regulate a huge amount of physiological processes, including development, reproduction, and metabolism. Their physiological significance is exemplified by the variety of ligands in current clinical and developmental treatments of metabolic disorders such as type 2 diabetes, atherosclerosis, dyslipidemia, and cancer. The human genome encodes 48 different nuclear receptors (49 in mouse). The glucocorticoid receptor was firstly isolated and cloned in 1985 (*69*). In the subsequent years, many other NRs were identified by screening of newly sequenced genomes.

From an evolutionary point of view, nuclear receptors are ancient and arose together with the need of multicellular organisms to regulate metabolism and development. The NR ancestor probably acted as a ligand-independent monomer. With acquiring the ability for homo- and heterodimerization and for being regulated by ligands, the increasing functional complexity of gene regulation potentially expedited the evolution of higher organisms (*70*). The evolutionary oldest NRs (e.g. the retinoid X receptor RXR) were found in Coelenterata and a major diversification occurred in insects. Steroid receptors have evolved in the chordate lineage (*71*). Taken together, the complexity of nuclear receptors has been increased in parallel to the complexity of the transcriptional machinery rising during evolution.

All nuclear receptors share the common structural architecture depicted in **Figure 4**. The highly variable N-terminal region comprises the ligand-independent transactivation domain (AF1), which is constitutively active and can be regulated by covalent modification (*72*). The central DNA-binding domain (DBD) consists of two highly conserved zinc-finger motifs that target the nuclear receptor to its specific DNA response elements. In general, the response element is composed of two copies of a (A/G)GGTCA hexanucleotide or a modification thereof. The hexanucleotides are arranged in an inverted, direct, or everted repeat, and they are separated by a NR-specific number of nucleotides. The amino acids between the last two cysteins of the first zinc finger form the P-loop that is mainly responsible for the binding to the NR-specific DNA response element (*71*). The DBD of the NR is connected to the C-terminal region via a flexible, non-conserved hinge region, which optionally contains a nuclear localisation signal (*71*). The C-terminal ligand-binding domain (LBD) is less conserved among the NRs but functionally unique – the LBD enables ligand recognition, dimerisation with other NRs, and interaction with cofactors (*72*). In general, the LBD comprehends 11-12 α-helices arranged with 2-4 β-sheets in an antiparallel, three-layered sandwich. Small molecule ligands bind to a hydrophobic cavity in the core of the LBD. The size of the binding pocket ranges from 350 to more than 1300 $Å^3$ and determines the promiscuity and affinity of potential ligands (*73*). The C-terminal end of the LBD often contains the conserved activation function 2 (AF2) domain, allowing ligand-dependent interaction with transcriptional cofactors (**Figure 4**).

Figure 4. Canonical structure of nuclear receptors. The architecture comprises the N-terminal activation function 1 (AF1) domain, the DNA binding domain (DBD), the flexible hinge region, the ligand binding domain (LBD) and the C-terminal activation function 2 (AF2) domain.

The ligand binding is accompanied by a conformational change within the LBD, especially in the last α-helix (often helix 12) (*74*). This spatial rearrangement modulates the interaction with various coactivators and corepressors (*72*). According to the classical concept, in the absence of a ligand the NR is associated with corepressors (e.g. nuclear receptor corepressor (N-CoR) and HDAC3 histone deacetylases), leading to transcriptional inhibition. In contrast, binding of agonists results in the release of corepressors and recruitment of coactivators (e.g. members of the steroid receptor coactivator (SRC) and CBP/p300 histone acetyltransferases) and thus triggers transcriptional activation (*75*) (**Figure 5**). Hence, the structural property of the bound ligand determines the induced conformational change and thus the specific release or recruitment of different transcriptional cofactors. Some NRs (e.g. the estrogen-related receptor ERR) contain an AF2 domain fixed in an active conformation, so that the nuclear receptor becomes constitutively active. If so, the activity of the NR is modulated by cofactor availability, NR expression itself or covalent modification like phosphorylation or acetylation (*72*).

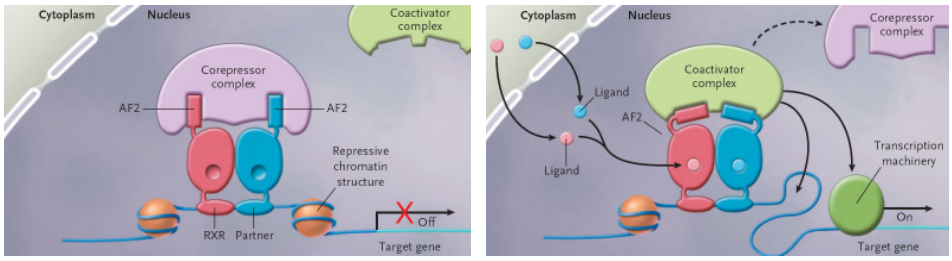

Figure 5. Mechanism of transcriptional activation through heterodimeric nuclear receptors. **(Left)** In absence of ligand these nuclear receptors repress target gene expression by recruitment of transcriptional corepressor complexes via the activation function 2 (AF2) domain. **(Right)** Binding of ligands triggers conformational changes in the AF2 domain leading to replacement of corepressors by coactivators, which facilitate the recruitment of the transcription machinery and target gene expression. Adopted from ref. (*189*)

Several classification strategies have been reported. Based on their dimerisation and DNA binding behaviour the nuclear receptor superfamily is divided into four groups. The *first* subfamily comprises steroid hormone receptors that are localised in the cytoplasm and translocate to the nucleus upon ligand binding. The NRs then form homodimers and bind palindromic response elements on the DNA. The *second* subfamily consists of NRs, which are retained in the nucleus independently of ligand binding and form heterodimers with RXR to recognize directly repeated response elements. The second group comprises the peroxisome proliferator-activated receptor (PPAR) amongst others. The *third* subfamily of NRs are homodimeric, direct repeat-binding, orphan receptors, with their ligands still unknown. The members of the *fourth* group are monomeric orphan receptors (*71, 76*). Accounting for evolutionary relationships using sequence alignment procedures the nuclear receptor superfamily can also be divided into 7 groups (0 to 6) (*77*). This phylogeny-based nomenclature is approved by the Nuclear Receptor Nomenclature Committee and is integrated in the official gene symbol.

1.3.1 The peroxisome proliferator-activated receptor (PPAR)

The peroxisome proliferator-activated receptor (PPAR) was first cloned by Issemann and Green in 1990 (*78*). The term PPAR is based on early observations of peroxisome proliferation after treatment of rodents with PPAR ligands (*79*) (*80*). Nevertheless, PPARs do not induce peroxisome proliferation in primates or humans (*81*). However, they are key regulators of metabolic pathways like energy metabolism, adipogenesis and insulin sensitivity (*82, 83*). According to the evolutionary relationship, the PPARs belong to the first group. The PPAR forms heterodimers with RXR and binds to the response element composed of the consensus sequence AGGTCA with a single nucleotide spacing between two repeats (direct repeat 1). The PPAR response element (PPRE) is often present in multiple copies in the promoter region but can also be located in the transcribed region of target genes (*83*).

A wide variety of natural or synthetic compounds was identified as PPAR ligands. Binding of ligands occurs with high promiscuity, and known PPAR ligands are strikingly structurally diverse. This is due to the large solvent-accessible cavity in the ligand binding pocket, which is over 1000 $Å^3$ in volume (*73*). PPARs are capable of binding to a variety of fatty acids and their metabolites with medium to low affinity, indicating that their physiological activation is not restricted to a single ligand, but rather involves interactions with numerous fatty acids and their metabolites (*73*). Hence, PPARs act as lipid sensors that induce lipid storage or catabolism and thus translate "what you eat" in "what you are" (*84*). Among the synthetic ligands, several glucose- or lipid-lowering drugs are PPAR agonists, underscoring the important role of PPARs as therapeutic targets. The PPAR/RXR heterodimers are permissive as they can be activated by PPAR agonists as well as by RXR ligands alone (*85*).

Three PPAR subtypes characterised by distinct tissue distribution, target genes and ligands, each encoded in a separate gene, have been identified: PPARα, PPARβ/δ and PPARγ. PPARα was the first murine PPAR subtype characterized in 1990 (*78*), many decades after the clinical introduction of the PPARα-activating fibrates (see below). Two years later, the group of Walter Wahli reported the cloning of three different PPAR subtypes in *Xenopus laevis*, which were named PPARα, PPARβ and PPARγ (*86*). Subsequently, the mammalian orthologs of PPARβ and PPARγ were characterized (*73*). Since the sequence of murine PPARβ was less conserved in *Xenopus laevis*, it originally was named PPARδ in mice. In 2000, orthologous evolution was proven, terming the receptor PPARβ/δ (*87*).

1.3.1.1 PPARα

PPARα has been shown to play a key role in the regulation of fatty acid catabolism, glucose homeostasis and lipoprotein metabolism (*78*). It is expressed in metabolically active tissues such as liver, heart, skeletal muscle and kidney (*88*), and also in immune cells like macrophages (*89*). Target genes of PPARα are

involved in uptake, intracellular transport and β-oxidation of fatty acids (*90*). This include the fatty acid transport protein (FATP), carnitine palmitoyltransferase I (CPT1) and acyl-CoA oxidase 1 (ACOX1). Besides, further enzymes for lipoprotein metabolism are transcriptionally regulated (*83, 91*). PPARα-null mice show hepatic steatosis when fed a high-fat diet (HFD), and display hypoglycemia, hypoketonemia, and hypothermia besides elevated plasma free fatty acid levels under fasted conditions (*92*). It recently was shown that PPARα can be activated by endogenous α-linoleic acid (*93*) and 1-palmitoyl-2-oleoyl-sn-glycerol-3-phosphocholine (*94*) besides other such as unsaturated fatty acids and eicosanoids (*95*). Chemical activation of murine PPARα results in decreased serum triglyceride levels, increased high density lipoprotein (HDL) levels (*82*), improved insulin sensitivity and lowered blood glucose and insulin concentrations (*96*). Synthetic fibrates (e.g. bezafibrate, fenofibrate) are potent agonists of PPARα and are widely used in the clinical treatment of hypertriglyceridemia for about 50 years (*97*). In addition to cholesterol-lowering statins, fibrates are often combined with niacin and omega-3 fatty acids. Some side effects comprise gastrointestinal symptoms (*98*).

1.3.1.2 PPARβ/δ

PPARβ/δ is ubiquitously expressed in all tissues and involved in the regulation of fatty acid oxidation, epidermal development, cell proliferation, cancer and inflammation (*83, 99*). Transgenic mice overexpressing PPARβ/δ in adipose tissue are protected from obesity during a HFD, whereas adipose tissue-specific deletion leads to obesity (*100*). Concordantly, pharmaceutical activation of PPARβ/δ was shown to ameliorate insulin resistance in different mouse models due to increased lipid catabolism (*99*). Furthermore, its activation in mice enhanced running endurance without exercise (*101*). Specific ligands (e.g. GW1516, MBX-8025) are currently in various stages of clinical development (*102*).

1.3.1.3 PPARγ

PPARγ plays a key role in glucose and lipid homeostasis. It is a regulator of several developmental processes such as adipogenesis and bone formation, and additionally, has anti-inflammatory and cancer-modulating properties (*84, 103, 104*). While the PPARγ1 isoform is predominantly expressed in liver, intestine, kidney, macrophages and adipocytes, PPARγ2, exhibiting an additional N-terminal 28 amino acid residue, is exclusively expressed in adipose tissue (*104, 105*).

Various target genes of PPARγ have already been identified. These include the fatty acid binding protein (FABP), the acyl-CoA synthetase (ACS), the lipoprotein lipase (LPL) (*106*) and the fatty acid transport protein 1 (FATP1) (*107*). These gene products are required for adipogenesis and uptake of serum fatty acids. The phosphoenolpyruvate carboxykinase (PEPCK) (*108*), the glycerol kinase (GyK) (*109*) and the glycerol transporter aquaporin 7 (*110*) promote the intracellular storage of detrimental lipids (*104*). Taken together, these pathways lead to the net flux of fatty acids from serum and other tissues (e.g. liver, muscle) into adipocytes. Thus, the level of free fatty acids in serum is decreased. Furthermore, activated PPARγ increases the transcription of the insulin responsive glucose transporter GLUT4 in fat and muscle cells, thereby reducing blood glucose levels (*107*). In addition, expression of secreted adipokines like TNFα, leptin and resistin is decreased, while expression of adiponectin is up-regulated upon PPARγ activation (*107*). Consequently, PPARγ activation results in decreased insulin resistance and has anti-inflammatory and anti-atherogenic properties (**Figure 6**).

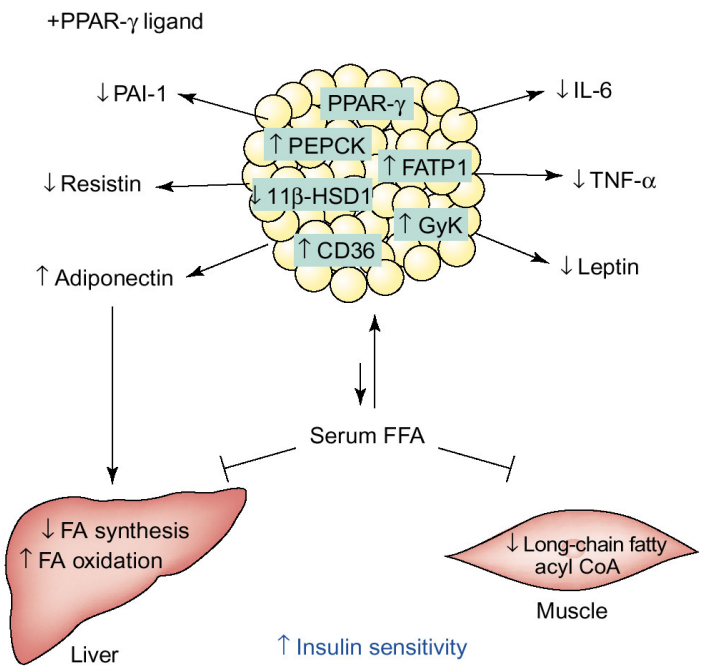

Figure 6. Potential mechanism of insulin sensitisation by PPARγ ligands. In adipose tissue, activation of PPARγ leads to increased gene expression of PEPCK, FATP1, 11β-HSD1, GyK and CD36, resulting in an influx of free fatty acids (FFA) from serum and other tissues into adipocytes. This decreases the level of detrimental free fatty acids in serum. Further, expression of secreted adipokines such as TNFα, leptin, resistin, IL-6 and PAI-1 is reduced, while expression of adiponectin stimulating fatty acid oxidation is increased. Consequently, PPARγ activation results in improved insulin sensitivity and anti-inflammatory effects. Adopted from ref. (*107*).

Several mechanisms for the anti-inflammatory effects of PPARγ have been observed, including increased expression of anti-inflammatory molecules and negative regulation of pro-inflammatory genes (derepression). Further anti-inflammatory processes are independent of direct DNA-binding of PPARγ (transrepression). This comprises binding of PPARγ and subsequent inhibition of pro-inflammatory AP1 and NF-κB, and nucleocytoplasmatic redistribution of the p65 subunit of NF-κB. Transrepression is further achieved by modulation of MAPK14 (mitogen-activated protein kinase 14) activity and competition for

limiting pools of coactivators (*111*). Additionally, it was shown in macrophages that activated PPARγ becomes SUMOylated and subsequently binds to corepressors, which prevents its degradation by the 19S proteasome. Consequently, pro-inflammatory genes are maintained in a repressed state (*112*).

Generation of PPARγ-null mice results in embryonic lethality due to placental dysplasia and dyslipidemia (*113*). Transgenic mice lacking PPARγ in fat, muscle or liver develop insulin resistance (*114-117*). Further conditional knockout studies confirm the protective role of PPARγ in glucose and lipid homeostasis (*83*). Macrophage-specific PPARγ knockout mice show reduced cholesterol efflux leading to atherosclerosis (*118*). Intriguingly, heterozygous PPARγ knockout mice reveal reduced adiposity and are *protected* from HFD-induced insulin resistance (*119, 120*). Additionally, human genetic studies demonstrated that a specific Pro12Ala substitution with lessened PPARγ activity observed in Pima Indians and others is correlated to *improved* insulin sensitivity and *reduced* risk of type 2 diabetes (*121-123*). By contrast, the rare Pro115Gln mutation leads to constitutive activation of PPARγ and, noteworthy, to obesity (*124*). Complete loss of function mutations (Phe388Leu, Pro495Leu, Arg425Cys) have been associated with lipodystrophy and diabetes (*84*).

Endogenous ligands for PPARγ comprise 15-deoxy-prostaglandin J2 (*125*), linoleic acid, linolenic acid, eicosapentaenoic acid, 9- and 13-hydroxyoctadecadienoic acid (9-HODE, 13-HODE) (*126*), and 15-hydroxyeicosatetraenoic acid (15-HETE) (*127*) beside other fatty acid- and arachidonic acid derivatives.

Thiazolidinediones such as rosiglitazone (Avandia) and pioglitazone (Actos) are widely used as anti-diabetic drugs and have been shown to strongly activate PPARγ (*128, 129*). Originally, thiazolidinediones were derived from clofibrate due to its glucose lowering effects (*130*), without any knowledge about the molecular target (*128*). Unfortunately, thiazolidinedione treatment is accompanied by several side effects such as weight gain, congestive heart failure, and

osteoporosis amongst others (*104, 131, 132*). Recently, the regulatory agencies therefore restricted or even suspended rosiglitazone in the US and in the EU, respectively (*131*).

The adverse safety profile of these fully activating PPARγ agonists and the genetic studies mentioned above demonstrate that *partial* rather than full activation of PPARγ may improve insulin sensitivity while unlinking unwanted side effects. These considerations led to the concept of selective PPAR modulators (SPPARMs) (*133*). This model is derived from the approved selective estrogen receptor modulators (SERMs) such as tamoxifen (*134, 135*). According to the SPPARM concept, chemically diverse PPARγ ligands bind in distinct manners to the LBD of PPARγ. This results in different conformational changes of the nuclear receptor, especially at helix 12, and thus, in ligand-specific interactions between PPARγ and transcriptional coactivators and corepressors. Consequently, different genes in specific tissues are modulated in differential manners. Beneficial gene regulation may become uncoupled from adverse effects by SPPARMs, providing an optimized insulin-sensitizing compound (*74, 104, 136*). Currently, several SPPARγMs are in clinical and preclinical development. For instance, telmisartan, nTZDpa and halofenate could be shown to partially activate PPARγ without inducing weight gain (*137*).

Another promising approach for the development of novel PPARγ ligands is the concept of dual PPARα/γ or even pan PPARα/β/δ/γ agonist. As single activation of the three isotypes has different clinical outcomes, e.g. on the lipid profile, a combination of therapeutic effects is thought to show improved efficacy for the treatment of type 2 diabetes and dyslipidemia (*138*). Among these dual PPARα/γ agonists, the glitazars are in the most advanced stage of development. In clinical trials muraglitazar (*139*), aleglitazar (*140*), tesaglitazar (*141*) improved insulin sensitivity and ameliorated the lipid profile. But the development of many glitazars had to be discontinued due to severe side effects such as carcinogenic effects, weight gain, edema and cardiovascular events (*142*).

Recent studies suggest that a small molecule targeting all three PPAR subtypes may provide improved efficacy and safety profiles. The therapeutically used bezafibrate, already introduced in 1977, is rather a pan-PPAR agonist than a specific PPARα ligand, as it activates all three PPARs with similar effectiveness (*143*). Indeed, bezafibrate not only reduces triglycerides and increases high-density lipoprotein-cholesterol, but further reduces insulin and glucose levels without long-time safety concerns (*143*). However, its low potency in activating PPARs necessitates the development of more powerful compounds. Candidates in early development stages include indeglitazar (*144*) and sodelglitazar (GW677954) (*145, 146*). In spite of the promising preclinical and clinical data for novel PPAR agonists, further studies, especially investigating long-time safety, are required.

The concerns about safety of PPAR agonists raised scepticism on PPAR as therapeutic target in the last years. Though, recent findings (*147*) raise hope for the success of novel PPARγ ligands. Obesity is associated with inflammation-derived PPARγ phosphorylation at serine 273 in adipose tissue. Inhibition of this phosphorylation was achieved by PPARγ ligands, and strikingly, ligand-induced inhibition of the phosphorylation was independent from the magnitude of receptor agonism. The partial PPARγ agonist MRL-24 showing low transcriptional activation was as efficient as the full agonist rosiglitazone in inhibition of Ser-273-phosphorylation, indicating that agonist and phosphorylation effects are independent from each other. This suggests that the tremendous effects of obesity and high-fat diet are mediated by Ser-273-phosphorylation of PPARγ and could be prevented by ligands with less transcriptional activation. This may reduce the risk of potential side effects (*147*). Whereas the primary aim in the field was to develop highly activating PPARγ agonists, ligands with low or even without agonism now seem to have promising properties by separating anti-diabetic from unwanted side effects (*148-150*).

1.4 Pharmacological treatment of type 2 diabetes

The aim of pharmacological treatment is to reduce hyperglycemia but to avoid disabling hypoglycaemia in parallel to lifestyle and dietary interventions. Whereas individuals with type 1 diabetes are strictly dependent on insulin administration due to pancreatic defects, for treating type 2 diabetes oral anti-diabetic drugs are usually sufficient. Besides several insulin formulations and analogues, the following drug classes are currently approved for the treatment of diabetes: biguanides, sulfonylureas, meglitinides, thiazolidinediones, α-glucosidase inhibitors, GLP-1 analogues, DPP-4 inhibitors and amylin analogues.

Metformin (dimethylbiguanide) is the worldwide most prescribed anti-diabetic drug (*151*) and it is the agent of first choice for the treatment of type 2 diabetes (*152*). Its mode of action is to activate the AMP-activated protein kinase (AMPK) in the liver (*153*), that regulates cellular glucose and lipid metabolism (*154*). Thus, metformin reduces hepatic production and secretion of glucose and partially increases extrahepatic insulin sensitivity (*155*).

Sulfonylureas (e.g. glimepiride) have been extensively used for decades. They stimulate ATP-dependent potassium channels on the cell membrane of pancreatic β-cells resulting in calcium influx and subsequent insulin secretion (*156*). Sulfonylureas considerably lower blood glucose levels but involve the risk of hypoglycemia. Weight gain may aggravate insulin resistance (*155*). If either sulfonylureas or metformin alone fail to control blood glucose, a combination of both is established, partly in combination with thiazolidinediones (*152*).

Meglitinides (e.g. repaglinide) also stimulate insulin release in a manner similar to sulfonylureas, but are only short-lived, rendering the use of meglitinides suitable prior to meal. Side effects are similar to that of sulfonylureas but with lower risk of hypoglycaemia (*155*).

Thiazolidinediones (TZDs, e.g. rosiglitazone, pioglitazone) act as insulin sensitizers by activation of the nuclear peroxisome-proliferator-activated receptor γ (PPARγ). In the past years, TZDs commanded the majority of the global market

share (*1*). However, TZDs additionally provoke side effects that resulted in restriction of their use (*157, 158*). New concepts of PPARγ modulation offer a promising approach. Selective modulation of PPARγ (SPPARγM) and the other isotypes (dual and pan PPAR agonists) will improve the efficacy and safety profile of current PPARγ agonists (see 1.3.1.3). Several SPPARγMs and dual PPAR agonists showed minimized side effects like weight gain in clinical studies and thus are promising drugs for the treatment of diabetes and associated disorders (*136*). However, a lot of dual PPARα/PPARγ activators (glitazars) have been discontinued due to toxicity problems (*138*).

The α-glucosidase inhibitors (e.g. acarbose) reduce digestion and uptake of carbohydrates by blocking intestinal α-glucosidase (*1*). Thus, postprandial hyperglycemia is reduced. The α-glucosidase inhibitors have less potent glucose-lowering efficacy compared to the aforementioned agents but have a good safety profile (*155*).

GLP-1 analogues and DPP-4 inhibitors are novel anti-diabetic drugs that affect the incretin system. Incretins such as GLP-1 (glucagon-like peptide 1) are secreted from colon cells shortly after food intake via activation of neuro-endocrine pathways. They act on the pancreatic β-cells by enhancing insulin release and production. GLP-1 is rapidly degraded by the ubiquitous dipeptidyl peptidase-4 (DPP-4). Thus, the underlying mechanism is glucose-dependent and presents an attractive anti-diabetic target, since the risk of hypoglycaemia is minimized (*155*). GLP-1 analogues (exenatide, liraglutide) need parenteral administration and trigger insulin secretion in the presence of glucose. DPP-4 inhibitors (gliptins) are orally active and reversibly inhibit DPP-4. Both GLP-1 analogues and DPP-4 inhibitors revealed a promising efficacy and safety profile so far and will a have a valuable role in future (*1, 155*).

Amylin analogues (pramlintide) are occasionally injected in parallel to insulin and lower serum glucose by decreasing glucagon release, slowing gastric emptying, and decreasing food intake (*159*).

Due to the causative linkage between diabetes and obesity, it should be noted that only orlistat is currently applied as long-term obesity treatment. Orlistat inhibits intestinal lipoprotein lipase and thus reduces fat absorption and provokes weight loss (*160*). Unfortunately, the promising centrally acting anoretics sibutramine and rimonabant have been withdrawn due to side effects (*160*).

Novel targets for the treatment of type 2 diabetes including 11β-hydroxysteroid dehydrogenase 1 (HSD11B1), G protein-coupled receptor 119 (GPR119), sodium/glucose cotransporters (SGLT1 and 2) and stearoyl-CoA desaturase (SCD) are described in plenty of current patent claims (*161*).

1.5 Prevention of type 2 diabetes

Considering the growing incidences of obesity and type 2 diabetes strategies for the prevention of metabolic disorders before their development are of central importance. Although obesity and insulin resistance are reversible to a certain condition (*17*), their progression lead to irreversible damages such as pancreatic β-cell failure. It is obvious that a paradigm shift *from treatment to prevention* of metabolic diseases is required. As the pathogenesis of type 2 diabetes is causally linked to physical inactivity and hypercaloric diet (*11, 17*), changes in life style and nutrition are fundamental for health management. Classically, diet was characterized by its energy content, and the amount of calories was the major marker of healthy nutrition. In the past decades, it was recognized that specific molecular compounds can influence the metabolism, and that so called nutraceuticals, food-derived products with pharmaceutical benefits, add additional profits for reducing the risk for metabolic disorders (*162*). The emerging field of nutrigenomics aims to unravel the dietary impacts on metabolism and homeostatic control (*163*). Nuclear hormone receptors as PPARs have a key position therein, as they are nutrient sensors involved in energy homeostasis *and* metabolic disorders (*164*). Nuclear receptors can not only be activated by macronutrients (e.g. PPARs or LXRs by fats) and micronutrients (e.g. retinoic acid receptors by vitamin A), but further can be modulated by a magnitude of dietary small

molecules such as flavonoids and polyphenols. This is addressed by the application of functional foods, modified diets that hold beneficial effects on health, which gain increasing importance for the food industry (*165*). Recent innovative ingredients include cholesterol-lowering phytosterols, triglyceride-reducing unsaturated fatty acids and chocolate enriched with blood-pressure-lowering flavonoids (*166*). Several nutraceuticals have also been reported to reduce insulin resistance. For instance, vitamin D may increase insulin sensitivity (*167*) and also was shown to prevent the onset of diabetes (*168*). Additionally, soluble fibers such as glucomannan and chlorogenic acid decrease insulin resistance by slowing carbohydrate absorption similar to α-glucosidase inhibitors (see 1.4) (*162, 169*). Further improvement in insulin sensitivity was observed during studies with chromium, magnesium and α-lipoic acid (*169*). Since 2006 the European Food Safety Authority (EFSA) requires detailed scientific justification of health claims to avoid consumer misleading (*170*). The beneficial effects of nutraceuticals on diabetes and obesity therefore need additional clinical studies in healthy volunteers and/or diabetic patients. However, due to low long-term effects measuring *preventive* effects in healthy volunteers is more difficult than detecting *therapeutic* effects in diabetic patients. The future will show if nutraceutical companies will endeavour sophisticated long-term studies for prevention, or if anti-diabetic nutraceuticals will be primarily approved for co-treatment of insulin resistance.

1.6 Mother Nature's medicine chest - Natural products in drug discovery

The current decline in new drug approvals and progressive loss of patent protection require new strategies for the development of new chemical entities (*171*). Natural products are still promising sources of new drugs, albeit their application for drug screening is regressive (*171*). Natural products are secondary metabolites, small molecules that are not essential for that organism. Often in form of crude plant extracts, natural products were the first drugs available to mankind and are still the major medicine worldwide (e.g. by Traditional Chinese

Medicine) (*172*). Natural products also played an essential role for the development of pharmacology in the Western world, as about half of the current approved drugs are based on natural products (*173*).

For instance, statins used for the treatment of hypercholesterolemia are derivatives of the natural polyketide compactin (mevastatin), which was isolated from the mold *Penicillium citrinum* in 1976 (*174*). Of note, the derivative atorvastin (Lipitor) was the best selling drug in 2008 and brought about 12 billion US dollars annual sales (*175*). The widespread analgesic acetylsalicylic acid (Aspirin) has its origin in nature, too. Already the ancient Greek used extracts from willow bark to treat pain and fever, and 2000 years later the active natural product salicin was isolated and improved (*176*). Therapy of severe pain is often administered with morphine, which was discovered and isolated from opium in 1804 (*177*). Pain patients that are intolerant to morphine are alternatively treated with the peptide ziconotide (Prialt) derived from the marine cone snail *conus magus* (*178*). Also the popular antiphlogistics tacrolimus (FK506) and cyclosporine were isolated from bacterial and fungal sources, respectively (*179, 180*).

Since combating microbial invaders is a major challenge for plants and fungi they evolved a huge amount of antibiotics that are also beneficial for human health management. Penicillin, isolated from the mould *Penicillium notatum* by Alexander Fleming in 1928 (*181*), and other β-lactam antibiotics play a pivotal role for the treatment of infections. Besides, artemisinin, isolated from the plant *Artemisia annua*, was established as standard medication of malaria (*182*). Moreover, treatment of cancer is a growing field in pharmacology. The taxanes (taxol) were first isolated from the Pacific yew tree *Taxus brevifolia* and are of major importance in chemotherapy of various types of cancer (*183*).

Noteworthy, also some anti-diabetic drugs are natural products or analogues thereof. For instance, the development of the biguanide metformin was attributed to the isolation of guanides from *Galega officinalis* (French lilac), which was used because of its hypoglycemic properties for hundreds of years (*184*). Additionally, the novel GLP-1 analogue exenatide is a synthetic version of exendin-4, a

hormone found in the saliva of the Gila monster that was first isolated in 1992 (*185*).

But not only pure chemical compounds are used for the medication of common diseases. There is also a growing interest for the usage of mixtures of natural products based on traditional remedies. For instance, besides various bioactive plant extracts available without prescription (e.g. Saint John's wort extracts), a defined mixture of compounds extracted from green tea (sinecatechins, Veregen) was recently approved officially for the treatment of genital warts (*173*).

These examples impressively illustrate the high potential of natural resources to combat disorders and to serve as leads for the development of derivatives. As natural sources, the current focus is on plant-, fungi- and actinomycetes-derived compound libraries. Though, collections of compounds from marine organism and cyanobacteria are increasingly investigated (*171*).

Screening of natural product libraries has several advantages over the investigation of synthetic combinatorial libraries. In general, the success rate of natural product library screening is much higher (*171*), because natural products have a higher chance to interact with biological target molecules. This can be explained by the different structural properties of synthetic and natural compounds. There is a huge chemical space that can potentially be occupied by *synthetic compounds*. A theoretical library of compounds with up to 30 atoms (carbon, nitrogen, oxygen and sulfur) may contain more than 10^{60} different molecules (*186*). On the other hand, the chemical space of *biological* targets is modest in size – e.g. the human genome encodes about 25,000 genes (*187*). For the three-dimensional folding of proteins only a strict set for stable conformational interactions is allowed. The bottleneck of *combinatorial chemistry* is the lack of knowledge about the areas of chemical space that are suited to interact with biological space. On the other side, *natural products* are produced by proteins and thereby naturally interact with these biological molecules. Consequently, *natural products* can more likely interact with biological targets in a screening approach (*171*).

Several disadvantages of natural product library screening account for their decreased application in the pharmaceutical industry. Access and supply to the natural resources have to be assured, but are subjected to biological variation, risk of extinction and loss of biodiversity, political restrictions and intellectual property concerns (*171, 173*). In the process of high-throughput screening problems of purity, solubility and stability can occur. In addition, considerable time can be required for structural characterisation of novel natural products. Since many known natural products have already been patented, the driven force is reduced in many pharmaceutical organizations, leading to a drop in natural product-based drug development in the last years (*171*).

However, only few microorganisms and plants have been examined for bioactivity. Advances in plants collections, microbe cultivation and systematic classification using the metagenomics approach, and development of new natural resources (e.g. marine organisms and insects) will provide many novel compounds.

1.7 Aims of this thesis

In consideration of the high pandemic prevalence of type 2 diabetes, new anti-diabetic compounds are required for pharmaceutical and nutraceutical development. The nuclear receptor PPARγ is an important target for insulin sensitizing drugs, but treatment with current PPARγ-activating drugs is associated with severe side effects. The objective of this work was to identify and characterize novel PPARγ ligands. A large natural product library has to be screened with different biophysical and cellular approaches. For the screening hits potency and selectivity of PPARγ activation has to be characterized. In different cell models the influence of novel PPARγ modulators on gene expression has to be systematically investigated and compared to known PPARγ ligands. Effects on prevention and therapy of type 2 diabetes have to be further investigated in different mouse models. Various metabolic tests in mice, gene expression analyses and biochemical experiments in isolated tissues have to be performed.

The final aim is to discover a novel class of potent natural products that have promising *in vivo* properties for the application as pharmaceutical or nutraceutical compound for prevention or therapy of type 2 diabetes or other PPARγ-related diseases.

2 Materials and Methods

2.1 Compounds and natural products

Compounds were purchased from the following sources: rosiglitazone (Cayman, Biozol, Eching, Germany), nTZDpa (Tocris, Biozol, Eching, Germany), pioglitazone (Sigma Aldrich, Taufkirchen, Germany), telmisartan, troglitazone, GW0742, GW7647 (all from Sigma-Aldrich, Taufkirchen, Germany), amorfrutin 1 (NP-003520), amorfrutin 2 (NP-003521), amorfrutin 3 (NP-006430), amorfrutin 4 (NP-009525), other natural products including the natural product library (all available from Analyticon Discovery, Potsdam, Germany). We used a diverse library of natural products, consisting of approximately 8,000 compounds. It contained pure plant-derived and microbial metabolites representing a great variety of different substance classes and structures. Purity of natural compounds was determined by high performance liquid chromatography (HPLC) or nuclear magnetic resonance (NMR) spectroscopy and on average 95 % was achieved. Structural elucidation was performed by NMR and liquid chromatography coupled to mass spectrometry (LC/MS). The amorfrutins were isolated from roots of *Glycyrrhiza foetida* (approximately 3.5 g per kg plant material) and alternatively from fruits of *Amorpha fruticosa* (approximately 500 mg per kg plant material) using organic extraction and iterative HPLC separation of organic fractions. Amorfrutins 1, 5, and 5ME were additionally synthesized in-house as described below.

2.2 Chemical synthesis of amorfrutins

Investigation of the effects of amorfrutins *in vivo* required the development of a chemical synthesis to gain multigram quantities of compound. A synthesis route for the amorfrutins was developed by Dr. Frank C. Schroeder (Boyce Thompson Institute and Department of Chemistry and Chemical Biology, Cornell University, Ithaca, NY 14853, USA). Amorfrutins 1, 5, and 5ME were synthesized by Aman Prasad and Dr. Frank C. Schroeder with purities greater than 99%.

2.3 Time-resolved FRET assays

Identified PPARγ ligands were validated and characterized by a time-resolved fluorescence resonance energy transfer (TR-FRET)-based competitive binding assay. FRET involves a radiationless energy transfer from stimulated electrons (s_1) of a donor fluorophor to ground state electrons (s_0) of an acceptor fluorophor, provided that the emission spectrum of the donor overlaps the excitation spectrum of the acceptor dye. The efficiency of the energy transfer is highly dependent on the intermolecular distance, so that a minimal spatial distance of the dyes of ca. 8 nm is required (*190*). For time-resolved FRET lanthanide complexes are used as fluorescence donor. Lanthanides have long fluorescence life times (µs- to ms-scale), and thus, their fluorescence can be detected after a certain time delay (e.g. 200 µs), while the common short-lived background fluorescence is already decayed. This leads to an increased signal-to-background ratio. The common large Stokes shift of lanthanides further enhances the signal-to-background ratio.

To characterize molecular binding to PPAR the LanthaScreen competitive binding assays (Invitrogen, Darmstadt, Germany) were used. This technology makes use of terbium-labelled anti-GST-antibodies bound to GST-tagged PPAR and fluorescein-labelled dexamethasone. Increasing the concentration of potential ligands results in displacement of the labelled PPAR-ligand and hence in a decrease of the TR-FRET signal.

To determine ligand-induced cofactor recruitment to PPAR the LanthaScreen coactivator assays (Invitrogen, Darmstadt, Germany) were used. This approach involves terbium-labelled anti-GST-antibodies bound to GST-tagged PPAR and fluorescein-labelled cofactor peptides. Increasing the concentration of ligands leads to conformational change of PPAR and thus to enhanced or decreased binding of labelled cofactor peptides observed as change in the TR-FRET signal. This experiment not only discloses the ligand's effective concentrations, but further elicits the ligand-specific recruitment efficacy, that means the degree of cofactor association at PPARγ/ligand-saturated conditions. The efficacy thus is the maximal magnitude of cofactor recruitment achievable with this ligand.

Experiments were performed according to the manufacturer's protocols. To save resources the assays were miniaturized to a final volume of 5 to 10 µl end volume without loss in performance as determined by a Z'-factor > 0.7 (*191*). Competitive binding was measured in black small volume high bind polystyrene 384-well plates (Greiner Bio-One, Frickenhausen, Germany). Cofactor recruitment was detected in black low volume non-treated polystyrene 384-well plates (Corning Life Sciences, Fisher Scientific, Schwerte, Germany). The terbium chelate was excited at 340 nm and fluorescence was measured after 200 µs over 100 µs at 490 nm for terbium and at 520 nm for fluorescein. Fluorescence was measured with the POLARstar Omega (BMG LABTECH, Offenburg, Germany). For FRET calculation relative fluorescence units for 520 nm were divided by 490 nm.

Data were fitted using GraphPad Prism 5.0. Competitive binding data were fitted according to equation:

Y=Top + (Bottom - Top)/(1+10^((LogIC50-X)*HillSlope))

with variable Hill slope. 'Y' means FRET ratio (520nm/490nm), 'X' is titrated ligand concentration in logarithmic unit, 'Bottom' and 'Top' represent the plateaus in the units of the FRET ratio, Hill slope describes the steepness of the curve, and 'IC50' is the ligand concentration at 50% binding that has to be determined. IC50 values were converted to general Ki values according to Cheng and Prusoff (*192*). Cofactor recruitment data were fitted according to equation:

Y=Bottom + (Top-Bottom)/(1+10^((LogEC50-X)*HillSlope)).

'EC50' is the ligand concentration at 50% cofactor binding. Efficacy ('Top') of cofactor recruitment is normalized to the full PPARγ agonist rosiglitazone (set to 100%).

2.4 Reporter-gene assay

Reporter gene assays allow the verification and characterization of PPARγ agonists in a cellular environment, but are limited by artificial overexpression of the chimeric PPARγ-construct and by very simplified promoter architecture. Cellular activation of PPARγ was assessed in a reporter gene assay according to

the manufacturer's protocol (GeneBLAzer PPARγ DA Assay, Invitrogen). In brief, HEK 293H cells stably express a GAL4-PPARγ-LBD fusion protein and an UAS-beta-lactamase reporter gene. Upon binding on the PPARγ-LBD the ligand induces transcriptional activity of the fusion protein. This leads to expression of beta-lactamase, which subsequently catalyzes the cleavage of a fluorophor that consists of a coumarin (donor) and a fluorescein (acceptor) molecule linked by a lactam moiety. After cleavage both fluorophores become separated, resulting in a decrease of FRET efficiency. Thus, PPARγ activation is detected by an increase in coumarin fluorescence.

Cells were incubated with indicated concentrations of compounds. FRET was measured in a black polystyrene cell culture 384-well plate (Corning Life Sciences) in the POLARstar Omega with excitation at 410 nm and emission at 460 and 530 nm. For FRET calculation relative fluorescence units for 530 nm were divided by 460 nm. Obtained data were fitted using GraphPad Prism 5.0 according equation:

Y=Bottom + (Top-Bottom)/(1+10^((LogEC50-X)*HillSlope))

with variable Hill slope. Efficacy ('Top') of PPARγ activation is normalized to the full PPARγ agonist rosiglitazone (set to 100%).

2.5 Crystallization and structure determination

Crystallization and structure determination of the human ligand binding domain of PPARy in complex with amorfrutin 1 was kindly done by Jens C. de Groot and Dr. Konrad Büssow (Division of Structural Biology, Helmholtz Centre for Infection Research, Braunschweig, Germany). Briefly, crystallization was performed using hanging drop-vapour phase diffusion. The structure was solved by molecular replacement with PDB entry 1PRG (*193*) and refined to a resolution of 2.0 Å.

2.6 Cell culture

Gene expression studies were performed in adipocytes, in which PPARγ is highly expressed. Mouse 3T3-L1 cells (kindly provided by Dr. Schürmann, DifE, Potsdam-Rehbrücke, Germany) were cultured in Dulbecco's modified Eagle's medium (DMEM, Invitrogen) and 10% calf bovine serum (ATCC, LGC Promochem, Wesel, Germany) prior differentiation. Two-day post-confluent cells were differentiated in DMEM supplemented with 10% fetal bovine serum (FBS, Biochrom, Berlin, Germany), 10 µg/ml human insulin, 1 µM dexamethasone and 500 µM 3-isobutyl-1-methylxanthine (all Sigma-Aldrich). After 2 days of differentiation, medium was changed to DMEM supplemented with 10% FBS and 10 µg/ml human insulin for additional 2 days. Thereafter, cells were maintained in DMEM/10% FBS for 4 days with medium change every other day. To investigate the compound effects on PPARγ target genes, differentiated adipocytes were incubated for 24 hours with indicated amounts of substances, whereas 0.1% DMSO was used as vehicle control.

Primary subcutaneous preadipocytes isolated from human patients were provided by Zen-Bio (BioCat, Heidelberg, Germany). Cells were differentiated and modified after the manufacturer's protocol. Briefly, preadipocytes were maintained on nunclon plates (Nunc, Wiesbaden, Germany) in preadipocyte medium (PM-1, Zen-Bio) until differentiation. Cells were differentiated using PPARγ agonist-free adipocyte medium (AM-1, Zen-Bio) supplemented with 500 µM IBMX for 7 days. Thereafter, medium was changed to pure AM-1 for additional 7 days. Mature adipocytes were treated with indicated compounds diluted in AM-1 for 24 hours, whereas 0.1% DMSO was used as vehicle control.

2.7 PPARγ knockdown

Specificity of compound-dependent gene expression effects was investigated in siRNA-mediated PPARγ knockdown in adipocytes with subsequent qPCR analysis. Therefore, differentiated human adipocytes were seeded in 24-well-

plates at a confluence of 30 to 60%. Cells were transfected with 10 nM PPARγ Silencer Select Validated siRNA (ID s10888) or 10 nM Silencer Select Negative Control #1 siRNA (all Ambion, Applied Biosystems) using DeliverX Plus siRNA Transfection Kit (Panomics, BioCat). Transfection was carried out in serum- and antibiotic-free AM-1 medium (AM-1-PRF-SF, Zen-Bio) for 4 hours and continued for 3 days in standard AM-1 medium. Afterwards, compounds and vehicle control were added to PPARγ-knockdown and negative control cells for 24 hours.

2.8 RNA purification, cDNA synthesis and qPCR

Total RNA was isolated using the RNeasy Mini Kit (QIAGEN) according to their manual. For gene expression analysis in mice, tissues were first lysed and homogenized in RLT buffer (QIAGEN) with 5 mm steel beads at 20 Hz for 4 min (TissueLyser, QIAGEN). Genomic DNA was digested on column using the DNase-Set (QIAGEN). The concentration of extracted RNA was measured using the Nanodrop ND-1000 Spectrophotometer (Fisher Scientific). RNA was reversely transcribed into cDNA applying the High Capacity cDNA Reverse Transcription Kit (Applied Biosystems) with random primers.

Quantitative real-time PCR (qPCR) was carried out on the ABI Prism 7900HT Sequence Detection System using the SYBR Green PCR Master Mix (Applied Biosystems) to investigate the effects of natural products on PPARγ target gene expression. Briefly, after an initial denaturation at 95 °C for 10 min, the cDNA was amplified by 40 cycles of PCR (95 °C, 15 s; 60 °C, 60 s). The relative gene expression levels were normalized using β-actin gene and quantified by the $2^{-\Delta\Delta Ct}$ method (*194*). If not otherwise denoted, primers were designed with the Primer3 software (*195*) following specificity check with NCBI BLAST search (*196*). Primers with following sequences were used.

Symbol	Species	Forward primer	Reverse primer	Ref.
ACTB	human	CAGCCATGTACGTTGCTATCCAGG	AGGTCCAGACGCAGGATGGCATG	
ADIPOQ	human	GGTGAGAAGGGTGAGAAAGG	TCCTTTCCTGCCTTGGATT	
CD36	human	GTTGATTTGTGAATAAGAACCAGAGC	TGTTAAGCACCTGTTTCTTGCAA	
FABP4	human	GGTGGTGGAATGCGTCATG	CAACGTCCCTTGGCTTATGC	
HSD11B1	human	GGCCTCATAGACACAGAAACAGC	TGATCTCCAGGGCACATTCC	
LPL	human	ACAGAATTACTGGCCTCGATCC	CTGCATCATCAGGAGAAAGACG	
NR1H3	human	CACCTACATGCGTCGCAAGT	GACAGGACACACTCCTCCCG	
PLTP	human	GACACCGTGCCTGTGCG	GGTGGAAGCCACAGGATCCT	
PPARG	human	CATGGCAATTGAATGTCGTGTC	CCGGAAGAAACCCTTGCAT	
PPIB	human	ACGACAGTCAAGACAGCCTGG	CTTCCGCACCACCTCCAT	
Acadl	mouse	AGCCTGGGGCTGGAAGTGACTTA	CACGGTTGGTGACGGCCACG	
Acly	mouse	CAGCCAAGGCAATTTCAGAGC	CTCGACGTTTGATTAACTGGTCT	*(147)*
Acox1	mouse	CAGCACTGGTCTCCGTCATG	CTCCGGACTACCATCCAAGATG	
Actb	mouse	TGTCCACCTTCCAGCAGATGT	AGCTCAGTAACAGTCCGCCTAGA	
Aplp2	mouse	GTGGTGGAAGACCGTGACTAC	TCGGGGGAACTTTAACATCGT	*(147)*
Car3	mouse	TGACAGGTCTATGCTGAGGGG	CAGCGTATTTTACTCCGTCCAC	*(147)*
Ccl2	mouse	CCAGCACCAGCACCAGCCAA	TGGGGCGTTAACTGCATCTGGC	
Ccl3	mouse	GCTCCCAGCCAGGTGTCATTTTCC	GGGGTTCCTCGCTGCCTCCA	
Ccl5	mouse	CTCACTGCAGCCGCCCTCTG	CCGAGCCATATGGTGAGGCAGG	
Ccr2	mouse	TCAGCTGCCTGCAAAGACCAGA	CGGTGTGGTGGCCCCTTCAT	
Ccr5	mouse	AGACTCTGGCTCTTGCAGGATGGA	GGCAGGAGCTGAGCCGCAAT	
Cd24a	mouse	GTTGCACCGTTTCCCGGTAA	CCCCTCTGGTGGTAGCGTTA	*(147)*
Cfd	mouse	CATGCTCGGCCCTACATGG	CACAGAGTCGTCATCCGTCAC	*(147)*
Cidec	mouse	ATGGACTACGCCATGAAGTCT	CGGTGCTAACACGACAGGG	*(147)*
Cpt1a	mouse	TCTGCAGACTCGGTCACCACTCAAG	GGCTCAGGCGGAGATCGATGC	
Cpt2	mouse	AAGCAGCGATGGGCCAG	GAGCTCAGGCAGGGTGACC	
Cxcl1	mouse	GAGCTGCGCTGTCAGTGCCT	TGTGGCTATGACTTCGGTTTGGGT	
Cyp2f2	mouse	GTCGGTGTTCACGGTGTACC	AAAGTTCCGCAGGATTTGGAC	*(147)*
Ddx17	mouse	TCTTCAGCCAACAATCCCAATC	GGCTCTATCGGTTTCACTACG	*(147)*
Emr1	mouse	ACCCTCCAGCACATCCAGCCAA	TCACAGCCCGAGGGTGTCCA	
Fabp4	mouse	TGATGCCTTTGTGGGAACCT	GCAAAGCCCACTCCCACTT	
Il1b	mouse	CCCTGCAGCTGGAGAGTGTGGA	GCTCTGCTTGTGAGGTGCTGA	
Il6	mouse	TCTGCAAGAGACTTCCATCCAGTTGC	AGGCCGTGGTTGTCACCAGC	
Lgals3	mouse	TGGGGCCTACCCCAGTGCTC	GGCACCGTCAGTGGTCCAGC	
Nr1d1	mouse	TACATTGGCTCTAGTGGCTCC	CAGTAGGTGATGGTGGGAAGTA	*(147)*
Nr1d2	mouse	TGAACGCAGGAGGTGTGATTG	GAGGACTGGAAGCTATTCTCAGA	*(147)*

Nr1h3	mouse	GCTCTGCTCATTGCCATCAG	TGTTGCAGCCTCTCTACTTGGA	
Nr3c1	mouse	AGCTCCCCCTGGTAGAGAC	GGTGAAGACGCAGAAACCTTG	*(147)*
Peg10	mouse	TGCTTGCACAGAGCTACAGTC	AGTTTGGGATAGGGGCTGCT	*(147)*
Pgc1a	mouse	TCCCATACACAACCGCAGTCGC	GGGGTCATTTGGTGACTCTGGGGT	
Ptgs2	mouse	CCCTGCTGCCCGACACCTTC	CCAGCAACCCGGCCAGCAAT	
Rarres2	mouse	GCCTGGCCTGCATTAAAATGG	CTTGCTTCAGAATTGGGCAGT	*(147)*
Rybp	mouse	CGACCAGGCCAAAAAGACAAG	CACATCGCAGATGCTGCATT	*(147)*
Selenbp1	mouse	ATGGCTACAAAATGCACAAAGTG	CCTGTGTTCCGGTAAATGCAG	*(147)*
Slc2a4	mouse	GCGGATGCTATGGGTCCTTA	GTCCGGCCTCTGGTTTCA	
Tbl1x	mouse	CACAAGTTGCACGGCTCGCG	AGTGTGAGCCACCCTCGTCACA	
Tnf	mouse	AGCCCACGTCGTAGCAAACCA	CATGCCGTTGGCCAGGAGGG	
Txnip	mouse	TCTTTTGAGGTGGTCTTCAACG	GCTTTGACTCGGGTAACTTCACA	*(147)*

2.9 Viability assays

Cytotoxic effects of the natural products were assessed in HepG2 and 3T3-L1 cells cultured in DMEM/10%FCS using the WST-1 reagent (Roche) according to the manufacturer's protocol. Cells were incubated with different concentrations of compounds for 24 h. Experiments were performed in triplicate.

2.10 Genome-wide gene expression analyses

RNA quality was determined using the Bioanalyzer 2100 (Agilent). Biotin-labelled cRNA was produced using the Illumina TotalPrep RNA Amplification Kit (Ambion) following the manufacturer's instructions. Cy3-stained cRNA was hybridised on HumanHT-12 v3.0 or MouseWG-6 v2.0 Expression BeadChips (Illumina, Eindhoven, The Netherlands). Scanning was performed using the Illumina BeadStation 500 platform and reagents were used according to the protocols supplied by the manufacturer. Samples were hybridised at least in biological triplicates. All basic expression data analysis was carried out using BeadStudio 3.1 (Illumina). Raw data were background-subtracted and normalized using the cubic spline algorithm. Processed data were then filtered for significant detection (P value ≤ 0.01) and differential expression vs. vehicle treatment

according to the Illumina t-test error model and were corrected according to the Benjamini-Hochberg procedure (P value ≤ 0.05) in the Beadstudio software. Gene expression data were submitted in MIAME-compliant form to the Gene Expression Omnibus database (GSE28384). Heatmaps and hierarchical clustering of samples were carried out with Mayday 2.8 (*197*). K-Means clustering of genes was calculated with Euclidean distance in MeV 4.3. Genes from these clusters were checked for functional annotation enrichment using DAVID 2008 (*198, 199*). Enrichment scores > 1.0 were considered as significant.

A common disadvantage of singular gene analysis is attributed to the use of stringent filtering. Consequently, small expression changes of several genes important for a certain pathway are lost during analysis, although the overall pathway might be significantly regulated. This concern was addressed by the development of Gene Set Enrichment Analysis (GSEA) (*200*), which tests for enrichment of whole sets of genes (e.g. pathways) instead of single genes. GSEA was performed using the following parameters: 1000 gene set permutations, weighted enrichment statistic, and signal-to-noise metric. Microarray data were analyzed using the curated C2 gene sets from the Molecular Signature Database (MSigDB) including KEGG pathways and data from chemical and genetic perturbation experiments (version 2.5, 1892 gene sets) if not otherwise denoted.

The high-dimensionality of whole-genome expression analyses is a problem for visualization and investigation of biologically relevant data. Principal component analysis (PCA) is often used for microarray data to reduce the dimensionality of the data while retaining most of the variation in the data set. Each compound profile is represented by few principal components instead of thousands of values. Thus, PCA allows for comparison of compound effects on genome-wide expression in a clearly arranged plot (*201*). PCA was performed in MeV 4.3 (*202*) using median centering. Principal components were calculated based on the mean expression profile of rosiglitazone, pioglitazone, nTZDpa and telmisartan and non-averaged sample profiles of amorfrutins. Principal components were then

averaged and plotted onto the axis with error bars representing standard deviations.

In contrast to PCA, gene distance matrix (GDM) analyses include all gene expression data of a compound, without restriction to a set of genes. Data reduction is achieved by collapsing the expression data of every gene to a vector sum in Euclidean space. The Euclidean distance between the vector sums of different compounds therefore is a measure of the similarity between the expression profiles. GDM comparison was performed in MeV 4.3.

Comparison of gene expression profiles of diseases or treatments with different small molecules reveals further insight into their mechanisms. The Connectivity Map approach provides a database of gene expression profiles of cells treated with small molecules and a pattern-matching software for expression data comparison (*203, 204*). To unravel the mechanism of action of identified PPARγ ligands we therefore compared the gene lists observed for rosiglitazone and amorfrutin 1 treatment to published data (Connectivity Map build 02).

2.11 Animal studies

Animal studies have been validated and approved State Office of Health and Social Affairs Berlin (LAGeSo) and were carried out according internationally approved guidelines. All animals were maintained one per cage under temperature-, humidity- and light-controlled conditions (22°C, 50% humidity, 12 hours light/12 hours dark-cycle). Mice had *ad libitum* access to food and water. Mice and food were weighed in a regularly manner to determine changes in body weight and food intake.

To explore the potential of our compound of interests in the prevention of diabetes we designed a long-term and low-dose study in C57BL/6 mice. Therefore, male C57BL/6 mice at age of 9 weeks were weighed and distributed equally to 4 groups (n=12). Mice were fed over 15 weeks with either low-fat diet (LFD, D12450B, 10 kcal% fat, ssniff, Soest, Germany), high-fat diet (HFD, D12492, 60

kcal% fat, ssniff) or high-fat diet with 4 mg/kg/d rosiglitazone (HFD+R) or 37 mg/kg/d amorfrutin 1 (HFD+A1). After 8 weeks of dosing blood was taken from the submandibular vein of conscious mice for testing of blood parameters. After 10 weeks an oral glucose tolerance test (OGTT) was carried out. Mice were fasted overnight before being subjected to an oral dose of 2 g/kg body weight of glucose (Sigma-Aldrich). Blood was taken from tail vein at the indicated time points. Blood glucose was analysed in a Hemocue B-Glucose analyser (Hemocue, Großostheim, Germany). Blood was collected using Microvette lithium-heparin coated capillary tubes (CB300, Sarstedt, Nürnbrecht, Germany). After centrifugation for 5 min at 2,000g, 4 °C, plasma was collected and analysed for metabolic parameters. After 13 weeks of feeding an intraperitoneal insulin sensitivity test (IPIST) was performed. Mice were fasted overnight and then had *ad libitum* access to food for 1 hour before the test. One U/kg body weight of insulin was injected intraperitoneally. Blood was taken from tail vein at the indicated time points. After 15 weeks of dosing, fasted mice were killed by cervical dislocation. Plasma and tissues were collected and stored at -80 °C before use.

For the therapy study we subjected diet-induced obesity (DIO) mice to a short-term-medium-dose treatment. Male C57BL/6 mice at age of 6 weeks were fed with high fat diet (HFD) for 12 weeks to induce obesity and insulin resistance. The mice were then weighed and distributed equally to 3 groups (n=13 each). Mice were fed over 3 weeks with HFD without compound (vehicle), HFD with 4 mg/kg/d rosiglitazone or with 100 mg/kg/d amorfrutin 1. After 17 days of treatment, an OGTT (2g/kg glucose) and after 23 days an IPIST (1.5 U/kg insulin) were performed as described above. After 24 days of dosing fasted mice were killed by cervical dislocation. Plasma and tissues were collected and stored at -80 °C before use.

To test the compounds in another diabetic model, leptin receptor deficient db/db mice (Charles River Laboratories, Sulzfeld, Germany) at age of 9 weeks were fed with standard diet (V1324, ssniff) without compound (vehicle), with 4 mg/kg/d

rosiglitazone or 100 mg/kg/d amorfrutin 1 over 3 weeks. After 17 days of treatment an IPIST (2.0 U/kg insulin) was carried out, and after 23 days an OGTT (2 g/kg glucose) was performed as described above. After 25 days of dosing fasted mice were killed by cervical dislocation. Plasma and tissues were collected and stored at -80 °C before use.

2.12 Metabolic parameters measurements

Plasma was used for the analysis of blood parameters. Glucose was measured using the Amplex Red Glucose Assay Kit (Invitrogen), while triglycerides, free fatty acids and plasma alanine transaminase (ALT) were determined with colorimetric quantification kits (Biovision, BioCat). Proinsulin, insulin and leptin were determined with mouse ELISA (Proinsulin Mouse ELISA and Insulin Ultrasensitive EIA, ALPCO, Immundiagnostik, Bensheim, Germany; Mouse Leptin ELISA, BioVendor, Heidelberg, Germany, respectively). All assays were performed according to the manufacturer's instructions. HOMA-IR was determined according to ref. (*205*).

For determining liver TNFα concentrations, murine liver (100 mg/ml) was lysed in a tissue lysis buffer (*206*) containing 20 mM Tris, 150 mM NaCl, 1 % Nonidet P-40, 0.5 % sodium deoxycholate, 1 mM EDTA, 0.1 % SDS and protease inhibitor cocktail (Roche). Samples were lysed and homogenized using disruption with 5 mm steel beads at 20 Hz for 4 min (TissueLyser, QIAGEN). After centrifugation for 10 min at 20,000 g, 4 °C, the supernatants were collected and used for TNFα ELISA (TNFα ELISA Ready-SET-Go, eBioscience, NatuTec, Frankfurt, Germany). The assay was miniaturized to a sample incubation volume of 25 µl and performed on a clear high bind polystyrene 384-well plate (Corning Life Sciences). For normalization of samples DNA content was measured using PicoGreen assay (Quant-iT, Invitrogen).

To measure liver and pancreatic triglycerides, tissues were weighed and disrupted at a concentration of 44 mg/ml in 100 % isopropanol for liver or 100 mg/ml in

50 % isopropanol/PBS (pH 7.4) for pancreas. Disruption was performed with 5 mm steel beads at 20 Hz for 4 min (TissueLyser). After centrifugation for 10 min at 20,000 g, 4 °C, the supernatants were collected and measured in the colorimetric assay (Biovision).

For the determination of glycogen in liver, tissues were weighed and disrupted at a concentration of 28 mg/ml in 200 mM sodium acetate (pH 4.8) using 5 mm steel beads at 20 Hz for 4 min (TissueLyser). The glycogen determination protocol (*207*) was modified as follows. Briefly, tissue lysates were heated to 70 °C for 10 min to inactivate endogenous enzymes. Samples were centrifuged for 10 min at 6,000 g, 4 °C. Subsequently, 3 µl of sample supernatants were added to 57 µl of 27 U/ml amyloglucosidase (Sigma-Aldrich) in 200 mM sodium acetate (pH 4.8) and incubated at 41 °C for 2 hours. To determine the free glucose in liver this incubation was also done with 3 µl of sample supernatant and 57 µl of 200 mM sodium acetate (pH 4.8) without amyloglucosidase. After incubation all samples were neutralized with 15 µl of 280 mM sodium hydroxide solution. Digested samples with or without enzyme were measured with the glucose assay kit (Invitrogen). For the calculation of liver glycogen, free glucose was subtracted from total glucose of each liver sample. Liver glycogen was presented as nmol released glucose per mg tissue.

2.13 Immunoblotting

To determine PPARγ phosphorylation vWAT of HFD-fed mice was lysed in UEES lysis buffer (9 M Urea, 100 mM EDTA/EGTA, 4% SDS with protease and phosphatase inhibitors) using 5 mm steel beads at 20 Hz for 4 min (TissueLyser). After centrifugation for 10 min at 10,000 g, the supernatants were stored at -80 °C until use. Samples were denatured and separated using a NuPAGE Novex 4-12% Bis-Tris gel (Invitrogen) and blotted onto nitrocellulose membranes. Membrane was blocked with a solution containing 2.5% milk powder, 2.5% BSA in PBS-T (0.05%) and 0.5x phosphatase inhibitor for 1 hour at room temperature. Membranes were washed in PBS-T (0.05%). A rabbit polyclonal phospho-specific

antibody against PPARγ Ser 273 was produced by Eurogentech (Seraing, Belgium) with the phosphopeptide Ac-KTTDKpSPFVIYDC-amide (*147*). For detection, 0.8 µg/mL PPARy-pSer273 and 0.5 µg/mL PPARy (E-8, Santa Cruz, Heidelberg, Germany) antibody, respectively, were diluted in PBS-T (0.05%) with 1.5% milk powder and 1.5% BSA. Membranes were shaked overnight at 4°C and subsequently incubated with anti-rabbit IgG-HRP (Santa Cruz, sc-2004) and anti-mouse IgG-HRP (Santa Cruz, sc-2005), respectively, prior to detection with Western Lightning ECL solution (Perkin Elmer) on a Fujifilm LAS-1000 camera system using the Image Reader LAS-1000 Pro V2.61 software. Membranes were stripped with Restore Plus Western Blot Stripping Buffer (Thermo Scientific) for 10 min. Densitometry was performed in ImageQuant TL (GE Healthcare). The rate of PPARy phosphorylation was normalized to total PPARy protein.

2.14 Statistical analyses

Data are presented as mean ± standard error of mean (s.e.m.) if not otherwise denoted. Statistical significance was determined by unpaired two-tailed Student's t-test for single comparisons and one-way ANOVA with Dunnett's post test for multiple comparisons using GraphPad Prism 5.0. Pearson correlation analyses were performed in GraphPad Prism 5.0. A P-value $\leq$ 0.05 was defined as statistically significant.

2.15 Equipment and reagents

2.15.1 Reagents

Reagent	Manufacturer/Provider
DMSO	Merck (Darmstadt, Germany)
Natural products	AnalytiCon Discovery (Potsdam, Germany)
Amorfrutin 1 (synthetic)	Kindly provided by Dr. Frank C. Schroeder (Cornell University, Ithaca, USA)
Amorfrutin 5	Kindly provided by Dr. Frank C. Schroeder (Cornell University, Ithaca, USA)

Amorfrutin 5ME	Kindly provided by Dr. Frank C. Schroeder (Cornell University, Ithaca, USA)
GW0742	Sigma-Aldrich (Taufkirchen, Germany)
GW7647	Sigma-Aldrich (Taufkirchen, Germany)
nTZDpa	Tocris (Biozol, Eching, Germany)
Pioglitazone	Sigma-Aldrich (Taufkirchen, Germany)
Rosiglitazone	Cayman (Biozol, Eching, Germany)
Telmisartan	Sigma-Aldrich (Taufkirchen, Germany)
Troglitazone	Sigma-Aldrich (Taufkirchen, Germany)
Amplex Red Glucose Assay Kit	Invitrogen (Karlsruhe, Germany)
Amyloglucosidase (A1602)	Sigma-Aldrich (Taufkirchen, Germany)
FFA quantification kit	Biovision (Biocat, Heidelberg, Germany)
Triglyceride quantification kit	Biovision (Biocat, Heidelberg, Germany)
Lanthascreen PPARa competitive binding assay (PV4892)	Invitrogen (Karlsruhe, Germany)
Lanthascreen PPARb/d competitive binding assay (PV4893)	Invitrogen (Karlsruhe, Germany)
Lanthascreen PPARγ competitive binding assay (PV4894)	Invitrogen (Karlsruhe, Germany)
Lanthascreen PPARγ Coactivator Assay (PV4548)	Invitrogen (Karlsruhe, Germany)
Lanthascreen Fl-CBP-1 Peptide (PV4596)	Invitrogen (Karlsruhe, Germany)
Lanthascreen Fl-NCOR ID2 Peptide (PV4624)	Invitrogen (Karlsruhe, Germany)
Lanthascreen Fl-PGC1A Peptide (PV4421)	Invitrogen (Karlsruhe, Germany)
Lanthascreen Fl-PRIPRAP250 Peptide (PV4604)	Invitrogen (Karlsruhe, Germany)
GeneBLAzer PPARγ DA Assay (K1419)	Invitrogen (Karlsruhe, Germany)
Mouse Insulin Ultrasensitive EIA	ALPCO (Immundiagnostik, Bensheim, Germany)
Mouse Leptin ELISA	BioVendor (Heidelberg, Germany)
Mouse Proinsulin EIA	ALPCO (Immundiagnostik, Bensheim, Germany)
Mouse TNFα ELISA Ready-SET-Go	eBioscience (NatuTec, Frankfurt, Germany)
ALT Assay Kit	Biovision (Biocat, Heidelberg, Germany)
Dulbecco's modified Eagle's medium (DMEM)	ATCC (LGC Promochem, Wesel, Germany)
Preadipocyte medium (PM-1)	Zen-Bio (BioCat, Heidelberg, Germany)

Adipocyte medium (AM-1)	Zen-Bio (BioCat, Heidelberg, Germany)
Serum- and antibiotic-free AM-1 medium (AM-1-PRF-SF)	Zen-Bio (BioCat, Heidelberg, Germany)
Phosphate buffered saline solution (PBS), pH 7.4	GIBCO (Invitrogen, Karlsruhe, Germany)
Calf Serum (CS)	ATCC (LGC Promochem, Wesel, Germany)
Fetal Calf Serum superior (FCS)	Biochrom (Berlin, Germany)
TrypLE Express	GIBCO (Invitrogen, Karlsruhe, Germany)
Trypan Blue Stain	Invitrogen (Karlsruhe, Germany)
3-Isobutyl-1-methylxanthine (IBMX)	Sigma-Aldrich (Taufkirchen, Germany)
Dexamethasone	Sigma-Aldrich (Taufkirchen, Germany)
WST-1	Roche (Mannheim, Germany)
DeliverX Plus siRNA Transfection Kit	Panomics (BioCat, Heidelberg, Germany)
PPARγ Silencer Select Validated siRNA (ID s10888)	Ambion (Applied Biosystems, Darmstadt, Germany)
Silencer Select Negative Control #1 siRNA	Ambion (Applied Biosystems, Darmstadt, Germany)
Ethanol	Merck (Darmstadt, Germany)
Isopropanol	Merck (Darmstadt, Germany)
RNase-free water	Ambion (Applied Biosystems, Darmstadt, Germany)
TRIzol reagent	Invitrogen (Karlsruhe, Germany)
β-Mercaptoethanol	Sigma-Aldrich (Taufkirchen, Germany)
RNeasy Plus Mini Kit	QIAGEN (Hilden, Germany)
DNase set	QIAGEN (Hilden, Germany)
High Capacity cDNA Reverse Transcription Kit	Applied Biosystems (Darmstadt, Germany)
Illumina TotalPrep RNA Amplification Kit	Ambion (Applied Biosystems, Darmstadt, Germany)
SYBR GREEN PCR Master Mix	Applied Biosystems (Darmstadt, Germany)
Real-time PCR Primer	Sigma-Aldrich (Taufkirchen, Germany)
Picogreen Quant-iT	Invitrogen (Karlsruhe, Germany)
Animal diets	ssniff (Soest, Germany)
Glucose	Sigma-Aldrich (Taufkirchen, Germany)
Insulin solution (human)	Sigma-Aldrich (Taufkirchen, Germany)
Urea	Sigma-Aldrich (Taufkirchen, Germany)

Sodium dodecyl sulfate (SDS)	Sigma-Aldrich (Taufkirchen, Germany)
Tween-20	Sigma-Aldrich (Taufkirchen, Germany)
1x Phosphatase Inhibitor Cocktail	Sigma-Aldrich (Taufkirchen, Germany)
1x Protease Inhibitor Cocktail	Roche (Mannheim, Germany)
Tris(hydroxymethyl)aminomethane (Tris)	Sigma-Aldrich (Taufkirchen, Germany)
Ethylenediaminetetraacetic acid (EDTA)	Sigma-Aldrich (Taufkirchen, Germany)
Ethyleneglycoltetraacetic acid (EDTA)	Sigma-Aldrich (Taufkirchen, Germany)
Coomassie Brillant Blue R250	Bio-Rad Laboratories (München, Germany)
Precision Plus Protein all blue standards	Bio-Rad Laboratories (München, Germany)
Milk powder	Sigma-Aldrich (Taufkirchen, Germany)
Bovine serum albumin (BSA)	Sigma-Aldrich (Taufkirchen, Germany)
Anti-PPARy antibody (E-8, mouse monoclonal)	Santa Cruz (Heidelberg, Germany)
Anti-pSer273-PPARy antibody (rabbit polyclonal)	Eurogentech (Seraing, Belgium)
Anti-mouse IgG-HRP (sc-2005, goat)	Santa Cruz (Heidelberg, Germany)
Anti-rabbit IgG-HRP (sc-2004, goat)	Santa Cruz (Heidelberg, Germany)
Restore Plus Western Blot Stripping Buffer	Pierce (Fisher Scientific, Schwerte, Germany)
Western Lightning ECL solution	Perkin Elmer (Rodgau, Germany)

2.15.2 Cells and animals

Cell/Animal model	**Provider**
3T3-L1 cell line	Kindly provided by Dr. Schürmann (DIfE, Nuhtetal, Germany)
HepG2 cell line	ATCC (LGC Promochem, Wesel, Germany)
Human primary preadipocytes	Zen-Bio (BioCat, Heidelberg, Germany)
C57BL/6 mice	In-house breeding
db/db mice	Charles River Laboratories (Sulzfeld, Germany)

2.15.3 Equipments and consumables

Product	Manufacturer
384 Well Flat Bottom Polystyrene High Bind Microplate, clear (3700)	Corning Life Sciences (Fisher Scientific, Schwerte, Germany)
384 Well low volume black Polystyrene nontreated microplate (3677)	Corning Life Sciences (Fisher Scientific, Schwerte, Germany)
384 Well Polystyrene cell culture microplate, black (781091)	Greiner Bio-One (Frickenhausen, Germany)
384 Well Polystyrene cell culture microplate, white (781098)	Greiner Bio-One (Frickenhausen, Germany)
384 Well Small Volume HiBase Polystyrene Microplates, black (784076)	Greiner Bio-One (Frickenhausen, Germany)
384 Well Small Volume HiBase Polystyrene Microplates, clear (784101)	Greiner Bio-One (Frickenhausen, Germany)
Thermowell 96-well PCR plate	Corning Life Sciences (Fisher Scientific, Schwerte, Germany)
Nunclon cell culture plate	Nunc (Wiesbaden, Germany)
75 cm² flask	TPP (Biochrom, Berlin, Germany)
POLARstar Omega	BMG LABTECH (Offenburg, Germany)
Steel beads (5 mm)	QIAGEN (Hilden, Germany)
TissueLyser	QIAGEN (Hilden, Germany)
ABI Prism 7900HT System	Applied Biosystems (Darmstadt, Germany)
Nanodrop ND-1000	Nanodrop (Fisher Scientific, Schwerte, Germany)
Bioanalyzer RNA 6000 Pico Kit	Agilent Technolgies (Böblingen, Germany)
Bioanalyzer 2100	Agilent Technolgies (Böblingen, Germany)
HumanHT-12 v3 Expression BeadChips	Illumina (Eindhoven, The Netherlands)
MouseWG-6 v2.0 Expression BeadChips	Illumina (Eindhoven, The Netherlands)
BeadStation 500	Illumina (Eindhoven, The Netherlands)
Microvette lithium-heparin coated capillary tubes (CB300)	Sarstedt (Nürnbrecht, Germany)
Hemocue B-Glucose analyser	Hemocue (Großostheim, Germany)
NuPAGE 4-12% Bis-Tris Gel	Invitrogen (Karlsruhe, Germany)
Hybond ECL nitrocellulose membrane	GE Healthcare (München, Germany)
LAS-1000 camera system	Fujifilm (Düsseldorf, Germany)

2.15.4 Software

Software	Provider
GraphPad Prism 5	GraphPad Software (La Jolla, CA, USA)
Primer-BLAST	National Center for Biotechnology Information (NCBI)/Primer3 (http://www.ncbi.nlm.nih.gov/tools/primer-blast)
SDS 2.2	Applied Biosystems (Darmstadt, Germany)
BeadStudio 3.1	Illumina (Eindhoven, The Netherlands)
DAVID 2008	National Institute of Allergy and Infectious Diseases (NIAID) (Frederick, MD, USA, http://david.abcc.ncifcrf.gov)
Mayday 2.8	Center for Bioinformatics Tuebingen (ZBIT) (University of Tuebingen, Tuebingen, Germany, http://www.zbit.uni-tuebingen.de/pas/software.htm)
MeV 4.3	Dana-Farber Cancer Institute (Boston, MA, USA, http://www.tm4.org/mev)
Gene Set Enrichment Analysis (GSEA)	Broad Institute (Cambridge, MA, USA, www.broadinstitute.org/cmap)
Connectivity Map, build 02	Broad Institute (Cambridge, MA, USA, www.broadinstitute.org/gsea)
Image Reader LAS-1000 Pro V2.61	Fujifilm (Düsseldorf, Germany)
ImageQuant TL	GE Healthcare (München, Germany)

3 Results

3.1 From plant to tube: *In vitro* characterization of novel PPAR ligands

3.1.1 Amorfrutins are a novel class of PPAR-binding natural products

To identify novel natural products that could act as anti-diabetic PPARγ ligands, we initially screened a natural product library consisting of approximately 8,000 pure compounds of herbal and microbial origin by using a mass spectrometry-based binding assay. The screen revealed several potential new PPARγ ligands, including a family of isoprenoyl-substituted benzoic acid derivatives, the amorfrutins (**Figures 7 and S1, and table S1**). This natural product class was mainly isolated from the edible roots of licorice, *Glycyrrhiza foetida*, and the fruits of the related legume *Amorpha fruticosa*, from which the name of the compound class was derived (*208*).

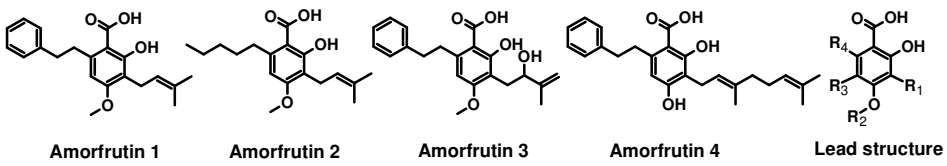

Figure 7. Structures of the four amorfrutins that were further analysed and corresponding lead structure. R1: Isoprenoyl residues; R2: H or Me; R3: H or isoprenoyl residues; R4: H, aliphatic or aromatic residues or a combination thereof.

Time-resolved fluorescence resonance energy transfer (TR-FRET) assays revealed further biophysical characteristics of identified PPARy ligands. In a competitive binding assay the affinity constants (Ki) for binding of the amorfrutins to the PPARγ-LBD ranged from low-nanomolar to low-micromolar range (**table S1**). For instance, amorfrutin NP-015142 strikingly bound to PPARγ with a Ki of 19 nM, which is in the range of the anti-diabetic drug rosiglitazone (7 nM, **table 1**). This is the first report of a natural product binding to PPARγ with such high affinity. Amorfrutins 1 to 4, which were used in subsequent experiments, showed

Ki values of 236 nM, 287 nM, 352 nM and 278 nM, respectively (**Figure 8A and table 1**).

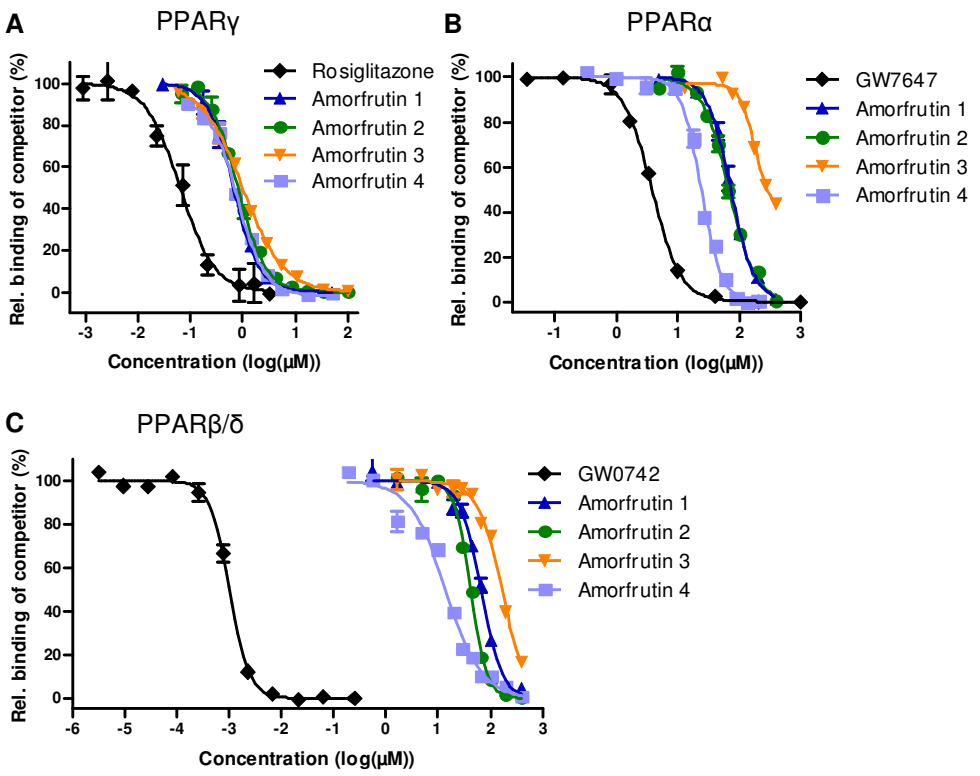

Figure 8. Binding of compounds on the ligand binding domain (LBD) of **(A)** PPARγ, **(B)** PPARα and **(C)** PPARβ/δ in a competitive TR-FRET assay. Data are expressed as mean ± s.d. (n=3).

The amorfrutins also showed micromolar binding to PPARα and PPARβ/δ with selectivities ranging from 10-fold to 200-fold for PPARγ (**Figures 8B, 8C and table S1**). For instance, amorfrutin 3 is a very selective nanomolar PPARγ ligand, as its binding constants are 115 µM and 68 µM for PPARα and β/δ, respectively. In contrast, amorfrutin NP-015142 also has high affinity to PPARα and β/δ with binding constants of about 2 µM (**table S1**), indicating that NP-015142 is a pan PPAR agonist. In summary, dependent on the compound concentration, amorfrutins are potent PPARγ ligands with the potential to additionally activate PPARα and PPARβ/δ. This suggests that these natural products could contribute

to treatment of diabetes and related diseases such as dyslipidemia and hypercholesterolemia (*74*).

Table 1. Affinity constants (Ki) and effective concentrations (EC50) of investigated compounds binding to PPARγ. Ki values were obtained by using a competitive TR-FRET assay, EC50 and efficacy values were determined from a reporter gene assay. Efficacy is the maximum activation relative to the rosiglitazone-induced activation of PPARγ.

Compound	PPARγ		
	Ki	EC50	Efficacy
Amorfrutin 1	236 nM	458 nM	39%
Amorfrutin 2	287 nM	1.2 µM	30%
Amorfrutin 3	352 nM	4.5 µM	22%
Amorfrutin 4	278 nM	979 nM	15%
Rosiglitazone	7 nM	2 nM	100%
Pioglitazone	584 nM	n.d.	n.d.
nTZDpa	29 nM	n.d.	n.d.
Telmisartan	1.7 µM	n.d.	n.d.

n.d., not determined.

To gain further insight into the interaction of amorfrutins with PPARγ, the structure of the complex of the PPARγ-ligand binding domain (LBD) and amorfrutin 1 was determined by X-ray crystallography in cooperation with Jens C. de Groot and Dr. Konrad Büssow (Division of Structural Biology, Helmholtz Centre for Infection Research, Braunschweig, Germany). Binding of full agonists such as rosiglitazone or pioglitazone is known to stabilize helix H12 of PPARγ (*73*). In contrast, the novel agonist amorfrutin 1 was bound between helix H3 and the β-sheet, thus stabilizing this region. The structure showed that amorfrutin 1 was recognized by PPARγ in a similar way as the partial agonists nTZDpa and MRL-24, and also the intermediate agonist BVT.13 (*209*). Similar to these selective PPARγ modulators (SPPARγMs), amorfrutin 1 was bound by Ser342 and Arg288 of the LBD via hydrogen bonds, especially to the carboxyl group of the amorfrutins. Disruption of these interactions by methylating the carboxyl

group in amorfrutin 5 weakened the binding to PPARγ by a factor of 40 (**Figure 9**). The structure also revealed that the ortho-phenyl and meta-isoprenoyl residues of amorfrutin 1 have extensive van der Waals contacts with the LBD, thus explaining the high binding affinity. The structure clearly described the amorfrutins as a new class of SPPARγMs.

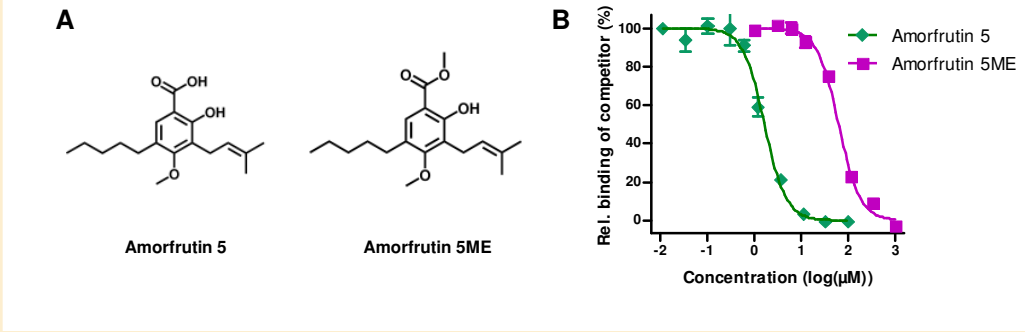

Figure 9. Effect of esterification of amorfrutins acidic head group. **(A)** Structure of amorfrutin 5 and its methylester (ME) derivative. **(B)** Binding on PPARγ in a competitive TR-FRET assay. Esterification increased the binding constant from 590nM to 23µM. Data are expressed as mean ± s.d. (n=3).

3.1.2 Amorfrutins partially recruit transcriptional cofactors to PPARγ

It is a well accepted model that binding of different ligands induce specific conformational changes in the LBD and AF2-domain of PPARs, and that this consequently leads to compound-specific interactions of the nuclear receptor with different sets of transcriptional cofactors, and further to different effects on gene expression (*74, 75*). In an *in vitro* cofactor recruitment assay amorfrutins and the other partial ligands nTZDpa (*210*) and telmisartan (*211*) only partially recruited the coactivators TRAP220/DRIP-2, PGC1α (PPARγ coactivator 1α), PRIP/RAP250 and CBP (CREB binding protein) relative to the full PPARγ agonists rosiglitazone and pioglitazone (**Figure 10 and table S2**). Compared to rosiglitazone, binding of amorfrutins led to reduced release of the transcriptional corepressor NCOR2 (nuclear receptor corepressor 2). The corresponding EC50 values were in the nanomolar or low-micromolar range. Intriguingly, although the

binding affinities are similar for all four amorfrutins, they exhibited distinct cofactor recruitment profiles, e.g. with an EC50 range from 0.1 to 77 µM with corresponding efficacy ranging from 6 to 24% in case of CBP recruitment. Thus, small variations in the ligand structure more likely affect the cofactor recruitment profile than the binding affinity. These experiments indicate that amorfrutins are SPPARγMs - PPARγ ligands with reduced modulation of receptor agonism.

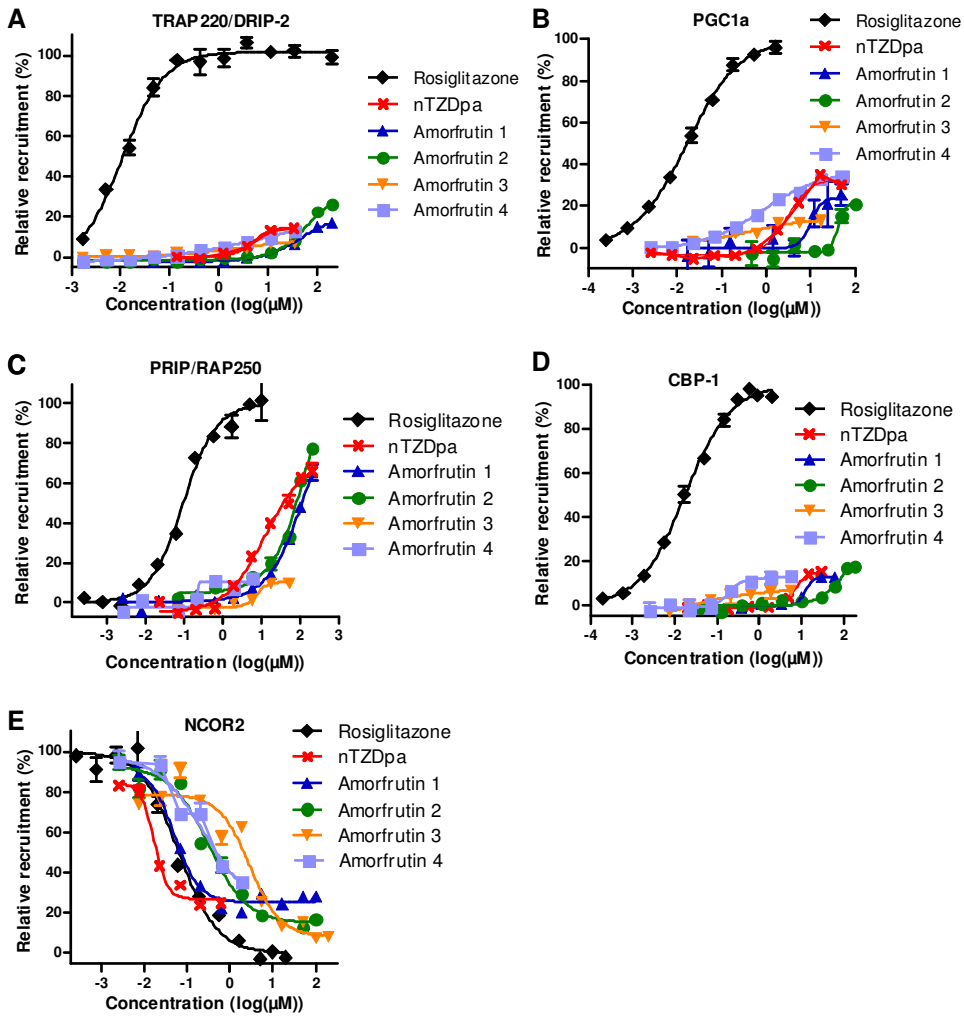

Figure 10. Recruitment of various cofactor peptides to PPARγ-LBD that is bound to different compounds. Peptides are derived from coactivators **(A)** TRAP220/DRIP-2, **(B)** PGC1α, **(C)** PRIP/RAP250, **(D)** CBP-1, or **(E)** corepressor NCOR2. Data are expressed as mean ± s.d. (n=3).

3.1.3 Amorfrutins partially activate PPARγ in cell culture

Cell-based transactivation of PPARγ was carried out using a reporter gene assay, revealing that amorfrutins are partial PPARγ agonists with activation values of 15 to 39 % compared to rosiglitazone. The EC50 values were 458 nM, 1.2 µM, 4.5 µM and 979 nM for amorfrutin 1, 2, 3 and 4, respectively (**Figure 11 and table 1**). Since the detection of only slightly activating ligands is hindered by low signal intensities, we additionally measured PPARγ activation in presence of non-saturating concentrations of rosiglitazone (**Figure S2**). This experimental modification verified the partial PPARγ agonism of the amorfrutins.

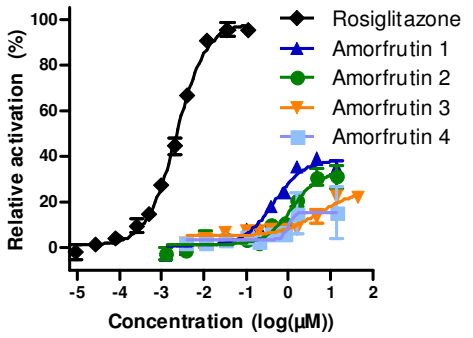

Figure 11. Cellular activation of PPARγ determined in a reporter gene assay. Data are expressed as mean ± s.d. (n=3).

3.2 From tube to bench: Effects of amorfrutins in target cells

3.2.1 Amorfrutins induce expression of PPARγ targets in adipocytes

Nuclear receptors such as PPARγ regulate the expression of hundreds or thousands of genes involved in metabolism. Subsequent to the *in vitro* binding and transactivation experiments, the amorfrutins were investigated in target cells of metabolic diseases. Therefor, differentiated 3T3-L1 mouse adipocytes were incubated for 24 h with 20 µM of each amorfrutin and gene expression was analyzed by quantitative real-time PCR (qPCR). The amorfrutins significantly upregulated classical PPARγ target genes such as the fatty acid binding protein 4 (Fabp4), the glucose transporter 4 (glut4, Slc2a4) and the liver x receptor alpha (lxra, Nr1h3). Consistent with the concept of partial agonism, the upregulation of

gene expression was reduced for amorfrutins compared to the full agonist rosiglitazone (**Figure 12**).

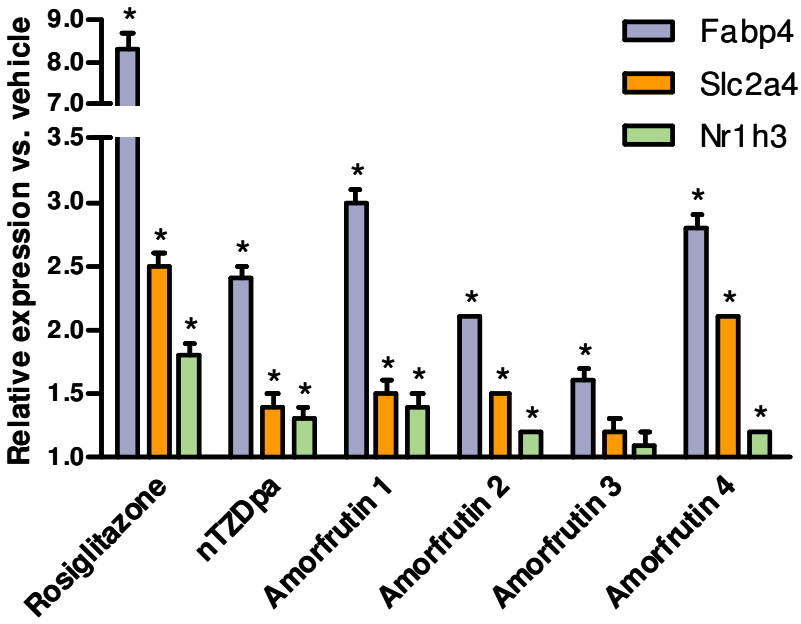

Figure 12. Gene expression analysis of compound-treated 3T3-L1 adipocytes determined by qPCR. Data are expressed as mean ± s.e.m. (n=4). *, P≤0.05 vs. vehicle.

3.2.2 PPARγ knockdown confirms selectivity of amorfrutins

To verify the supposed mechanism of gene expression modulation via PPARγ activation, specificity of compound effects was investigated in siRNA-mediated PPARγ-knockdown in human primary adipocytes. A protocol for chemically induced siRNA-transfection of primary adipocytes was established, which was not reported so far. The PPARγ knockdown efficiency reached 82% on transcript level compared to unspecific negative siRNA (**Figure 13A**). In presence of negative siRNA amorfrutin 1 and 2 activated expression of HSD11B1, LPL, CD36 and PLTP. Knockdown of PPARγ significantly reduced or abolished the amorfrutin-induced gene expression modulation, verifying the specificity of PPARγ activation by these natural products (**Figure 13B**).

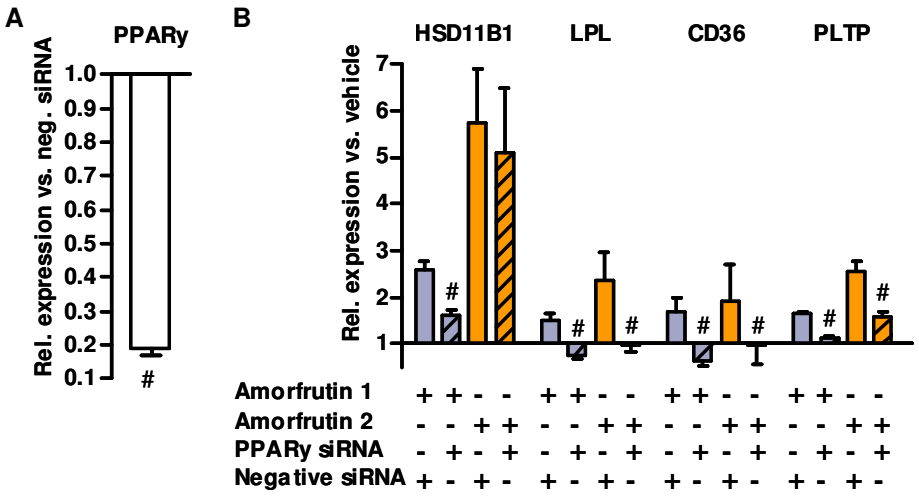

Figure 13. Effects of RNA interference with PPARγ-siRNA **(A)** on PPARγ gene expression and **(B)** on amorfrutin-mediated effects in human primary adipocytes. Data are expressed as mean ± s.e.m. (n=4). #, P≤0.05 vs. negative siRNA.

3.2.3 Amorfrutins regulate metabolism and immunity in adipocytes

Genome-wide gene expression analyses in primary human adipocytes were performed on Illumina Beadchip arrays. Real-time qPCR was used to validate the array experiments. Therefor, four genes were randomly chosen from the array data and correlated to qPCR-derived expression values. The bead array data were in correlation with the qPCR data, with Pearson correlation coefficients of 0.79, 0.78, 0.57 and 0.51 for ADIPOQ, NR1H3, HSD11B1 and FABP4, respectively (**Figure S3**). This led to an average Pearson correlation coefficient of 0.66 for all genes tested by qPCR, indicating an adequate congruence between both techniques.

Whole-genome gene expression analyses of human primary adipocytes treated with amorfrutins, the full PPARγ agonists rosiglitazone and pioglitazone, the selective PPARγ modulators nTZDpa (*210*) and telmisartan (*211*), or vehicle only, revealed striking expression patterns. Rosiglitazone and nTZDpa affected the

expression of 309 and 177 genes, respectively, whereas amorfrutin 1 and amorfrutin 2 regulated 137 and 120 genes, respectively (**Figure 14**).

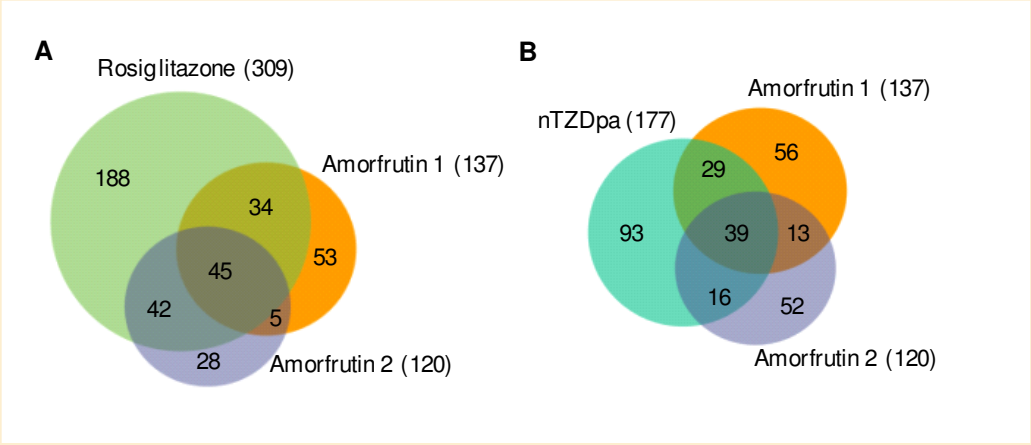

Figure 14. Venn diagrams of differentially expressed genes after treatment of human adipocytes with different compounds. **(A)** Comparison of amorfrutins with rosiglitazone. **(B)** Comparison of amorfrutins with nTZDpa. Numbers in circles indicate up- and down-regulated genes, numbers in parentheses represent a total of regulated genes for that compound.

The most highly significant up- and down-regulated genes after treatment with amorfrutin 1 and 2 are shown in **table 2**. Classical genes involved in lipid metabolism and insulin signalling were regulated upon treatment with amorfrutins. For instance, amorfrutin 1 induced the expression of phosphodiesterase 3B (PDE3B), which was shown to be down-regulated in the adipose tissue of rodent models of type 2 diabetes (*212, 213*). Furthermore, amorfrutin 1 increased the gene expressions of adiponectin (ADIPOQ) and lipoprotein lipase (LPL). In previous studies adiponectin was found to reduce body adiposity by affecting the mRNA expression of uncoupling proteins (UCPs) in adipose tissue and skeletal muscle (*214*). The lipoprotein lipase catalyzes the hydrolysis of triglycerides of circulating lipoproteins and was thought to mediate the hypotriglyceridemic effects of fibrates and thiazolidinediones (*215*). Amorfrutin 2 up-regulated genes such as the hormone-sensitive lipase (LIPE), the fatty acid binding protein 5 (FABP5) and the uncoupling protein 2 (UCP2), which

play important roles in the release and the uptake of fatty acids and thermogenesis, respectively.

Table 2. The 12 most highly significant up- and down-regulated genes after treatment of human adipocytes with amorfrutin 1 and 2. Fold change means gene expression relative to vehicle-treated cells. Data are expressed as mean (n=4).

Amorfrutin 1		Amorfrutin 2	
Gene	Fold Change	Gene	Fold Change
HLA-DMA	2.5	PPP1R1A	4.9
AP3B2	2.4	AP3B2	2.7
SLC19A3	2.3	MLSTD1	2.5
PDE3B	2.1	FABP5	2.4
KIAA1881	2.1	SHROOM4	2.4
MRAP	2.0	HLA-DMA	2.3
CSAD	2.0	UCP2	2.3
MLSTD1	2.0	LIPE	2.2
AOC3	2.0	CSAD	2.2
OSGIN1	1.9	PLIN4	2.2
ADIPOQ	1.8	MTHFD1	2.2
LPL	1.8	MESP1	2.1
PIK3IP1	0.7	PDE1A	0.7
SULF1	0.7	SOD2	0.7
C20ORF111	0.7	MXRA5	0.7
C5ORF23	0.7	OSAP	0.7
C20ORF82	0.7	KLF2	0.7
OMD	0.7	C11ORF2	0.7
TNFSF10	0.7	PENK	0.6
FLRT2	0.6	CCBP2	0.6
CABC1	0.6	PPP1R3C	0.6
PPP1R3C	0.5	SERPINA5	0.6
SERPINA5	0.5	MLPH	0.6
CYP4F22	0.3	CYP4F22	0.5

Hierarchical clustering of the compounds and k-means clustering of differentially expressed genes were carried out to systematically sort expression data. Then, gene clusters were checked for functional annotation enrichment using the Database for Annotation, Visualization and Integrated Discovery (DAVID) (**Figure 15**), resulting in six clusters of differentially regulated genes. The first cluster contained genes that were up-regulated by all PPARγ ligands and comprised genes involved in PPAR signalling including fatty acid metabolism (e.g. adiponectin), carbohydrate metabolism (e.g. pyruvate dehydrogenase kinase 4) and lipid synthesis (e.g. aquaporin 7). Almost all genes in the second cluster

were activated only by the TZD pioglitazone and were predominantly involved in protein biosynthesis and carboxylic and amino acid transport. Genes in the third cluster had functions in lipid and fatty acid metabolism and were mainly up-regulated by rosiglitazone. These genes were only slightly activated by amorfrutins and nTZDpa and encompassed the fatty acid binding protein 4 (FABP4) and the cortisone-regenerating enzyme hydroxysteroid 11-beta dehydrogenase 1 (HSD11B1) that is correlated to visceral adiposity (*216*). The 4th cluster contained genes with the most diverse regulation among the PPARγ ligands tested and comprised genes strongly involved in the secretion of molecules, which verified the function of adipose tissue as an endocrine organ (*31*). Additionally, genes of the 4th cluster play important roles in the metabolism of fatty acids, e.g. the gene lipin 1 is mainly involved in the oxidation of free fatty acids, which is controlled by the PPARα isotype (*217*). In this study lipin 1 was only upregulated by the dual PPARα/γ ligand telmisartan (*218*) and amorfrutin 4 that could be shown to bind PPARα as well (**Figure 8 and table 1**). Genes in the 5th cluster were differentially down-regulated by these compounds and had functions not only in the secretion but also in the inhibition of proteases and developmental processes. Remarkably, the 6th cluster contained genes that were mainly down-regulated by the full agonists rosiglitazone and pioglitazone. These genes are linked to ion homeostasis and inflammatory processes besides secretion and protease inhibition. Recently, it was reported that TZDs can cause edema due to an increased plasma volume (*219*). This could be a result of altered ion homeostasis, which was an enriched term in the 6th gene cluster. For instance, expression of the sodium exchanger SLC9A9 was specifically down-regulated after treatment with pioglitazone (**Figure 15**).

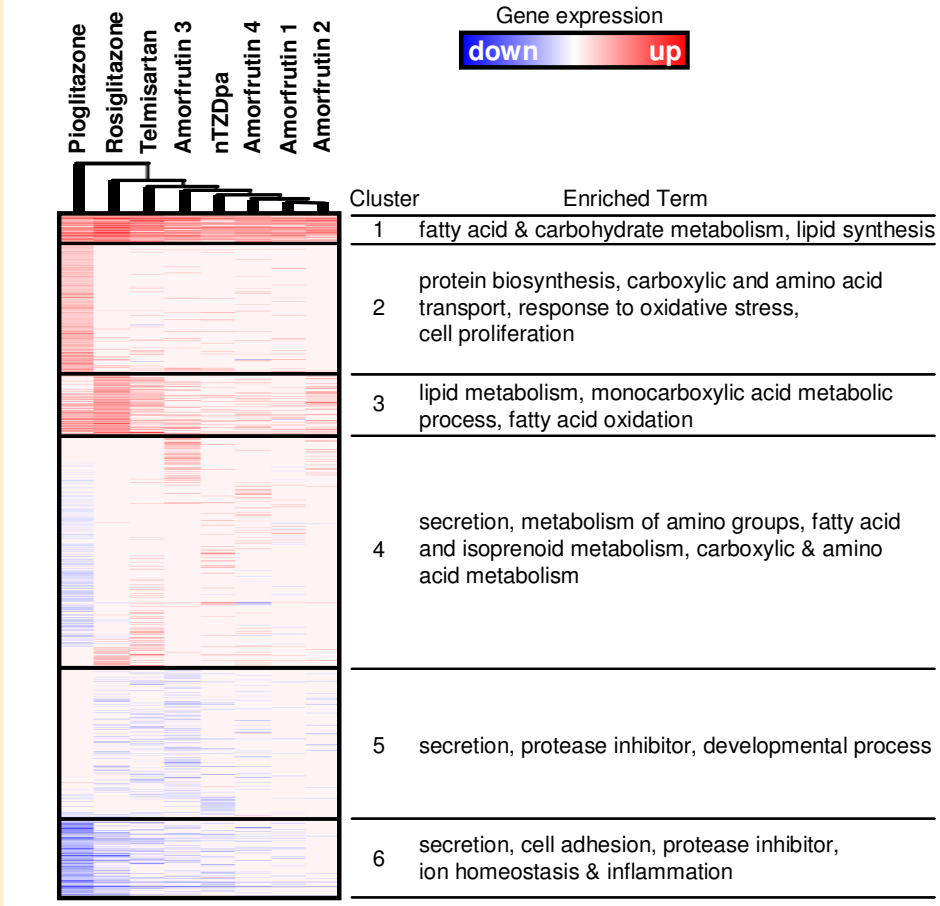

Figure 15. Heatmap of differentially expressed genes after treatment of human adipocytes with different compounds. Illumina BeadChip data were filtered for significance and clustered with the k-means clustering algorithm. Enrichmend of clustered genes were annotated using DAVID 2008. Genes are presented as either up-regulated (red) or down-regulated (blue).

In conclusion, the full and partial synthetic PPARγ agonists as well as the amorfrutins exhibited differential effects on gene expression in human adipocytes. The hierarchical clustering of the small molecules revealed similarity between the amorfrutin expression profiles. Nevertheless, gene expression profiles of the amorfrutins were partially distinct, indicating that small changes in ligand structure can considerably affect PPARγ activation patterns.

To circumvent the low sensitivity of singular gene enrichment analyses, Gene Set Enrichment Analysis (GSEA) was performed on the adipocytes expression data. The gene sets comprised canonical pathways and data from chemical and genetic perturbation experiments. Gene sets that were significantly changed (FDR≤0.25) by at least one compound are presented in **Figure S4**. Gene sets were displayed as either up-regulated (red) or down-regulated (blue) in the compound expression profiles. In contrast to the list of single genes (**Figure 15**), the compounds showed an overall correlation in the enrichment of gene sets, indicating a common mechanism of action, namely PPARγ agonism.

As expected for PPARγ agonists, the most enriched pathways for amorfrutin 1 and 2 include PPAR signalling, cholesterol biosynthesis, fatty acid elongation and fatty acid oxidation, which all were strongly upregulated (**Figure 16**).

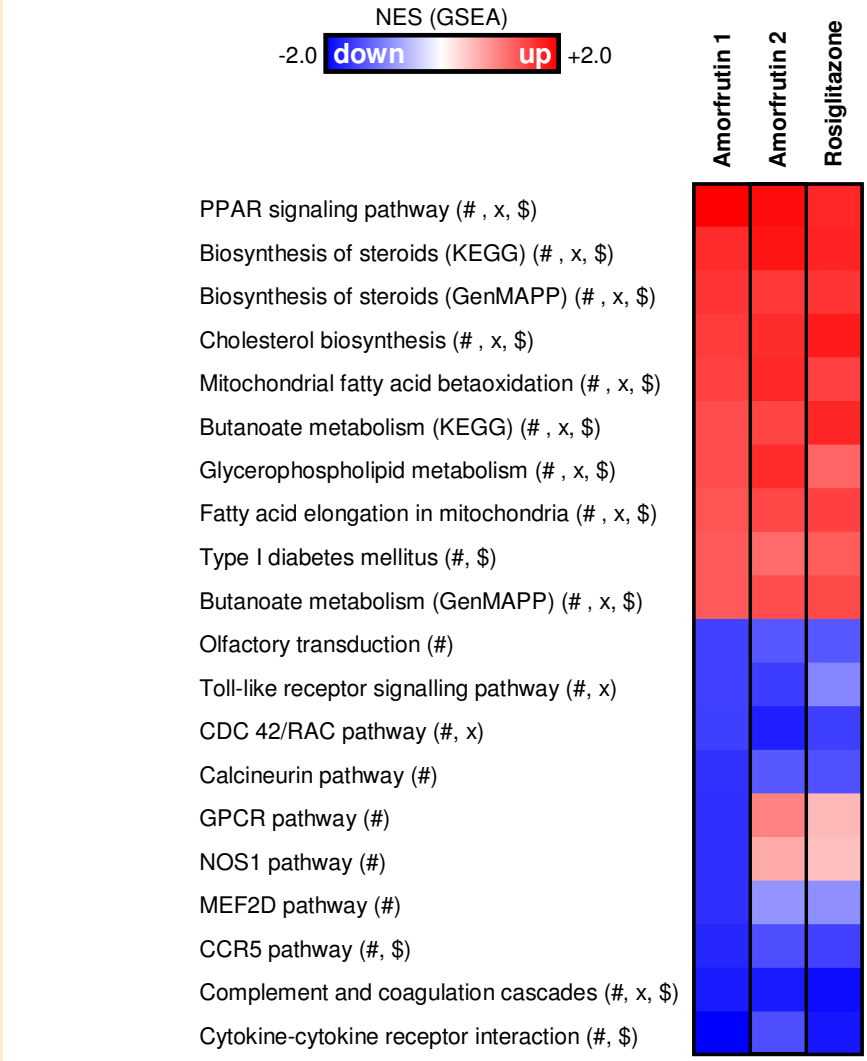

Figure 16. Enriched pathways after treatment of human primary adipocytes using GSEA. Ten most highly significant pathways for amorfrutin 1 and corresponding normalized enrichment scores (NES) are shown. #, x, $, $P \leq 0.05$ for amorfrutin 1, amorfrutin 2 or rosiglitazone.

Subsequently, we filtered out gene sets from the collection that were linked to either fatty acid metabolism or inflammation. As depicted in **Figure 17A**, fatty acid metabolism-related gene sets were significantly enriched in the gene expression data of all PPARγ agonists described in this study. The degree of enrichment, as described as normalized enrichment score (NES), was similar for the amorfrutins when compared to the well-known PPARγ ligands. Additionally,

pro-inflammatory gene sets were significantly under-represented in the expression profiles of the investigated PPARγ ligands (**Figure 17B and table S3**). This underscores the role of PPARγ in the inhibition of inflammatory responses (*220, 221*), and indicates anti-inflammatory properties of the amorfrutins, which should be investigated in further studies.

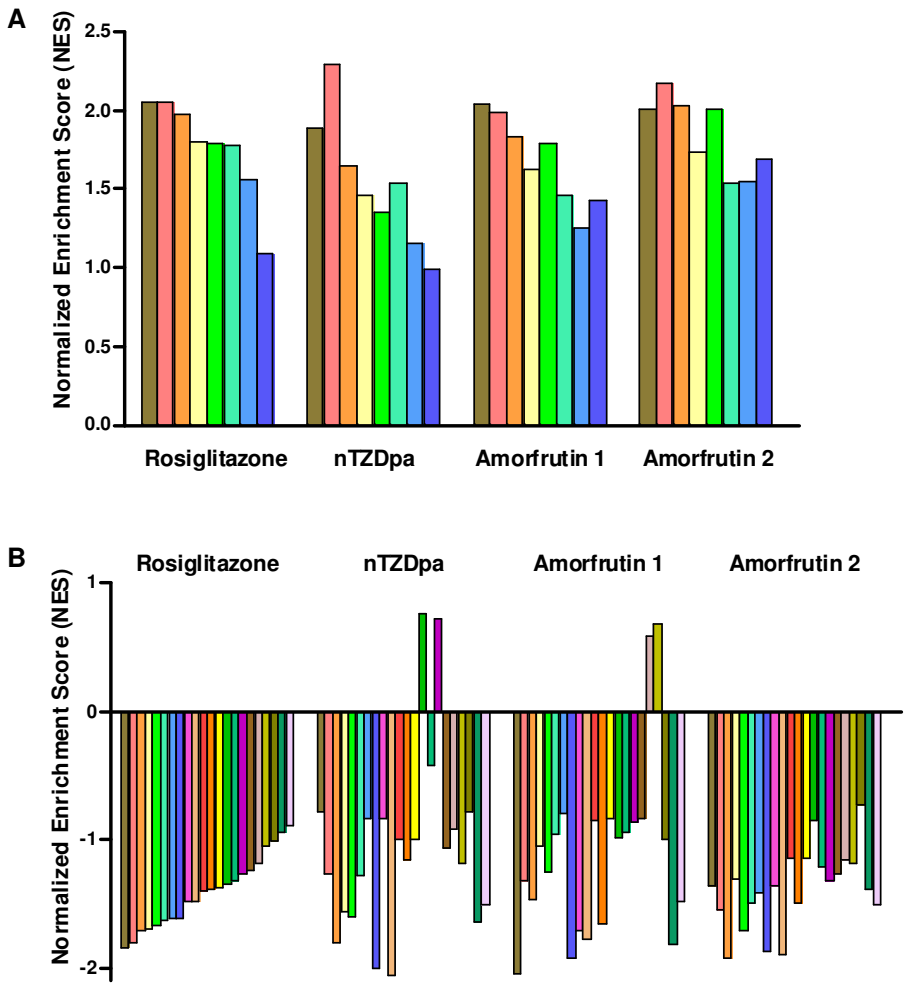

Figure 17. Effects on gene expression related to fatty acid metabolism **(A)** and inflammatory pathways **(B)**. Normalized enrichment scores for each gene set were calculated with compound-specific expression profiles by GSEA. Gene sets were filtered with FDR≤0.25 for at least one compound. For full description of corresponding gene set names see Supplementary table S3.

The Connectivity Map tool (*204*) can be used to connect small molecules sharing a mechanism of action. Gene expression data were validated by comparing with implemented data obtained from other research groups. Connection of the rosiglitazone profile in human adipocytes revealed similarities to other rosiglitazone data obtained in PC3 or HL60 cells. Four different rosiglitazone experiments appeared under the most highly significant 13 connections to small molecules, including the most significant experiment (**table S4**). Additional seven connections revealed similarity to the other TZDs pioglitazone and troglitazone and the endogenous PPARγ agonist 15-delta prostaglandin J2. This indicates that in spite of comparing to other human cell lines as adipocytes, our rosiglitazone data as an example of the signatures described in this study were in accordance with experiments done in other labs.

Furthermore, applying the Connectivity Map tool to our amorfrutin 1 gene expression profile unravelled the broad mechanism of action. A strong anticorrelation to the phosphoinositide 3-kinase (PI3K) inhibitor LY-294002 ($p<10^{-5}$, **table 3**) could be observed. Activation of PI3K is an early event in insulin signalling and it has been shown that insulin sensitizers as TZDs increase PI3K activity in adipocytes (*222*). Besides LY-294002, the mammalian target of rapamycin (mTOR) inhibitor sirolimus was also negatively connected to the amorfrutin 1 profile ($p<10^{-5}$). mTOR acting downstream of PI3K was recently shown to counteract PPARγ effects (*223*). Experiments with the insulin sensitizer troglitazone revealed positive connection with the amorfrutin 1 gene expression signature ($p<10^{-3}$). Enhancing insulin sensitivity could also be verified by collapsing the Connectivity Map implemented small molecule data to Anatomical Therapeutic Chemical (ATC) classification (**table 3**). The code A10BG (blood glucose lowering drugs, thiazolidinediones) includes different PPARγ ligands for the treatment of diabetes and showed the most significant connection to the amorfrutin data ($p<10^{-5}$). These results again revealed that amorfrutins are acting through PPARγ modulation and had high potential for application as insulin sensitizers.

Table 3. Connectivity of the amorfrutin 1 gene expression profile in human adipocytes with other small molecules using the Connectivity Map. **(Top)** The three most significant connections with small molecules from different experiments and cell lines. **(Bottom)** Best connection with small molecules sharing the same Anatomical Therapeutic Chemical (ATC) classification.

rank	cmap name	mean	n	enrichment	p	specificity	percent non-null
1	LY-294002	-0.538	61	-0.538	0.00000	0.0245	85
2	sirolimus	-0.505	44	-0.447	0.00000	0.1507	79
3	troglitazone	0.269	16	0.515	0.00018	0.0000	50

rank	atc code	mean	n	enrichment	p	specificity	percent non-null
1	A10BG	0.310	41	0.443	0.00000	0.0000	56

3.2.4 Amorfrutins are selective PPARγ modulators (SPPARγMs)

Since treatment with approved, strongly activating PPARγ agonists is associated with unwanted side effects, ligands with selective modulation profiles are required (*74, 104, 133, 136*). Hypergeometrical testing was applied to the lists of regulated genes to further compare the expression signatures of amorfrutins with those of full and partial PPARγ agonists. This analysis revealed an overlap with an enrichment factor of 26 for amorfrutin 1/rosiglitazone and an overlap with an enrichment factor of 67 for amorfrutin 1/nTZDpa relative to expectation by chance. Consequently, a first assessment of the expression data showed that the gene signatures of the natural products were more closely related to those of SPPARγMs than to the profiles of full PPARγ agonists.

To include the intensities of gene expression changes in gene signature comparison, principal component analyses (PCA) were performed. Gene expression profiles of amorfrutin 1 and 2 correlated in the first two principal components (~70% of the data variability) more efficiently with the SPPARγMs nTZDpa and telmisartan than with the full PPARγ agonists (**Figure 18**). The results were similar with the other amorfrutins described in this study (data not shown).

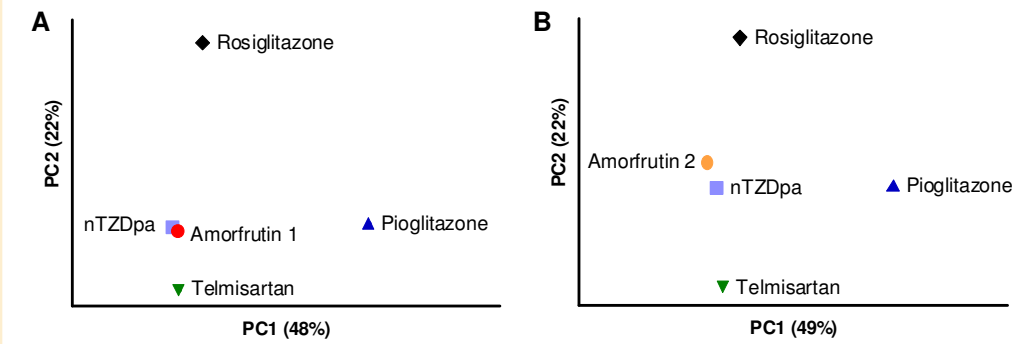

Figure 18. Principal Component Analysis (PCA) of differentially expressed genes after treatment with different PPARγ ligands, including the full agonists rosiglitazone and pioglitazone and the selective PPARγ modulators nTZDpa and telmisartan. The first two principal components (PC1, PC2) were plotted on the axis. Number in parentheses represent the variability of that principal component. The plots show 70% of the data variability **(A)** for amorfrutin 1 and 71% of the data variability **(B)** for amorfrutin 2.

distance matrix (GDM) analysis was additionally performed to compare the gene expression profiles (**Figure 19**). As expected, the amorfrutin gene expression profiles showed similarities among each other, and were closer to the SPPARγMs than to the TZDs. These gene expression analyses clearly showed that amorfrutins are a novel class of selective PPARγ modulators (SPPARγMs).

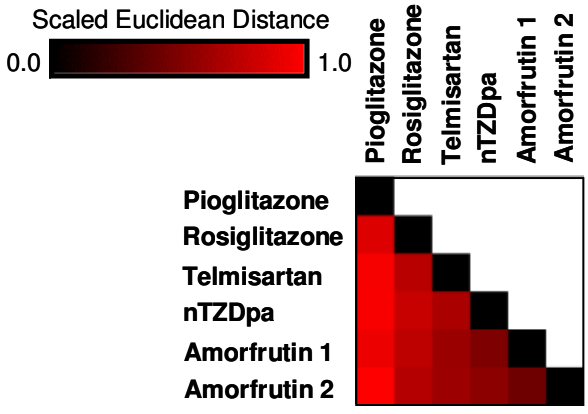

Figure 19. Gene distance matrix of gene expression profiles in human adipocytes. Squares show the distance of two compounds in Euclidean space, ranging from exactly the same profile (black) to completely different (red).

3.2.5 Amorfrutins show promising ADMET properties

Successful treatment of mice requires good ADMET (Absorption, Distribution, Metabolism, Excretion, Toxicity) parameters. To exclude cytotoxic effects of the amorfrutins the WST-1 assay was applied in HepG2 cells with different concentrations of amorfrutins. The amorfrutins revealed no effects on cell viability up to 50 µM compound concentration (**Figure S5**). Similar results were observed in other cell lines including adipocytes (data not shown).

Analyses in conjunction with the Lead Discovery Center (Dortmund, Germany) revealed that, *first*, the amorfrutins had a highly aqueous solubility, *second*, the amorfrutins showed good absorption and permeability in the PAMPA (parallel artificial membrane permeability assay) as well as in the Caco-2 cell model, and *third*, *in vitro* metabolic stability assays in liver microsomes indicated vulnerability for oxidation and glucuronidation under metabolic phase I and II conditions, respectively. Non-metabolized amorfrutin 1 was identified as the main form in murine plasma (66% abundance). Glucuronidated (25%) and oxidized (8%) metabolites were further detected. In summary, the amorfrutins had promising ADMET properties that accounted for further *in vivo* studies.

3.3 From bench to mouse: Animal studies

The anti-diabetic and anti-obesity potential of the amorfrutin class were validated by applying three different study designs: *first*, the prevention of diet-induced insulin resistance and obesity in C57BL/6 mice (37 mg/kg/d amorfrutin over 15 weeks), *second*, the therapy of distinctive insulin resistance and obesity in diet-induced-obesity (DIO) mice (100 mg/kg/d amorfrutin over 3 weeks), and *third*, the therapy of type 2 diabetes in leptin receptor deficient db/db mice (100 mg/kg/d amorfrutin over 3 weeks). Amorfrutin 1 was incorporated into the diet. The PPARγ agonist rosiglitazone (4 mg/kg/d), which is widely used for anti-diabetic treatment, was used as positive control. The same diet without compound incorporation was used as vehicle control.

3.3.1 Amorfrutin 1 has a safe profile on liver toxicity in mice

Liver toxicity indicating plasma alanine transaminase (ALT) assays showed significantly reduced ALT levels in high fat diet (HFD)-fed mice treated with amorfrutin 1 compared to HFD mice treated with vehicle control or rosiglitazone (**Figure S6**). Similarly, microarray-based gene expression analysis revealed no toxicity after amorfrutin treatment (**table S5**).

3.3.2 Amorfrutin 1 reduces insulin resistance, dyslipidemia and obesity in DIO mice

High-fat diet feeding of mice results in diet-induced obesity (DIO) and insulin resistance. Therefor, lean C57BL/6 mice were firstly fed for 12 weeks with high-fat diet (HFD). Subsequently, the mice were treated for 23 days with 100 mg/kg/d synthetic amorfrutin 1, 4 mg/kg/d rosiglitazone or vehicle control. Amorfrutin 1 considerably reduced plasma glucose, insulin, triglyceride and free fatty acid levels under fasted and fed conditions (**Figure 20 and tables S6 to S7**). Both amorfrutin 1 and rosiglitazone showed equal reduction of insulin resistance as assessed by homeostatic modelling (**Figure 20E**).

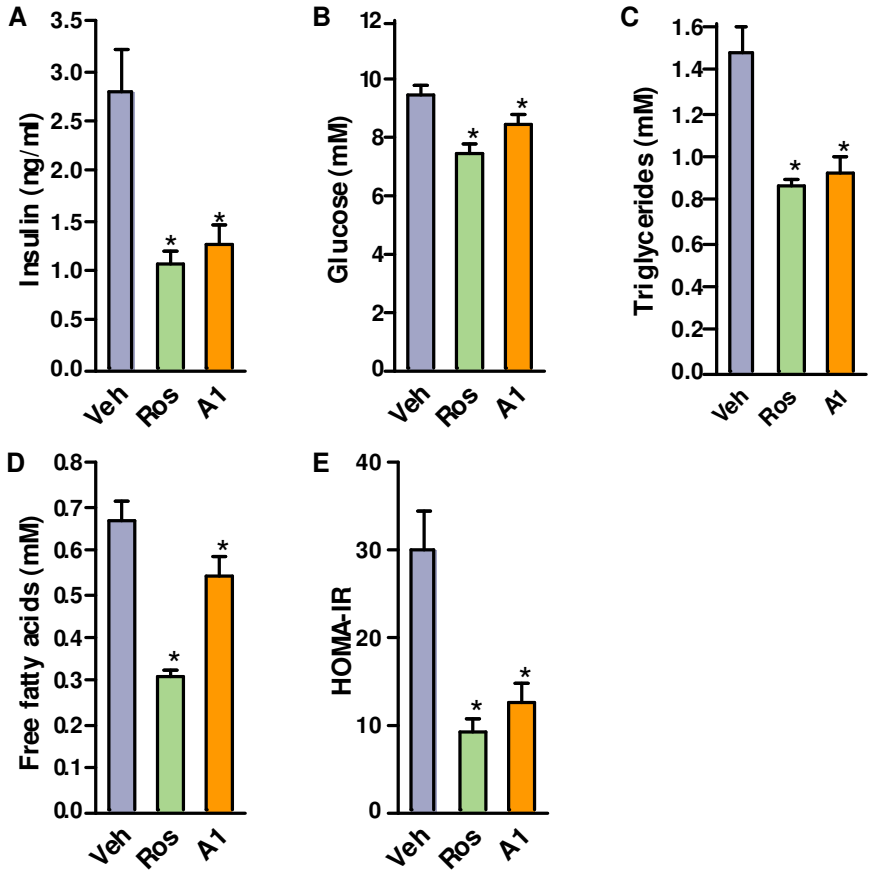

Figure 20. Effects of treatment over 17 days on plasma parameters in fasted DIO mice. **(A)** Insulin, **(B)** glucose, **(C)** triglycerides, **(D)** free fatty acids. **(E)** Insulin resistance was determined by homeostatic model assessment (HOMA). Data are expressed as mean ± s.e.m. (n=13). Veh, vehicle; Ros, rosiglitazone; A1, amorfrutin 1. *, P≤0.05 vs. vehicle.

Amorfrutin 1 considerably enhanced glucose tolerance (19% decrease in glucose area under the curve (AUC), 42% decrease in insulin AUC vs. vehicle) and insulin sensitivity (14% increase in glucose inverse area under the curve (AUC_i) vs. vehicle) during oral glucose tolerance tests (OGTT, **Figure 21A**) and intraperitoneal insulin sensitivity tests (IPIST, **Figure 21B**). In summary, amorfrutin 1 treatment of obese mice showed anti-diabetic efficacy similar to rosiglitazone.

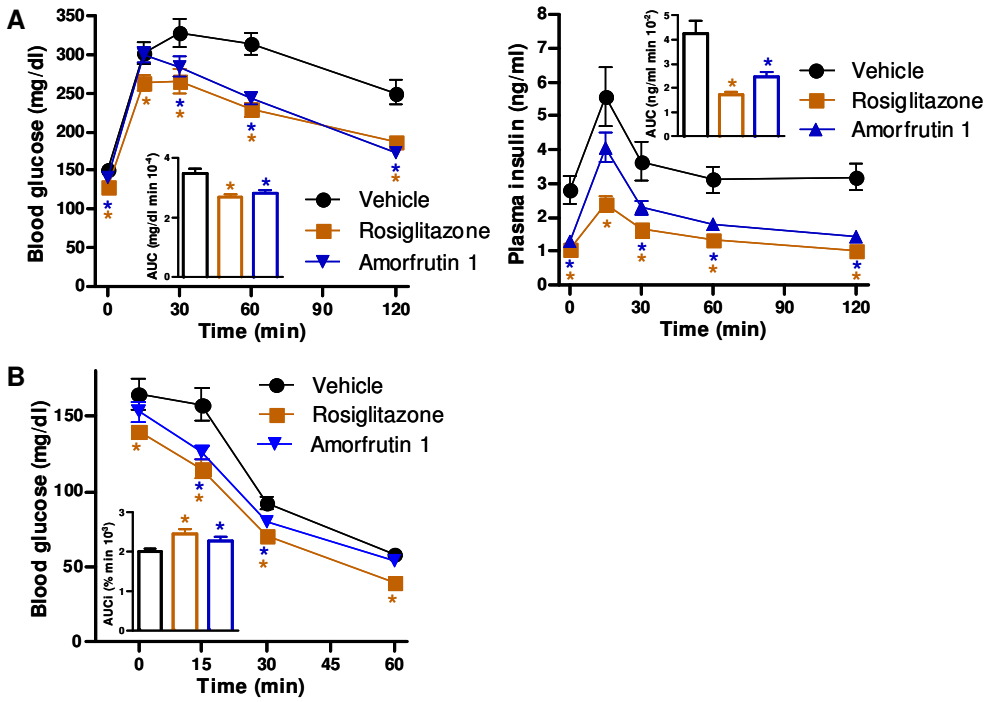

Figure 21. Effects on insulin resistance and glucose intolerance in DIO mice (n=13). **(A)** Glucose and insulin concentrations during oral glucose tolerance test (OGTT) treated with indicated compounds. Inlet, area under the curve (AUC). **(B)** Glucose level during intraperitoneal insulin sensitivity test (IPIST). Inlet, inverse area under the curve (AUC_i). Data are expressed as mean ± s.e.m. *, P≤0.05 vs. vehicle.

Strikingly, amorfrutin 1 clearly reduced the body weight in DIO mice by ~10%. Paradoxically, weight reduction was accompanied by an increase in food intake (**Figure 22**). In contrast, rosiglitazone treatment led to a raise in feeding without any weight change in this study. Increase of appetite has already been reported for several PPARγ ligands and is thought to attribute to the TZD-induced weight gain observed in many studies (*224*). However, amorfrutins probably regulates whole-body energy balance different to rosiglitazone. Importantly, weight loss upon amorfrutin treatment was not due to toxic effects that had been excluded by assaying plasma ALT concentrations and by liver gene expression analyses (**Figure S6 and table S5**).

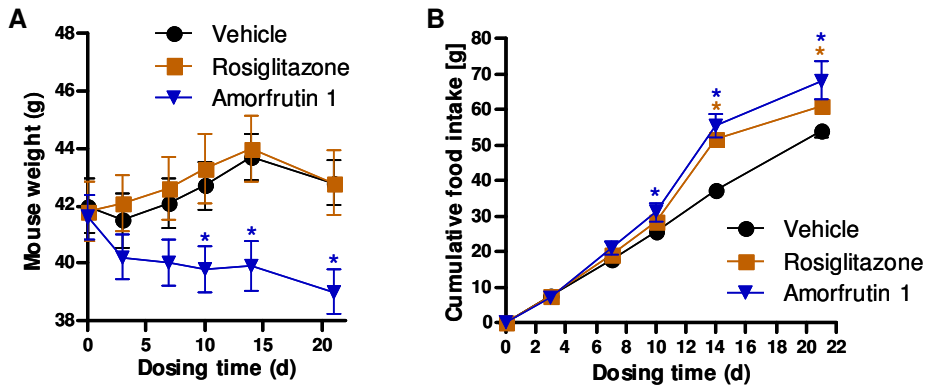

Figure 22. Effect of treatment on body weight **(A)** and food intake **(B)** in DIO mice (n=13). Data are expressed as mean ± s.e.m. *, P≤0.05 vs. vehicle.

3.3.3 Amorfrutin 1 prevents development of insulin resistance and dyslipidemia in HFD-fed mice

We further investigated the potential of amorfrutins to prevent early development of insulin resistance. C57BL/6 mice were fed either a low-fat diet (LFD) or a high-fat diet (HFD) in absence or presence of rosiglitazone (HFD+R, 4 mg/kg/d) or low-dose amorfrutin 1 (HFD+A1, 37 mg/kg/d), respectively, for 15 weeks. Amorfrutin 1 reduced the HFD-induced weight gain by 22% without reducing food intake (**Figure S7**), and significantly improved glucose tolerance (22% decrease in insulin AUC) and insulin sensitivity (21% increase in glucose AUC_i) (**Figure 23**).

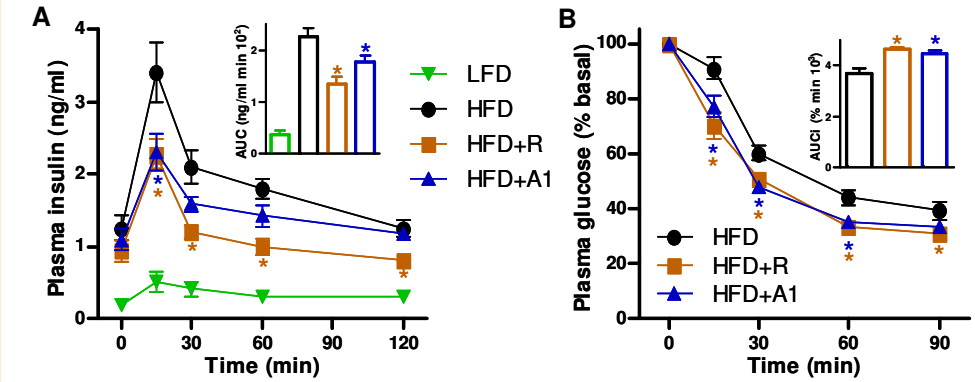

Figure 23. Effects of low-fat diet (LFD) or high-fat diet (HFD) without or with rosiglitazone (HFD+R) or amorfrutin 1 (HFD+A1) on glucose tolerance and insulin sensitivity in C57BL/6 mice (n=8-12). **(A)** Insulin concentrations during oral glucose tolerance test (OGTT) after 10 weeks of dosing. Inlet, area under the curve (AUC). **(B)** Glucose levels during intraperitoneal insulin sensitivity test (IPIST) after 13 weeks of dosing. Inlet, inverse area under the curve (AUC_i). Data are expressed as mean ± s.e.m. *, P≤0.05 vs. HFD.

Additionally, amorfrutin 1 substantially diminished the rise of plasma triglycerides, free fatty acids, insulin and glucose (**tables S8 to S9**). Besides, treatment with amorfrutin 1 led to increased liver glycogen content, which is a characteristic for anti-diabetic agents (**Figure 24A**) (*225*). Furthermore, amorfrutin 1 significantly reduced the increase of plasma concentrations of the

adipose derived hormone leptin (**Figure 24B**), which could have in part contributed to the improved metabolic profile observed. In summary, amorfrutin 1 partly prevented the diet-induced obesity, insulin resistance and dyslipidemia.

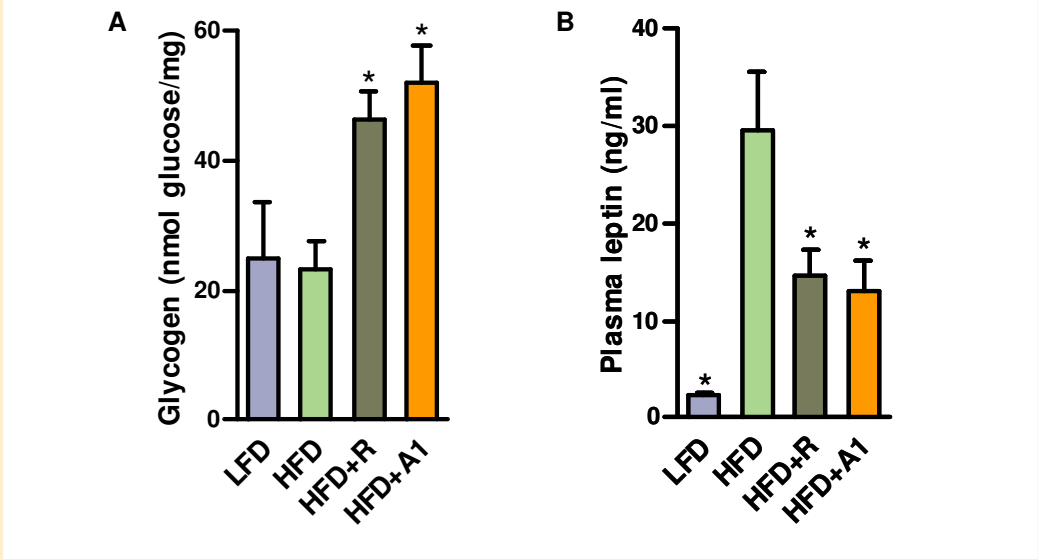

Figure 24. Effect of treatment over 15 weeks on **(A)** liver glycogen concentration (n=12) and **(B)** plasma leptin (n=9-12) in C57BL/6 mice. Data are expressed as mean ± s.e.m. *, P≤0.05 vs. HFD.

3.3.4 Amorfrutin 1 ameliorates insulin sensitivity and dyslipidemia in db/db mice

To figure out potential contributions of the leptin hormone and to validate the anti-diabetic effects in a model of severe type 2 diabetes, we also treated leptin receptor-deficient db/db mice with amorfrutin 1 (100 mg/kg/d), rosiglitazone (4 mg/kg/d) or vehicle for 3 weeks. In this model, rosiglitazone strongly increased the body weight by ~30% within 3 weeks, whereas amorfrutin 1 treatment had no significant effects on mouse body weight (**Figure 25**). Notably, in db/db mice amorfrutin 1 reduced plasma insulin concentrations more strongly than rosiglitazone (36% vs. 19% decrease after 24 days) (**Figure 26**). Amorfrutin 1 treatment decreased plasma concentrations of glucose, triglycerides and free fatty acids under fasted and fed conditions (**tables S10 to S11**). In conclusion,

amorfrutin 1 considerably prevented and ameliorated type 2 diabetes and dyslipidemia in three different mouse models.

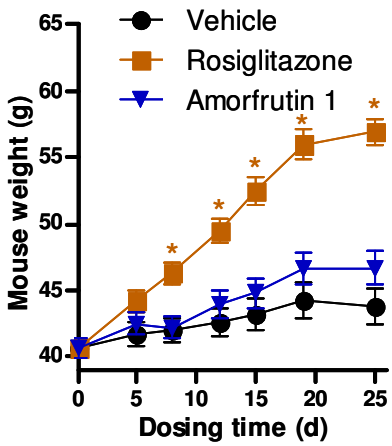

Figure 25. Effect of treatment over 3 weeks on body weight in db/db mice (n=13). Data are expressed as mean ± s.e.m. *, P≤0.05 vs. vehicle.

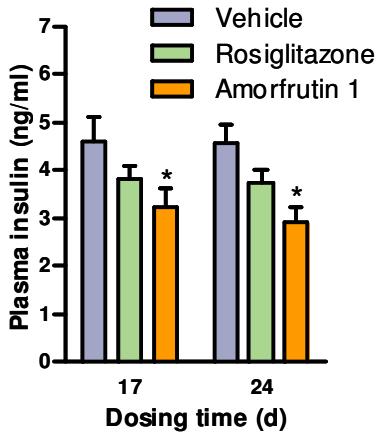

Figure 26. Effect of treatment on fasting plasma insulin level of diabetic db/db mice (n=7-12). Data are expressed as mean ± s.e.m. *, P≤0.05 vs. vehicle.

3.3.5 Amorfrutin 1 inhibits HFD-induced PPARγ phosphorylation

Recently, it was reported that the development of insulin resistance is associated with phosphorylation of PPARγ-Ser273, and that this phosphorylation can be inhibited by PPARγ ligands independently from PPARγ activation (*147*). Therefore, inhibition of Ser273-phosphorylation was proposed as a new strategy to increase specifically insulin sensitivity without activating the full range of PPARγ targets (see 1.3.1.3.). Indeed, treatment of HFD-fed mice with rosiglitazone inhibited the phosphorylation of PPARγ-Ser273 in vWAT. Moreover, treatment with the SPPARγM amorfrutin 1 led to similar reduction of phosphorylation (**Figure 27A**). Furthermore, decrease of PPARγ phosphorylation significantly correlated with improvement of insulin sensitivity (**Figure 27B**).

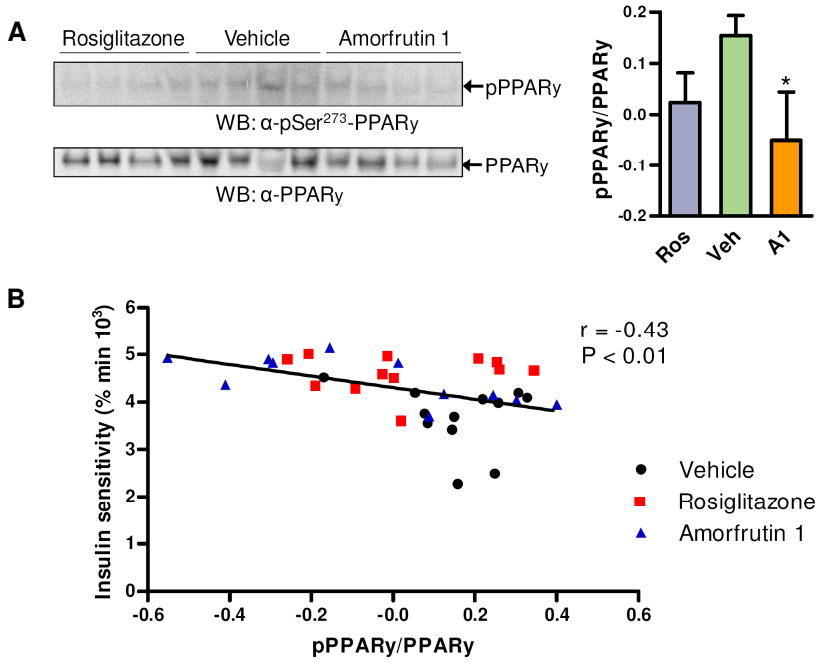

Figure 27. Correlation between inhibition of PPARγ phosphorylation and insulin sensitivity after treatment. **(A)** Phosphorylation of Ser273 PPARγ in visceral white adipose tissue (vWAT) of HFD-fed mice treated with rosiglitazone, amorfrutin 1 or vehicle for 15 weeks. The rate of PPARγ phosphorylation was normalized to total PPARγ protein using densitometric analyses. Data are expressed as mean ± s.e.m. (n=11-12). *, P≤0.05 vs. vehicle. **(B)** Correlation between insulin sensitivity measured in the insulin sensitivity test (expressed as AUC_i) and PPARγ phosphorylation. Pearson correlation coefficient and corresponding P value (two-tailed) are shown (n=35).

This experiment verifies the recent hypothesis that blocking of PPARγ phosphorylation is independent from transcriptional agonism, and that this inhibition but not PPARγ activity is linked to improved insulin sensitivity.

Choi et al. (*147*) further reported that inhibition of PPARγ phosphorylation resulted in specific transcription of 17 target genes. Indeed, 14 of them were significantly regulated upon treatment of mice amorfrutin 1 (**Figure 28**), consistent with the hypothesis that amorfrutins affect PPARγ-Ser273 phosphorylation.

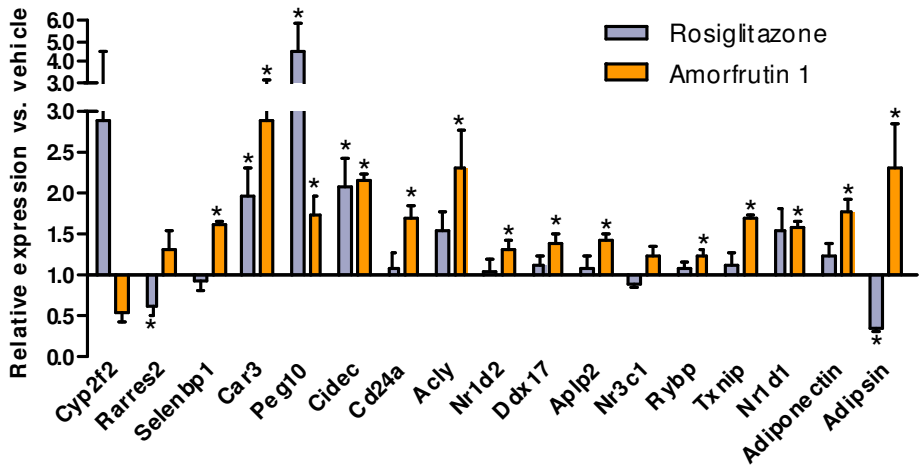

Figure 28. Expression of genes regulated by inhibition of PPARγ-Ser273 phosphorylation in white adipose tissue of DIO mice according to ref. (*147*). Gene expression of vehicle-treated mice is set to 1. Data are expressed as mean ± s.e.m. *, P≤0.05 vs. vehicle.

3.3.6 Amorfrutin 1 reduces detrimental deposit of lipids in various tissues

Accumulation of triglycerides and free fatty acids in non-adipose tissues contributes to lipotoxicity and tissue damage (*188, 226*). In addition to improvement of plasma lipid levels, amorfrutin 1 reduced the concentration of detrimental free fatty acids in the heart of db/db mice by 50% (**Figure 29A**), whereas rosiglitazone only had minor effects. Rosiglitazone further increased the triglyceride concentration in liver and pancreas, whereas amorfrutin 1 did not show lipogenic effects (**Figure 29B**). In stark contrast to rosiglitazone, amorfrutin 1 reduced HFD-induced accumulation of liver triglycerides by ~50% relative to untreated HFD control mice (**Figure 29C**).

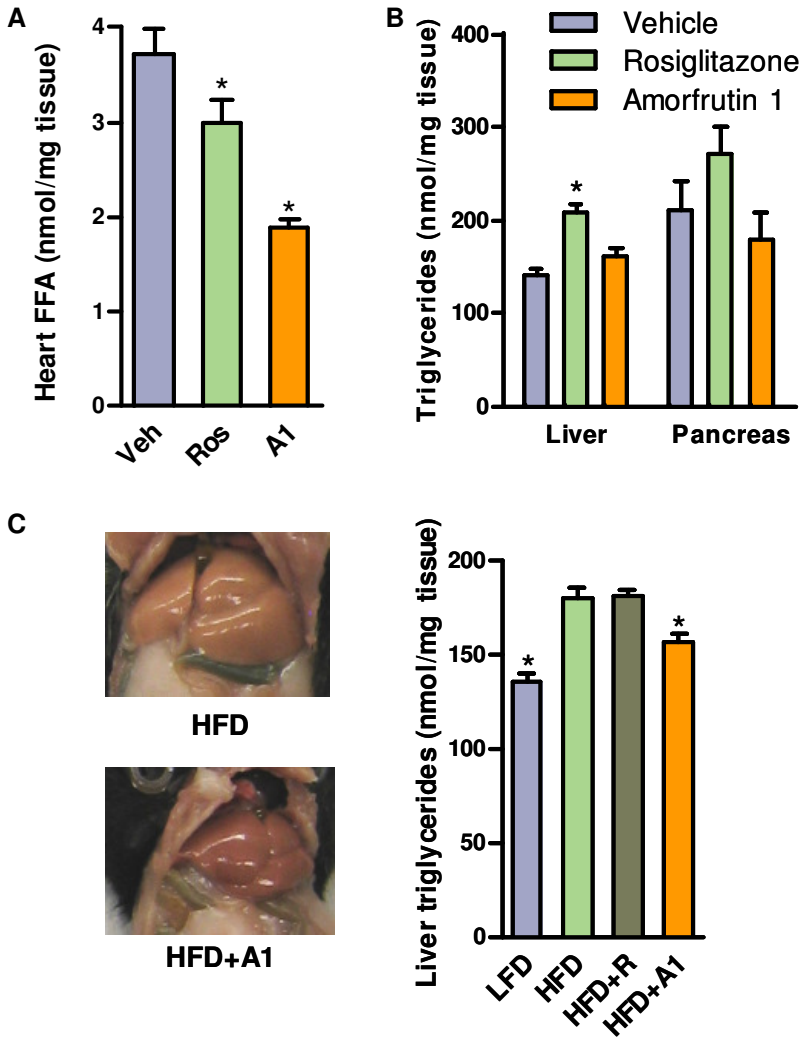

Figure 29. Effects of PPARγ modulators on lipid deposit in different mouse models of type 2 diabetes. **(A)** Effect of treatment over 3 weeks on free fatty acids in the heart of db/db mice (n=13). **(B)** Effect of treatment over 3 weeks on liver and pancreas triglycerides of db/db mice (n=10-13). **(C)** Effect of treatment over 15 weeks on liver histology (left) and liver triglycerides (right) of C57BL/6 mice (n=6-7). Data are expressed as mean ± s.e.m. *, P≤0.05 vs. vehicle or HFD only, respectively.

3.3.7 Amorfrutin 1 has protective effects on pancreas

A hallmark of the progressive development of diabetes is pancreatic tissue exhaustion. This is accompanied by decreased capacity of the β-cells to produce insulin, and by elevated plasma levels of the insulin precursor proinsulin (*227*). Possibly due to improved insulin sensitivity, amorfrutin 1 also appeared to prevent deterioration of pancreatic function in all mice models tested, as pancreatic insulin and plasma proinsulin levels improved compared to nontreated control mice (**Figure 30**).

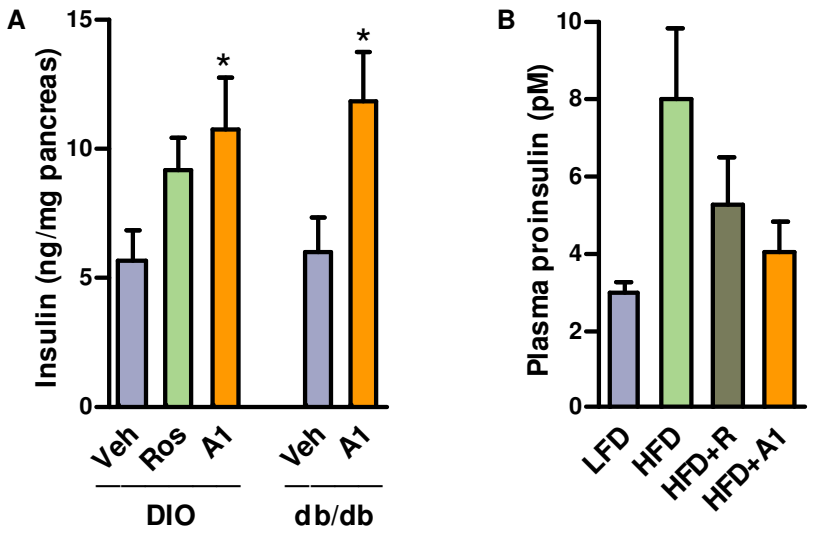

Figure 30. Effect of treatment on pancreas integrity. **(A)** Pancreatic insulin content in DIO mice (n=13) or db/db mice (n=7) after treatment over 3 weeks. **(B)** Plasma proinsulin levels in C57BL/6 mice (n=10-12) after treatment over 15 weeks. Data are expressed as mean ± s.e.m. *, P≤0.05 vs. vehicle or HFD only, respectively.

3.3.8 Amorfrutin 1 promotes expression of genes of lipid breakdown

Gene expression analyses in liver elucidated the underlying mechanism of reduced liver steatosis upon amorfrutin treatment. Rosiglitazone excessively activated expression of the fatty acid binding protein 4 (Fabp4) up to 55-fold, accounting for increased adipogenesis in the mouse liver (*228*). In contrast, amorfrutin 1 did not increase liver Fabp4 expression at all. Instead, amorfrutin 1 induced the expression of genes responsible for fatty acid oxidation such as PPARγ coactivator 1α (Pgc1α), acyl-Coenzyme A oxidase 1 (Acox1) and carnitine palmitoyltransferases 1a and 2 (Cpt1a and Cpt2), which could contribute to the observed reduction in liver steatosis (**Figure 31**).

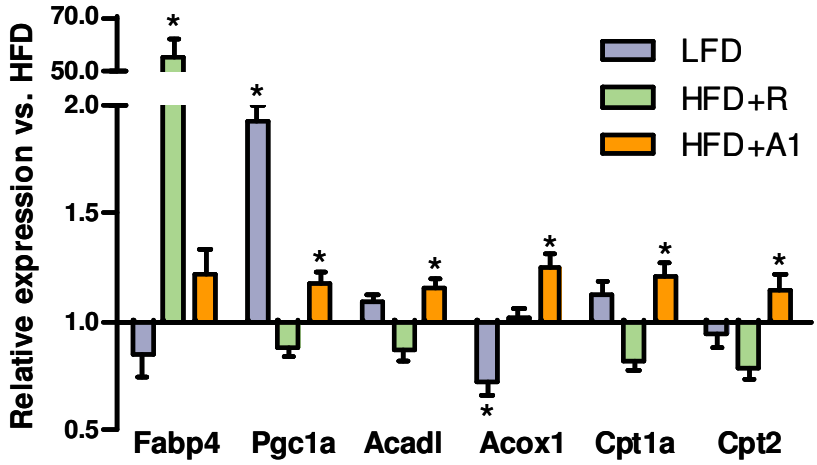

Figure 31. Regulation of liver gene expression after feeding with low fat diet (LFD) and high fat diet (HFD) without or with rosiglitazone (HFD+R) or amorfrutin 1 (HFD+A1) over 15 weeks in C57BL/6 mice (n=12). Expression of classical PPAR target genes was analyzed by qPCR. Gene expression of HFD-fed mice is set to 1. Data are expressed as mean ± s.e.m. *, P≤0.05 vs. HFD only.

Recently, it was reported that accumulation of triglycerides in liver is causally linked to decreased expression of transducin beta-like (TBL) 1 (*229*), a transcriptional cofactor of PPARα, which is the master regulator of fatty acid oxidation. Consistently, TBL1 expression negatively correlated with liver

steatosis (**Figure 32A**), and HFD feeding of mice led to a significant reduction in TBL1 expression compared to LFD-fed animals (**Figure 32B**). Strikingly, treatment with amorfrutin 1, but not rosiglitazone, completely inhibited the decrease in TBL1 expression, confirming the liver protective effects of amorfrutins.

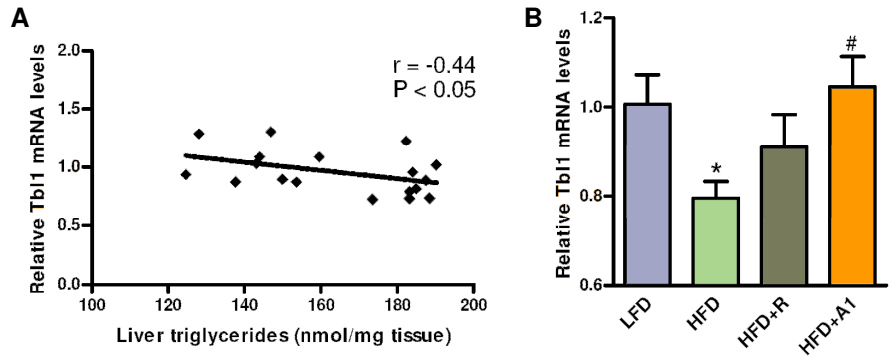

Figure 32. Gene expression of cofactor Tbl1 in murine liver. **(A)** Pearson correlation coefficient and P value (one-tailed) shown for normalized gene expression of cofactor Tbl1 versus triglyceride content in C57BL/6 liver samples (n=18). **(B)** Change in gene expression after feeding of low-fat diet (LFD) or high-fat diet (HFD) without or with rosiglitazone (HFD+R) or amorfrutin 1 (HFD+A1) over 15 weeks in C57BL/6 mice (n=12). Data are expressed as mean ± s.e.m. *, P≤0.05 vs. LFD; #, P≤0.05 vs. HFD.

3.3.9 Amorfrutin 1 reduces HFD-induced inflammation and macrophage invasion

Obesity is a chronic low-grade inflammation that is characterized by the expression of inflammatory mediators and macrophage recruitment to different tissues (*17*). In liver amorfrutin 1 reduced the transcript concentrations of the interleukins Il6 and Il1b, Lgals3, Ptgs2 and Ccl2 (MCP-1) (**Figure 33A**). Besides, amorfrutin 1 but not rosiglitazone decreased HFD-derived macrophage accumulation in liver as determined by expression of macrophage-specific transcripts of Ccl3, Ccl5, Ccr2, Ccr5, and Emr1. The reduction of macrophage

markers in amorfrutin 1-treated mice was comparable to that of lean LFD-fed mice (**Figure 33B**).

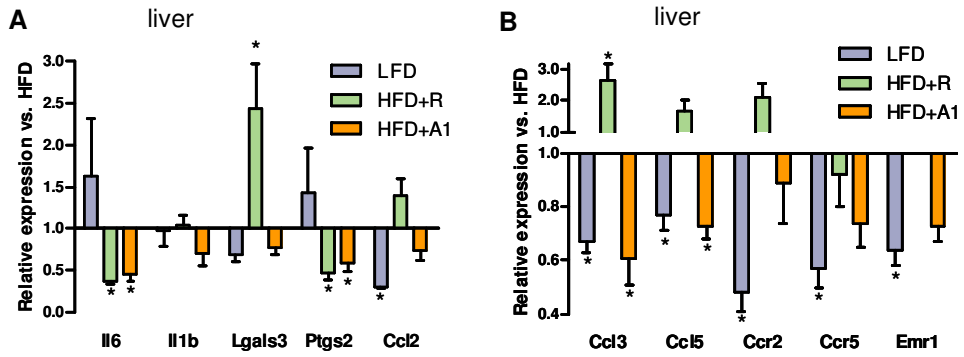

Figure 33. Regulation of liver gene expression after feeding with low-fat diet (LFD) or high-fat diet (HFD) without or with rosiglitazone (HFD+R) or amorfrutin 1 (HFD+A1) over 15 weeks in C57BL/6 mice (n=12). Expression of genes involved in inflammatory processes **(A)** and presence of macrophage-specific markers **(B)** were analyzed by qPCR. Gene expression of HFD-fed mice is set to 1. Data are expressed as mean ± s.e.m. *, P≤0.05 vs. HFD.

Accordingly, tumor necrosis factor α (TNFα) protein concentrations were lowered in liver (**Figure 34**). The anti-inflammatory effects of amorfrutin 1 were also verified by gene expression analyses in viscerale white adipose tissue (vWAT) (**Figure S8**). Consequently, amorfrutin treatment also led to reduction of obesity-derived inflammation in mice.

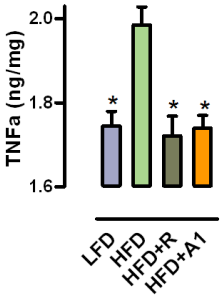

Figure 34. Effect of treatment on TNFα protein concentrations in liver of C57BL/6 mice (n=6). Data are expressed as mean ± s.e.m. *, P≤0.05 vs. HFD.

4 Discussion

The studies presented here introduces the amorfrutins, a novel natural product class of selective PPAR modulators, for effectively preventing and treating type 2 diabetes and the metabolic syndrome with minimized side effects.

4.1 The amorfrutin structure

The core structure of the amorfrutins consists of a simple 2-hydroxy benzoic acid with diverse isoprenyl and phenyl moieties (**Figure 7**). In a competitive TR-FRET-based binding assay binding affinity constants for these natural products could be determined. Affinity constants were in the high nanomolar range for PPARγ and in the medium to high micromolar range for PPARα and PPARβ/δ (**table S1**). The crystal structure of amorfrutin 1 in complex with the PPARγ-LBD in combination with the systematic synthesis of different derivatives revealed important information about the structure activity-relationship (SAR). The work of Jens C. de Groot and Dr. Konrad Büssow (Division of Structural Biology, Helmholtz Centre for Infection Research, Braunschweig, Germany) revealed that besides a plenty of van der Waals contacts between PPARγ and the ligands phenyl and isoprenyl residues a complex network of hydrogen bonds is formed between Ser342 and Arg288 and the amorfrutins carboxyl group. We further could show that disruption of these hydrogen bond network by esterification of the amorfrutin carboxyl group leads to loss of the high binding affinity. The methylester A5ME has a binding constant of 23 µM, in contrast to 590 nM for the carboxylate A5, thus esterification decreases the binding affinity by a factor of 39. The enthalpic contribution of the carboxyl group is

$$\Delta\Delta G = -RT\ln(K_{i1}/K_{i2}) \approx -8.31\,J/(mol\,K)\cdot 298\,K\cdot\ln(1/39) \approx 9\,kJ/mol \approx 2.2\,kcal/mol.$$

This is in the range of the common energy contribution of strong hydrogen bonds (*230*) as seen in the crystal structure, and thus is verifying the observed data.

We also discovered a series of related amorfrutins binding to PPARγ and further to PPARα as well as PPARβ/δ (**Figure S1 and table S1**). These examples disclosed that small modifications at the isoprenyl residue may dramatically increase the affinity to PPARγ, and generate ligands in the low-nanomolar range. This high affinity is extraordinary for nature-based PPARγ ligands, as most of the known non-synthetic ligands have affinities in the micromolar range (*83, 231*).

Slight modifications of the amorfrutin structure have a high impact on the transcriptional activation of target genes (**Figures 14 to 15**). Mediators of this specificity are the transcriptional cofactors. All amorfrutins presented here exhibited unique cofactor recruitment profiles (**Figure 10 and table S2**), probably as a result of different PPARγ conformations induced upon ligand binding. Therefore it is supposed that, consequently, pharmacologic properties – ADME parameters, anti-diabetic efficacy and safety – can directly be fine-tuned by derivatisation of the amorfrutin core structure. This principle has already been observed with other PPAR ligand classes. For instance, in clinical use rosiglitazone does barely improve lipid parameters (e.g. HDL- and LDL-cholesterol) (*232*) and increases the risk of congestive heart failure (*233*), while pioglitazone is associated with improvements in lipid parameters (*232*) and does not adversely affect cardiovascular diseases (*234*).

Albeit not endogenously present, structural similarity of the amorfrutins to potential physiologic ligands is a matter of discussion. The core structure of the amorfrutins is partly reminiscent to that of vitamin B6, especially of the pyridoxal form, which is required for amino acid catabolism and glycogenolysis (*235, 236*). It already has been reported that vitamin B6 deficiency is linked to impaired gluconeogenesis (*237*) and that administration of pyridoxal or pyridoxamine improves diabetes in several animal models (*238, 239*). Therefore the binding of pyridoxal to PPARγ was tested using the TR-FRET assay. However, pyridoxal showed no binding to the PPARγ-LBD. This may be attributed to the missing phenyl and isoprenyl residues that are needed for numerous van der Waals contacts. To systematically search for potential similar endogenous ligands we

scanned the Human Metabolom Database (HMDB) (*240*). The Tanimoto similarity search (threshold 0.6) revealed likeness to several intermediates of the ubiquinone biosynthesis, e.g. to 3-Hexaprenyl-4-hydroxy-5-methoxybenzoic acid and 3-Hexaprenyl-4,5-Dihydroxybenzoic acid. Ubiquinone is required as mobile electron transporter between complexes in the electron transport chain. Since it has an important role in the oxidative phosphorylation, it could be speculated that upon nutrient intake a balanced coregulation of ATP generation and glucose- and lipid metabolism would be beneficial. However, neither it was directly shown that intermediates of the ubiquinone biosynthesis bind to PPARγ nor it is likely that the intermediates located in the mitochondria and the nuclear receptor PPARγ have direct contact.

Since the Tanimoto coefficients only take into account exact congruence between query and library structures, I additionally applied the CATS (Chemically Advanced Template Search) software developed by Gisbert Schneider (*241, 242*). CATS compares topological pharmacophore descriptors (hydrogen-bond donor/acceptor, positively or negatively charged, lipophilic) of two molecules in Euclidean space, and thus allows for 'scaffold hopping'. Noteworthy, the best hits belong to the groups of free fatty acids, prostaglandines and thromboxanes, which have already shown to contain important physiologic PPAR activators (*243, 244*). Consequently, although amorfrutins are no endogenous ligands in mammals, they may mimic physiologic PPAR modulators in terms of metabolic regulation.

The structure of the widely applied glitazones was derived from the fibrate class (*73*), and other PPARγ ligands (e.g.ragaglitazar) in turn are adopted from the glitazone core structure (*245*). Amorfrutins are neither similar to thiazolidinediones nor to glitazars, both having been associated with tremendous side effects. In addition, the amorfrutin lead molecule is much less in molecular size, providing the opportunity for further derivatisation and optimisation by keeping the molecular weight in an advantageous range. According to Christopher A. Lipinski's rules, oral bioavailability as a property of druglikeness of a compound is favoured with less than 5 hydrogen bond donors and 10 hydrogen

bond acceptors, a molecular weight not greater than 500, and with a maximal calculated partition coefficient (ClogP) of 5 (*246*). This 'rule of 5' is fulfilled by all amorfrutins presented here, indicating a particular high druglikeness.

As recent reports disclosed an important role for PPARγ expressed also in the brain (see below) blood-brain-barrier penetration has to be considered. This pharmacological property could shown to be correlated with the polar surface area (PSA) of the small molecule, which can be approximately calculated (*247*). Amorfrutin 1 has a PSA of ~ 67 Å² (rosiglitazone ~ 72 Å²). It is an accepted assumption that drugs that act on the central nervous system must have a PSA below 70-80 Å² (*248*). This indicates that amorfrutins can penetrate the blood-brain-barrier. This is also supported by high membrane permeability experimentally determined in the PAMPA and Caco-2 model.

The amorfrutins have outstanding structural properties for natural products. In general, synthetic, combinatorial chemistry differs strongly from biosynthetic processes. Nature uses a relatively small set of building blocks and introduces diversity by sophisticated pathways and many functional groups, especially numerous different oxidation levels. In addition, natural compounds are products of enantioselective reactions. As a consequence, natural products typically have about 6 chiral centers, 4 rings, 6 oxygen atoms and 7 and 3 hydrogen bond acceptors and donors, respectively. In contrast, chemical synthesis pursues the strategy to repeat a moderate number of stereononselective reactions on a lot of building blocks. Consequently, synthetic compounds of the same molecular weight in average have no chiral centers, only 3 rings, 3 oxygen atoms and 4 and one hydrogen bond acceptors and donor, respectively. Comparing compounds from combinatorial libraries versus that from natural product collections and drug databases revealed the exceptional position of the amorfrutins. They have no stereocenter, only one to two aromatic rings, and in general only 5 carbon-oxygen bonds. To assess the chemical properties in a more systematic approach, we compared 10 compound properties, which are typical for that chemical class

(*249*), using a distance matrix (**Figure S9**). The amorfrutins are more similar to synthesized compounds and drugs than to complex natural products.

This indicates that chemically synthesizing amorfrutins may be a promising tool compared to extensive extraction from *Glycyrrhiza spec.* As there was no amorfrutin synthesis reported so far, our group together with Aman Prasad and Prof. Dr. Frank C. Schroeder (Boyce Thompson Institute and Department of Chemistry and Chemical Biology, Cornell University, Ithaca, NY, USA) developed a 6-stepped synthesis route for amorfrutins with more than 99% purity. The synthesis of pure amorfrutins in multigram quantities was a basic requirement for several subsequent applications: 1) it provided the crystallisation and structure determination of bound PPARγ due to high purity, 2) it allowed for first animal studies to verify the anti-diabetic effects *in vivo*, 3) it facilitates future in vivo studies in human patients, and 4) it permits the development of diverse amorfrutin analogues by chemical modification.

In conclusion, the amorfrutin class has a promising potential as lead for the chemical generation of optimised PPARγ ligands or even dual and pan PPAR agonists.

4.2 The *in vitro* properties of amorfrutins

Initial *in vitro* experiments showed that amorfrutins are potent PPARγ ligands with affinity constants in the nanomolar range (**table S1**). Such competitive binding studies are well established tools to quantify small molecule binding affinities, although the data of this artificial set-up could be completed by additional assays like isothermal binding calorimetry (ITC) and nuclear magnetic resonance (NMR) chemical shift perturbation approaches without the need of fluorescence labelling.

Additional cofactor binding experiments revealed recruitment profiles that were strikingly distinct from those of the thiazolidinedione class. Binding of different (but structural similar) ligands induced very specific cofactor recruitment

signatures. However, effective (amorfrutin) concentrations of cofactor recruitment varied between different amorfrutins and cofactor peptides. For instance, amorfrutin 1 (Ki = 236 nM) and amorfrutin 3 (Ki = 352 nM) recruited CBP-1 with EC50 of 12 µM and 110 nM, respectively, and they led to release of NCOR-2 with IC50 of 51 nM and 2.8 µM, respectively (**table S2**). The observed EC50 values are partly not in agreement with the compound binding affinities. Obviously, already under cell-free conditions with simplified peptides the biophysical processes of PPARγ activation are very sophisticated. The peptides are derived from the exposed cofactor interaction domain, which in general contains a conserved leucine-rich LXXLL motif that directly binds to the PPARγ-LBD in dependence of the receptor conformation (*71*). Thus, the EC50 value is not only defined by the compound affinity (Ki), but additionally is influenced by the affinity of the cofactor peptide to the different PPARγ conformations (which was not measured here). The effective concentration of cofactor recruitment consequently is composed of various equilibrium binding constants. Therefore it is probable that cofactor binding on the PPARγ apo form facilitates binding of the small molecule.

Certainly, the cofactor recruitment assay used here is limited by its artificial design. Since many coactivators contain more than one copy of the LXXLL motif, cooperative effects which largely influence cofactor binding to PPARγ cannot be assessed in such *in vitro* assays. Additionally, non-conserved amino acids terminal to the LXXLL motif, which are absent in the derived peptides, also account for specificity of cofactor binding (*250*). The performed cofactor recruitment studies present a valuable link between binding and transcriptional activation. Albeit several current publications about the role of transcriptional cofactors in metabolism (*251, 252*), few is known about their role in PPAR-driven gene expression, and further studies are required.

A possible approach to use such cofactor recruitment profiling without knowledge of the underlying transcriptional processes is a solely descriptive assay – with different datasets of compounds with beneficial effects (e.g. SPPARMs) and

compounds with adverse effects (e.g. glitazones) it should be possible to screen for novel SPPARMs in addition to simple receptor binding assays. This methodological concept was recently described in several publications (*253-256*). As inferred from the mouse studies, recruitment of the newly-discovered PPAR coactivator TBL1 should also be included to assess the compounds ability to enhance fatty acid oxidation.

In subsequent experiments, the amorfrutins were verified as transcriptional PPARγ activators with effective concentrations (458 nM to 4.5 µM) (**table 1**) that partly were above the binding affinities (Ki) up to ten-fold. A reason for the discrepancy could include a compound-specific retention outside of the cells, but the lipophilicity of the amorfrutins should facilitate diffusion over the cellular membrane. Contrary to the *in vitro* binding assay, transcriptional activation by the PPARγ construct only took place in dependence of numerous cellular cofactors. Thus, different effective concentrations for the amorfrutins were probably a result of different cofactor associations in the cells. That is also a common reason, why EC50 values (and efficacy) often are not reproducible in different cell types: changing the cellular environment is always accompanied by a different expression profile of the transcriptional cofactors.

Certainly, the reporter gene assay is a very artificial approach to measure nuclear receptor transactivation. It is especially limited by the usage of the nonphysiologic HEK293 cancer cell line, by overexpression of the chimeric GAL4/LBD construct and, in addition, by the reporter gene promoter design containing several copies of the upstream activator sequence (UAS). This limitation can be resolved by use of PPARγ full length assays with reporter genes under control of a natural PPAR response element carried out in common target cells such as adipocytes or macrophages.

The differential recruitment of cofactors to PPAR target genes is the key for understanding of transcriptional effects modulated by ligands. However, all reporter gene assays and in vitro recruitment studies disregard the importance of the complex gene promoter architecture, as different target genes expressed in the

same cell type can be variably associated with different cofactors (*257-259*). A more comprehensive view of compound-specific cofactor recruitment and gene expression will be gained by systematic whole-genome approaches such as chromatin immunoprecipitation coupled to next generation sequencing (ChIP-seq) (*260*). With a deeper knowledge about the association of certain cofactors and target genes responsible for beneficial and adverse effects in clinical usage directed screening assays will allow to separate the wheat from the chaff of nuclear receptor ligands.

4.3 Cell culture studies with amorfrutins

As shown in murine and human adipocytes, the amorfrutins modulate transcription of PPARγ target genes. To verify the specificity amorfrutins siRNA-mediated PPARγ knockdown studies were performed in primary adipocytes. Although PPARγ knockdown resulted in complete inhibition of amorfrutin effects at two of four genes, residual transcriptional activation persisted at two genes. It cannot be excluded that the remaining PPARγ expression of ca. 20% is sufficient to influence expression of target genes. Application of additional siRNA molecules with different sequences could further boost PPARγ knockdown. Efficiency should also be assessed on protein scale. Probably, transcriptional activation of the two persisting genes was modulated by PPARα and PPARβ/δ, since amorfrutin 1 and 2 also slightly activate these isotypes (**table 1**). The investigated common target genes are not specific for PPARγ and all three PPAR subtypes are expressed in adipocytes. Further validation may include simultaneous knockdown of PPARα and β/δ as well and use of a more specific PPARγ ligand, e.g. amorfrutin 3. Molecular targets of amorfrutins in cells could also be investigated with capture compound mass spectrometry (*261*). Coupling of a reactive biotinylated linker to amorfrutin, e.g. via the 4-hydroxy-residue that is presumably not involved in PPARγ binding, and subsequent analysis of captured cellular proteins would elucidate potential targets in the whole proteome.

To investigate the regulative effects on expression of the whole genome primary human adipocytes were treated for 24 hours with amorfrutins. The compound concentration was below the maximal concentration tested in the cellular toxicity assay, so that toxic effects are unlikely. An amorfrutin concentration of 30 µM was applied that was above the effective concentration determined in the reporter gene assay to ensure saturation of cellular PPARγ with the compound. Similar effects on gene expression have also been observed with only 10 µM of amorfrutin 4 (data not shown). Comparison of the different gene expression patterns figured out that the SPPARMs regulated fewer genes and that with reduced magnitude. The presented heatmap of differentially regulated genes (**Figure 15**) indicates that the different PPARγ ligands have very distinct gene expression patterns. However, due to filtering of regulated genes using an arbitrary threshold of $P < 0.05$ it has to be considered, if genes that were obviously not regulated are just (slightly) below this cut-off. To address this, a Gene Set Enrichment Analysis (GSEA) was performed on the whole-genome data (**Figures 16, 17 and S4**). This approach has the advantage to cumulate expression levels of many genes belonging to a certain gene set (e.g. pathway). Hence, also slight regulation of several genes becomes detectable and allows a reliable comparison of compound profiles. The GSEA approach revealed that important PPARγ pathways as lipid and glucose metabolism, but also anti-inflammatory processes were regulated with amorfrutins similar to rosiglitazone. Selective PPARγ modulation by amorfrutins was substantiated by use of principal component analysis and gene distance matrix, which integrated the majority and all of the gene expression data, respectively.

4.4 The effects of amorfrutins in mice

Three different mouse models were chosen to evaluate the *in vivo* anti-diabetic effects of amorfrutins in different stages of type 2 diabetes. The potential of prevention of insulin resistance was investigated in common C57BL/6 mice that were simultaneously fed for 15 weeks with a high fat diet, thus mimicking an

unhealthy Western diet. Amorfrutin 1 significantly inhibited the development of obesity, insulin resistance, hypertriglyceridemia, lipid deposit in non-adipose tissue and low-grade 'metaflammation'. The observed reduction in liver steatosis with amorfrutin treatment can be explained by activation of the PPARα isotype, which is not targeted by rosiglitazone. This observation clearly shows the advantage of amorfrutins and of dual PPAR ligands in general, thus predicting the success of other amorfrutin variants that activate PPARα to a greater extend. Although rosiglitazone was more efficient in reducing glucose intolerance the natural product amorfrutin class revealed a promising potential for the preventive application of diet-induced insulin resistance and associated disorders.

Anti-diabetic effects of amorfrutins were further proved in obese and insulin resistant C57BL/6 mice that were previously fed with HFD to induce these metabolic disorders. This gave the opportunity to analyze the compound effects in a therapeutic format that mimics the phenotype of the malnutrition-based early stages of type 2 diabetes. Amorfrutin 1 clearly improved insulin sensitivity, glucose tolerance and dyslipidemia as well as the standard drug rosiglitazone.

Strikingly, amorfrutin 1 decreased the body weight by ~10%, whereas rosiglitazone had no effect on body weight. Additionally expression of uncoupling proteins (Ucp) as markers of thermogenesis in various tissues was determined. However, expression of Ucp in vWAT and liver was more increased with rosiglitazone than with amorfrutin treatment (data not shown). This indicates that induced thermogenesis alone cannot explain the difference in body weight change between both PPARγ ligands. Treatment was not associated with decreased food intake, instead amorfrutin (and rosiglitazone) surprisingly led to *increased* food intake (**Figure 22**). The discrepancy between rosiglitazone-induced thermogenesis and weight gain was a subject of current publications. Several reports disclosed an involvement of central nervous system (CNS) PPARγ in the regulation of energy balance (*262-265*), especially by a cross-talk with the hypothalamic-pituitary-thyroid (HPT) axis. According to that some studies could shown that CNS PPARγ, which becomes activated during HFD-feeding by endogenous ligands or

by administered rosiglitazone, stimulates food intake and weight gain. This was accompanied by decreased concentrations of thyroid hormones. Conversely, blocking CNS PPARγ by antagonists or shRNA decreased feeding and weight gain and also elevated thyroid hormones. However, in the HFD-study presented here amorfrutin 1 increased food intake as PPARγ agonists (e.g. rosiglitazone), but *decreased* body weight such as PPARγ antagonists. To explain this observation, several pharmacologic effects have to be considered. First, affecting CNS PPARγ by amorfrutin requires the transport through the blood-brain-barrier, which was not addressed here (see below). Second, regulation of appetite and weight gain are separated processes (*266*) that involve action on CNS PPARγ and peripheral PPARγ (*267*). Thus, differential modulation of PPARγ in different tissues, a conceptual hallmark of SPPARγMs, may have opposing effects on food intake and weight gain. Third, the selectivity of PPAR ligands to the three PPAR subtypes influences energy intake and homeostasis (*266*), as PPARα and β/δ agonists seem to reduce body weight and food intake, whereas PPARγ agonists favor the reverse effects (*224*). Pan PPAR agonists, e.g. bezafibrate, have been reported to induce weight loss with or without increased food intake (*268-270*). Amorfrutin 1, which is able to activate all three PPAR subtypes *in vitro* (**Figure 8 and table 1**), apparently behaves as a pan agonist *in vivo*.

To address the cross-talk with the HPT axis, the plasma concentrations of thyroid hormones such as triiodothyronine (T3), tetraiodothyronine (T4) and thyroid-stimulating hormone (TSH) should be measured. Besides, isolation of hypothalamic tissue and analyzing expression levels of genes for thyroid hormone receptor and thyrotropin-releasing hormone could be performed. In addition, plasma concentrations of ketone bodies could be determined to explore catabolic effects. Furthermore, it has to be considered that appetite and energy homeostasis is also regulated by the endocannabinoid system (*271*), which is linked to leptin signalling (*272*) and can be modulated by PPAR ligands as well (*273*). The control of appetite and energy balance underlies a very sophisticated network of neuroendocrine processes, which cannot be easily addressed with few control experiments.

Of note, an increase in food intake became present not until day 10 of treatment with amorfrutin and rosiglitazone, whereas weight loss already started during the first days (**Figure 22**). It can therefore be speculated that orexigenic effects are secondary to anti-diabetic and antiobesity actions. Although not determined in this experiment, reduced leptin hormone concentration as characteristic of PPARγ activation probably led to increased appetite in the course of this treatment. Further animal studies of different PPAR-activating classes, e.g. with the more PPARγ specific ligand amorfrutin 3, and deciphering the complex regulative network of whole-body energy balance will gain deeper comprehension.

In addition to these two mouse models, leptin receptor-deficient db/db mice were treated with amorfrutin 1 in order to determine its anti-diabetic potential in a model of severe type 2 diabetes. Whereas rosiglitazone induced weight gain, amorfrutin 1 did not affect body weight or food intake, indicating that leptin has an important role in mediating orexigenic and anorexigenic effects of amorfrutins. However, treatment of diabetic mice clearly ameliorated insulin sensitivity and reduced pancreatic tissue exhaustion and dyslipidemia.

Recent studies showed that HFD-induced phosphorylation at serine 273 of PPARγ leads to dysregulation of a large number of obesity-related genes and is coupled to insulin resistance (*147*). Therefore, inhibition of Ser273-phosphorylation was proposed as a new strategy to specifically increase insulin sensitivity without activating the full range of PPARγ targets associated with side effects (*149*). This novel concept explains the good anti-diabetic properties of SPPARγMs, which only partially activate PPARγ. Indeed, amorfrutins block the phosphorylation and the subsequent dysregulation of diabetes-related genes (**Figures 27 to 28**). Although the new role of Ser273 PPARγ phosphorylation needs to be further studied, this work emphasizes the mechanistic overlap between compounds with similar anti-diabetic efficacy but completely different PPARγ activation. Amorfrutins thus may be promising members of next generation PPARγ ligands that separate anti-diabetic actions from common side effects.

To summarize the three animal studies, the amorfrutin class revealed prominent effects on the prevention and therapy of insulin resistance and associated disorders. Short-term treatment with high dose as well as long-term treatment with low dose revealed anti-diabetic effects in three mouse models similar to the standard drug rosiglitazone. Additionally, the amorfrutins showed promising improvement of dyslipidemia and abnormal lipid deposit superior to rosiglitazone. It further disclosed outstanding reduction in HFD-induced obesity and confirmed safety regarding liver toxicity. Amorfrutin 1 as well as rosiglitazone revealed similar anti-inflammatory and anti-diabetic properties in the mouse studies. It is speculative, if the improvements in insulin sensitivity are a result of anti-inflammatory effects, or if the reverse is true. Both processes are inevitably linked to each other and cannot be easily separated (*8*). To unravel the chain of cause and effect a more time-resolved study design would be required. For instance, the chronological occurrence of anti-inflammatory vs. anti-diabetic effects could be determined. Taken together, the presented mouse studies clearly showed that amorfrutins strongly improve insulin resistance as well as several other important metabolic and inflammatory parameters.

4.5 Future perspectives

4.5.1 Further studies

The ADMET studies elucidated well aqueous solubility and intestinal membrane permeability but only minor stability for amorfrutins during liver metabolic processes. Furthermore, oral application of amorfrutin 1 in mice led to glucuronidation of its carboxyl group and, to a minor extend, to oxidation of the isoprenyl residue. It should be a relevant purpose to optimize the ADMET properties of the amorfrutins. Based on the presented *in vitro* studies and X-ray structure of bound amorfrutin, it can be assumed that glucuronidation of the carboxyl group diminishes the pharmacological effects of PPARγ modulation. For a comprehensive view on the impact of that modification additional pharmacokinetic studies are required. It is speculative, if chemical protection of

the carboxyl function, e.g. by hydrolysable ester groups, will increase the cellular concentration of the carboxylated form.

In contrast, oxidation at the isoprenyl residue is believed to have no major effects on PPARγ affinity, since first, the high-affine amorfrutin 3 also has a similar residue in its parent form, and second, the X-ray structure does not indicate a major contribution of distinct single atoms within the exchangeable isoprenyl group. On the other side, this is apparently not true for the binding to PPARα or β/δ (**Figure 8 and table 1**). Furthermore, marginal structural changes within the amorfrutins have an important impact on the cofactor recruitment and on the selective expression of distinct sets of genes. Consequently, optimizing ADMET properties has always to be critically balanced with the pharmacological profile.

Another aspect of optimizing pharmacological parameters should focus on the blood-brain-barrier permeability in order to address neuronal disorders.

The presented study mainly focuses on the change in gene expression as a key marker of compound and diet-induced effects. However, enzymatic and hormonal processes are generally regulated by proteins. A major strategy to control the levels of proteins is their degradation, so that transcriptional changes are not obligatory translated into stable proteome alterations. It would therefore be an interesting objective to determine protein expression patterns in the corresponding tissues. The application of protein expression arrays is a complementary method to investigate compound and diet-induced effects. In addition, the supposed pivotal role of PPARγ-Ser273 phosphorylation underscores the importance of posttranslational modifications of the proteome. For such sophisticated purposes the usage of high resolution liquid chromatography mass spectrometry (LC-MS) with previous enrichment approaches seems obvious. For comparative profiling approaches such technologies yet requires labelling strategies to enable accurate quantification (*274, 275*).

To complete the systems biological investigation it would be interesting to analyze metabolomic data. Since nutritional alterations, progression of metabolic disorders and their pharmacological counteraction impair the homeostasis of

metabolites, metabolomics provide a valuable tool to complement gene expression profiles.

The presented work exclusively focuses on anti-diabetic effects of the amorfrutin class. In addition, further PPARγ ligands from synthetic libraries were identified. This includes a class of chalcones that bound to PPARγ with nanomolar binding constants. However, chalcone treatment of mice did not prevent the onset of HFD-induced insulin resistance, likely due to its low bioavailability observed in ADME experiments.

4.5.2 Pharmaceutical applications of amorfrutins

The studies presented here clearly show the high potential of the amorfrutin class for effectively preventing and treating type 2 diabetes and the metabolic syndrome with minimized side effects. Metabolic diseases evolved to a global epidemic with rapidly growing incidence (*1*). Since current pharmaceutical interventions are affected by severe side effects such as weight gain potentially counteracting the pharmaceutical purposes, amorfrutins offer an alternative for that use. This work introduced firstly that oral application of the amorfrutin class can attenuate the development of diabetes and obesity. Secondly, short-term treatment improves insulin sensitivity in mice with severe type 2 diabetes as efficiently as rosiglitazone. Therefore, amorfrutins could be used as *preventive* and *therapeutic* compound to combat type 2 diabetes. Amorfrutins and amorfrutin-containing plant extracts or fractions could be applied as non-prescriptive phytomedical agents by diabetes-prone patients and health-conscious consumers to prevent insulin resistance. Further preclinical and clinical studies are needed to validate efficacy and safety of amorfrutins. For treatment of patients with type 2 diabetes, additional studies should include combination therapies, e.g. with metformin or sulfonylurea.

Amorfrutins inhibit the progression of diet-induced obesity and lead to stable weight loss in obese mice within few days. Pharmaceutical strategies to treat

obesity are rare. Currently, only orlistat (Xenical) is approved for that indication, but it is linked to gastrointestinal side effects. Since obesity is a rapid growing epidemic and one leading cause for metabolic disorders, innovative drugs are required. Oral application of amorfrutins may be used for the safe prevention and treatment of obesity, although long-term studies are needed.

PPARγ also plays a central role in inflammatory and autoimmune diseases (*276, 277*). Of note, several non-steroidal anti-inflammatory drugs (e.g. indomethacin and ibuprofen) also possess activity on PPARγ (*278*), and it was postulated that these antiphlogistics partly act via PPARγ (*279*). Indeed, PPARγ ligands were shown to have therapeutic activity e.g. in acute inflammation (*280*), arthritis (*281, 282*), atherosclerosis (*111, 283*) and inflammatory bowel diseases (*284, 285*). Of note, amorfrutins were shown to inhibit LPS-induced inflammation in mice by an unknown mechanism (*286*). Thus, it is obvious to investigate the anti-inflammatory potential of amorfrutins in further animal models and clinical studies.

Its important role in inflammation and lipid metabolism let PPARγ become a promising target in skin diseases. For instance, in psoriasis and atopic dermatitis, which are characterized by impaired lipid barrier formation, systemic or local application of PPARγ ligands improved the severity of skin disorders (*287, 288*). Currently, for these applications the drug of first choice are glucocorticoids that are associated with side effects such as skin atrophy (*289*). This is especially a problem in younger patients, which are predominantly affected (*290*). Treatment of skin diseases with amorfrutins in order to facilitate the therapy with less or without glucocorticoids may become a new efficient approach.

Other application fields of PPARγ modulators include neurodegenerative diseases. PPARγ ligands exert neuroprotective activity in Parkinson's disease, Alzheimer's disease and multiple sclerosis beside others (*291*). As a prerequisite for drugs acting on the central nervous systems, blood-brain-barrier penetration has to be assured.

The development of a synthesis route was an important prerequisite for large-scale application, albeit the yield needs to be optimized. The chemical synthesis nevertheless allows for further modification of the amorfrutin lead, thus their core structure can serve as template for the development of analogues. Alternatively to synthesized agents, purified natural amorfrutins or special extract preparations can be used.

Despite their potential application forms, major challenges remain to bring amorfrutins to pharmaceutical use. Since several former PPAR ligands were associated with severe side effects, the question of long-term safety has to be addressed accurately. Thus, the regulatory agencies claim complete 2-year carcinogenicity studies in rodents before beginning clinical trials of at least 6 months duration (*142*). Furthermore, in the field of diabetes and dyslipidemia several established therapies, e.g. metformin, sulfunylureas, fibrates and statins, already exist. The amorfrutins therefore have not only been proven to be safe in single and combinatorial treatments, but additionally must possess superior efficiencies as established drugs to become approved. Consequently, application strategies have to include the other aforementioned disorders.

4.5.3 Nutraceutical applications of amorfrutins

The amorfrutins are a class of eatable natural products present in different legumes. In addition to an application as drug it therefore is conceivable to develop amorfrutin-based nutraceuticals, e.g. as dietary supplement in yoghurt or juices. Nutrition not only entails a risk factor for metabolic stress, but also can be the key to health. The class of amorfrutins has the potential to be used as nutraceutical to prevent the widespread emergence of insulin resistance. Generally, dietary modifications are applicable for the *prevention* of metabolic disorders, whereas pharmaceuticals are approved for the *treatment* of diseases (*292*). Furthermore, amorfrutin-based nutraceuticals could supportingly be used as medical food for treatment of present metabolic disorders, as this work clearly revealed that amorfrutins have preventive *and* therapeutic effects on health.

However, usage of pure natural products or fractions containing the amorfrutins requires high amounts of biomaterial. Alternatively, biotechnical approaches such as plant cell fermentation (*293*) with optimised yield have to be considered. As this work unambiguously has shown that a whole amorfrutin class has beneficial effects, synergistic actions of crude extracts with different amorfrutins may be applicable. The class of simple 2-hydroxybencoic acid derivatives is not restricted to *Glycyrrhiza spec.* and *Amorpha spec.*, since related compounds with PPARγ-modulating activity are also produced in other plants and fungi (**table S1**). The exploitation of other herbal or microbial sources thus seems reasonable.

In summary, besides its high potential for pharmaceutical applications amorfrutins constitute a promising natural-product class for the development of nutraceuticals to prevent metabolic diseases.

5 Summary

Considering the rising pandemic expansion of metabolic disorders there is an urgent need for new concepts addressing prevention and treatment of diseases such as type 2 diabetes and obesity. Diabetes and its complications are considered the major cause of death in many countries and entail a huge impact on public health systems. Having a key role in lipid and glucose homeostasis, the nuclear receptor PPARγ (peroxisome proliferator-activated receptor gamma) presents an important target for anti-diabetic compounds. However, treatment with currently approved PPARγ-modulating drugs is associated with severe side effects such as weight gain and necessitates the development of next-generation PPARγ ligands. The present work introduces a new class of potent PPARγ ligands. The 'amorfrutins' present a family of natural products isolated from the eatable legumes *Amorpha fruticosa* and *Glychyrrhiza foetida* (liquorice). The amorfrutins strongly bind to PPARγ and selectively modulate expression of PPARγ target genes. The expression signatures of amorfrutins are distinctly different compared to currently approved PPARγ agonists. In different diabetic mouse models, oral treatment with amorfrutins strikingly improved insulin sensitivity, hypertriglyceridemia and metabolic inflammation with similar efficacy to current anti-diabetic agents. In striking contrast to other PPARγ drugs the amorfrutins efficiently uncoupled insulin sensitization from undesired side effects and further reduced obesity and tissue lipid accumulation. This work clearly reveals the exceedingly high potential of amorfrutins for very effective prevention and therapy of type 2 diabetes and associated metabolic disorders with minimized side effects. The amorfrutins represent a novel class of selective PPARγ modulators with outstanding properties for further pharmaceutical and nutraceutical development.

6 Zusammenfassung

Die rapide steigende, globale Inzidenz von Adipositas und Typ 2-Diabetes erfordert dringend neue Strategien zur Prävention und Therapie von metabolischen Erkrankungen. Diabetes und seine Folgeerkrankungen sind für einen Großteil der Todesfälle verantwortlich und stellen eine globale Herausforderung für die öffentlichen Gesundheitssysteme dar. Der nukleare Hormonrezeptor PPARγ (Peroxisom-Proliferator-aktivierter Rezeptor gamma) besitzt eine Schlüsselposition bei der Lipid- und Kohlenhydrat-Homöostase und ist ein wichtiges pharmakologisches Ziel antidiabetischer Wirkstoffe. Der Einsatz derzeit zugelassener PPARγ-Aktivatoren ist jedoch mit schwerwiegenden Nebenwirkungen verbunden, sodass ein Bedarf an neuartigen, verbesserten PPARγ-Modulatoren besteht. Während der hier beschriebenen Promotion gelang es, eine neue Klasse an affinen PPARγ-Liganden zu identifizieren und eingehend zu untersuchen. Bei diesen sogenannten „Amorfrutinen“ handelt es sich um eine Stoffklasse von bioaktiven Naturstoffen, die aus Süßholzwurzeln (*Glychyrrhiza foetida*) und den essbaren Früchten des Scheinindigos (*Amorpha fruticosa*) isoliert wurden. Die Amorfrutine zeichnen sich durch eine hohe Bindungsaffinität zu PPARγ aus und modulieren dessen transkriptionelle Aktivität ausgesprochen selektiv. Infolgedessen führt die Behandlung mit Amorfrutinen zu Genexpressionsprofilen, die sich deutlich von denen derzeit zugelassener PPARγ-Aktivatoren unterscheiden. In verschiedenen diabetischen Maus-Modellen bewirkte die orale Applikation von Amorfrutinen eine starke Verbesserung der Insulin-Sensitivität, der Hypertriglyzeridämie sowie der metabolischen Inflammation. Die antidiabetischen Wirkungen waren vergleichbar mit denen klinisch verwendeter Medikamente. Im Gegensatz zu letzteren führte die Behandlung mit Amorfrutinen *nicht* zu den bekannten Nebenwirkungen, sondern verringerte darüber hinaus Adipositas und Fetteinlagerungen in Organen. Die vorliegende Arbeit zeigt das große Potential der nebenwirkungsarmen Amorfrutine, Typ 2-Diabetes und damit verbundene metabolische Erkrankungen zu verhindern und zu therapieren. Die Amorfrutine stellen einen vielversprechenden Ansatz für die Entwicklung pharmazeutischer Wirkstoffe und Nahrungsergänzungsmittel dar.

7 References

1. Smyth S., Heron A. (2006), *Diabetes and obesity: the twin epidemics*, Nat Med 12, 75-80.
2. World Health Organization (WHO), *Diabetes Programme - Fact Sheet*, (http://www.who.int/diabetes/en/).
3. International Diabetes Federation (IDF) (2009), *Diabetes Atlas 4th edition*.
4. American Diabetes Association (2003), *Report of the expert committee on the diagnosis and classification of diabetes mellitus*, Diabetes Care 26 Suppl 1, S5-20.
5. Kahn S. E. et al. (1993), *Quantification of the relationship between insulin sensitivity and beta-cell function in human subjects. Evidence for a hyperbolic function*, Diabetes 42, 1663-1672.
6. Goldney R. D. et al. (2004), *Diabetes, depression, and quality of life: a population study*, Diabetes Care 27, 1066-1070.
7. Neel J. V. (1962), *Diabetes mellitus: a "thrifty" genotype rendered detrimental by "progress"?*, Am J Hum Genet 14, 353-362.
8. Gregor M. F., Hotamisligil G. S. (2011), *Inflammatory mechanisms in obesity*, Annu Rev Immunol 29, 415-445.
9. Hotamisligil G. S. (2006), *Inflammation and metabolic disorders*, Nature 444, 860-867.
10. Brownlee M. (2001), *Biochemistry and molecular cell biology of diabetic complications*, Nature 414, 813-820.
11. Saltiel A. R., Kahn C. R. (2001), *Insulin signalling and the regulation of glucose and lipid metabolism*, Nature 414, 799-806.
12. Steinthorsdottir V. et al. (2007), *A variant in CDKAL1 influences insulin response and risk of type 2 diabetes*, Nat Genet 39, 770-775.
13. Saxena R. et al. (2007), *Genome-Wide Association Analysis Identifies Loci for Type 2 Diabetes and Triglyceride Levels*, Science 316, 1331-1336.
14. World Health Organization (WHO) (2003), *Obesity and Overweight - Fact sheet*, (http://www.who.int/hpr/NPH/docs/gs_obesity.pdf).
15. Sims, E. A. H. (1980), *From the NIH: Successful diet and exercise therapy is conducted in Vermont for "diabesity"*, Jama 243, 519-520.
16. World Health Organization (WHO) (2000), *Obesity: preventing and managing the global epidemic. Report of a WHO consultation*, World Health Organ Tech Rep Ser 894, i-xii, 1-253.
17. Kahn S. E. et al. (2006), *Mechanisms linking obesity to insulin resistance and type 2 diabetes*, Nature 444, 840-846.
18. Despres J. P. et al. (2001), *Treatment of obesity: need to focus on high risk abdominally obese patients*, BMJ 322, 716-720.

19. National Institutes of Health (1998), *Clinical guidelines on the identification, evaluation, and treatment of overweight and obesity in adults - the evidence report.*, Obesity Res 6, 51S-209S.
20. Maeda K. et al. (1997), *Analysis of an expression profile of genes in the human adipose tissue*, Gene 190, 227-235.
21. Montague C. T., O'Rahilly S. (2000), *The perils of portliness: causes and consequences of visceral adiposity*, Diabetes 49, 883-888.
22. Griffin M. E. et al. (1999), *Free fatty acid-induced insulin resistance is associated with activation of protein kinase C theta and alterations in the insulin signaling cascade*, Diabetes 48, 1270-1274.
23. Houmard J. A. et al. (2002), *Effect of weight loss on insulin sensitivity and intramuscular long-chain fatty acyl-CoAs in morbidly obese subjects*, Diabetes 51, 2959-2963.
24. Randle P. J. et al. (1963), *The glucose fatty-acid cycle. Its role in insulin sensitivity and the metabolic disturbances of diabetes mellitus*, Lancet 1, 785-789.
25. Ron D., Walter P. (2007), *Signal integration in the endoplasmic reticulum unfolded protein response*, Nat Rev Mol Cell Biol 8, 519-529.
26. Hotamisligil G. S. (2010), *Endoplasmic reticulum stress and the inflammatory basis of metabolic disease*, Cell 140, 900-917.
27. Nakamura T. et al. (2010), *Double-stranded RNA-dependent protein kinase links pathogen sensing with stress and metabolic homeostasis*, Cell 140, 338-348.
28. Moitra J. et al. (1998), *Life without white fat: a transgenic mouse*, Genes Dev 12, 3168-3181.
29. Reitman M. L., Gavrilova O. (2000), *A-ZIP/F-1 mice lacking white fat: a model for understanding lipoatrophic diabetes*, Int J Obes Relat Metab Disord 24 Suppl 4, S11-14.
30. Kim J. Y. et al. (2007), *Obesity-associated improvements in metabolic profile through expansion of adipose tissue*, J Clin Invest 117, 2621-2637.
31. Kershaw E. E., Flier J. S. (2004), *Adipose tissue as an endocrine organ*, J Clin Endocrinol Metab 89, 2548-2556.
32. Ahima R. S. (2006), *Adipose tissue as an endocrine organ*, Obesity (Silver Spring) 14 Suppl 5, 242S-249S.
33. Despres J. P., Lemieux I. (2006), *Abdominal obesity and metabolic syndrome*, Nature 444, 881-887.
34. Schaffler A., Scholmerich J. *Innate immunity and adipose tissue biology*, Trends Immunol 31, 228-235.
35. Clowes G. H., Jr. et al. (1978), *Blood insulin responses to blood glucose levels in high output sepsis and spetic shock*, Am J Surg 135, 577-583.

36. Bahtiyar G. et al. (2004), *Association of diabetes and hepatitis C infection: epidemiologic evidence and pathophysiologic insights*, Curr Diab Rep 4, 194-198.

37. Pao V. et al. (2008), *HIV therapy, metabolic syndrome, and cardiovascular risk*, Curr Atheroscler Rep 10, 61-70.

38. Sidiropoulos P. I. et al. (2008), *Metabolic syndrome in rheumatic diseases: epidemiology, pathophysiology, and clinical implications*, Arthritis Res Ther 10, 207.

39. Hotamisligil G. S. et al. (1993), *Adipose expression of tumor necrosis factor-alpha: direct role in obesity-linked insulin resistance*, Science 259, 87-91.

40. Borst S. E. (2004), *The role of TNF-alpha in insulin resistance*, Endocrine 23, 177-182.

41. Hotamisligil G. S. et al. (1994), *Reduced tyrosine kinase activity of the insulin receptor in obesity-diabetes. Central role of tumor necrosis factor-alpha*, J Clin Invest 94, 1543-1549.

42. Ragolia L., Begum N. (1998), *Protein phosphatase-1 and insulin action*, Mol Cell Biochem 182, 49-58.

43. Sartipy P., Loskutoff D. J. (2003), *Monocyte chemoattractant protein 1 in obesity and insulin resistance*, Proc Natl Acad Sci U S A 100, 7265-7270.

44. Pickup J. C. et al. (1997), *NIDDM as a disease of the innate immune system: association of acute-phase reactants and interleukin-6 with metabolic syndrome X*, Diabetologia 40, 1286-1292.

45. Festa A. et al. (2000), *Chronic subclinical inflammation as part of the insulin resistance syndrome: the Insulin Resistance Atherosclerosis Study (IRAS)*, Circulation 102, 42-47.

46. Yuan M. et al. (2001), *Reversal of obesity- and diet-induced insulin resistance with salicylates or targeted disruption of Ikkbeta*, Science 293, 1673-1677.

47. Hundal R. S. et al. (2002), *Mechanism by which high-dose aspirin improves glucose metabolism in type 2 diabetes*, J Clin Invest 109, 1321-1326.

48. Hirosumi J. et al. (2002), *A central role for JNK in obesity and insulin resistance*, Nature 420, 333-336.

49. Larsen C. M. et al. (2007), *Interleukin-1-receptor antagonist in type 2 diabetes mellitus*, N Engl J Med 356, 1517-1526.

50. Davis J. E. et al. (2008), *Tlr-4 deficiency selectively protects against obesity induced by diets high in saturated fat*, Obesity (Silver Spring) 16, 1248-1255.

51. Weisberg S. P. et al. (2003), *Obesity is associated with macrophage accumulation in adipose tissue*, J Clin Invest 112, 1796-1808.

52. Xu H. et al. (2003), *Chronic inflammation in fat plays a crucial role in the development of obesity-related insulin resistance*, J Clin Invest 112, 1821-1830.

53. Berg A. H., Scherer P. E. (2005), *Adipose tissue, inflammation, and cardiovascular disease*, Circ Res 96, 939-949.

54. Schaffler A. et al. (2007), *Adipose tissue as an immunological organ: Toll-like receptors, C1q/TNFs and CTRPs*, Trends Immunol 28, 393-399.

55. Winer S. et al. (2009), *Normalization of obesity-associated insulin resistance through immunotherapy*, Nat Med 15, 921-929.

56. Desruisseaux M. S. et al. (2007), *Adipocyte, adipose tissue, and infectious disease*, Infect Immun 75, 1066-1078.

57. Dhurandhar N. V. (2004), *Contribution of pathogens in human obesity*, Drug News Perspect 17, 307-313.

58. Frank D. N., Pace N. R. (2008), *Gastrointestinal microbiology enters the metagenomics era*, Curr Opin Gastroenterol 24, 4-10.

59. Mai V., Draganov P. V. (2009), *Recent advances and remaining gaps in our knowledge of associations between gut microbiota and human health*, World J Gastroenterol 15, 81-85.

60. Delzenne N. M., Cani P. D (2011). *Gut Microbiota and the Pathogenesis of Insulin Resistance*, Curr Diab Rep 11, 154-159.

61. Amar J. et al. (2008), *Energy intake is associated with endotoxemia in apparently healthy men*, Am J Clin Nutr 87, 1219-1223.

62. Erridge C. et al. (2007), *A high-fat meal induces low-grade endotoxemia: evidence of a novel mechanism of postprandial inflammation*, Am J Clin Nutr 86, 1286-1292.

63. Cani P. D. et al. (2008), *Changes in gut microbiota control metabolic endotoxemia-induced inflammation in high-fat diet-induced obesity and diabetes in mice*, Diabetes 57, 1470-1481.

64. Cani P. D. et al. (2007), *Metabolic endotoxemia initiates obesity and insulin resistance*, Diabetes 56, 1761-1772.

65. Backhed F. et al. (2004), *The gut microbiota as an environmental factor that regulates fat storage*, Proc Natl Acad Sci U S A 101, 15718-15723.

66. Backhed F. et al. (2007), *Mechanisms underlying the resistance to diet-induced obesity in germ-free mice*, Proc Natl Acad Sci U S A 104, 979-984.

67. Vijay-Kumar M. et al. (2010), *Metabolic syndrome and altered gut microbiota in mice lacking Toll-like receptor 5*, Science 328, 228-231.

68. Turnbaugh P. J. et al. (2007), *The human microbiome project*, Nature 449, 804-810.

69. Hollenberg S. M. et al. (1985), *Primary structure and expression of a functional human glucocorticoid receptor cDNA*, Nature 318, 635-641.

70. Owen G. I., Zelent A. (2000), *Origins and evolutionary diversification of the nuclear receptor superfamily*, Cell Mol Life Sci 57, 809-827.

71. Novac N., Heinzel T. (2004), *Nuclear receptors: overview and classification*, Curr Drug Targets Inflamm Allergy 3, 335-346.

72. Sonoda J. et al. (2008), *Nuclear receptors: decoding metabolic disease*, FEBS Lett 582, 2-9.

73. Kliewer S. A. et al. (2001), *Peroxisome proliferator-activated receptors: from genes to physiology*, Recent Prog Horm Res 56, 239-263.

74. Cho N., Momose Y. (2008), *Peroxisome proliferator-activated receptor gamma agonists as insulin sensitizers: from the discovery to recent progress*, Curr Top Med Chem 8, 1483-1507.

75. Chen T. (2008), *Nuclear receptor drug discovery*, Curr Opin Chem Biol 12, 418-426.

76. Mangelsdorf D. J. et al. (1995), *The nuclear receptor superfamily: the second decade*, Cell 83, 835-839.

77. Nuclear Receptors Nomenclature Committee (1999), *A unified nomenclature system for the nuclear receptor superfamily*, Cell 97, 161-163.

78. Issemann I., Green S. (1990), *Activation of a member of the steroid hormone receptor superfamily by peroxisome proliferators*, Nature 347, 645-650.

79. Reddy J. K., Rao M. S. (1986), *Peroxisome proliterators and cancer: mechanisms and implications*, Trends Pharmacol Sci 7, 438-443.

80. Willson T. M. et al. (2000), *The PPARs: from orphan receptors to drug discovery*, J Med Chem 43, 527-550.

81. Cattley R. C. et al. (1998), *Do peroxisome proliferating compounds pose a hepatocarcinogenic hazard to humans?*, Regul Toxicol Pharmacol 27, 47-60.

82. Brown J. D., Plutzky J. (2007), *Peroxisome proliferator-activated receptors as transcriptional nodal points and therapeutic targets*, Circulation 115, 518-533.

83. Michalik L. et al. (2006), *International Union of Pharmacology. LXI. Peroxisome proliferator-activated receptors*, Pharmacol Rev 58, 726-741.

84. Argmann C. A. et al. (2005), *Peroxisome proliferator-activated receptor gamma: the more the merrier?*, Eur J Clin Invest 35, 82-92; discussion 80.

85. Kliewer S. A. et al. (1992), *Convergence of 9-cis retinoic acid and peroxisome proliferator signalling pathways through heterodimer formation of their receptors*, Nature 358, 771-774.

86. Dreyer C. et al. (1992), *Control of the peroxisomal beta-oxidation pathway by a novel family of nuclear hormone receptors*, Cell 68, 879-887.

87. Takada I. et al. (2000), *Alteration of a single amino acid in peroxisome proliferator-activated receptor-alpha (PPAR alpha) generates a PPAR delta phenotype*, Mol Endocrinol 14, 733-740.

88. Berger J. P. et al. (2005), *PPARs: therapeutic targets for metabolic disease*, Trends Pharmacol Sci 26, 244-251.

89. Chinetti G. et al. (1998), *Activation of proliferator-activated receptors alpha and gamma induces apoptosis of human monocyte-derived macrophages*, J Biol Chem 273, 25573-25580.

90. Evans R. M. et al. (2004), *PPARs and the complex journey to obesity*, Nat Med 10, 355-361.

91. Duez H. et al. (2005), *Regulation of human apoA-I by gemfibrozil and fenofibrate through selective peroxisome proliferator-activated receptor alpha modulation*, Arterioscler Thromb Vasc Biol 25, 585-591.

92. Kersten S. et al. (1999), *Peroxisome proliferator-activated receptor alpha mediates the adaptive response to fasting*, J Clin Invest 103, 1489-1498.

93. Ashibe B., Motojima K. (2009), *Fatty aldehyde dehydrogenase is up-regulated by polyunsaturated fatty acid via peroxisome proliferator-activated receptor α and suppresses polyunsaturated fatty acid-induced endoplasmic reticulum stress*, FEBS Journal 276, 6956-6970.

94. Chakravarthy M. V. et al. (2009), *Identification of a physiologically relevant endogenous ligand for PPARalpha in liver*, Cell 138, 476-488.

95. Forman B. M. et al. (1997), *Hypolipidemic drugs, polyunsaturated fatty acids, and eicosanoids are ligands for peroxisome proliferator-activated receptors alpha and delta*, Proc Natl Acad Sci U S A 94, 4312-4317.

96. Guerre-Millo M. et al. (2000), *Peroxisome proliferator-activated receptor alpha activators improve insulin sensitivity and reduce adiposity*, J Biol Chem 275, 16638-16642.

97. Lalloyer F., Staels B. (2010), *Fibrates, glitazones, and peroxisome proliferator-activated receptors*, Arterioscler Thromb Vasc Biol 30, 894-899.

98. Jialal I. et al. (2010), *Management of hypertriglyceridemia in the diabetic patient*, Curr Diab Rep 10, 316-320.

99. Gervois P. et al. (2007), *Drug Insight: mechanisms of action and therapeutic applications for agonists of peroxisome proliferator-activated receptors*, Nat Clin Pract Endocrinol Metab 3, 145-156.

100. Wang Y. X. et al. (2003), *Peroxisome-proliferator-activated receptor delta activates fat metabolism to prevent obesity*, Cell 113, 159-170.

101. Narkar V. A. et al. (2008), *AMPK and PPARdelta agonists are exercise mimetics*, Cell 134, 405-415.

102. Billin A. N. (2008), *PPAR-beta/delta agonists for Type 2 diabetes and dyslipidemia: an adopted orphan still looking for a home*, Expert Opin Investig Drugs 17, 1465-1471.

103. Tontonoz P. et al. (1994), *Stimulation of adipogenesis in fibroblasts by PPAR gamma 2, a lipid-activated transcription factor*, Cell 79, 1147-1156.

104. Lehrke M., Lazar M. A. (2005), *The many faces of PPARgamma*, Cell 123, 993-999.

105. Fajas L. et al. (1997), *The organization, promoter analysis, and expression of the human PPARgamma gene*, J Biol Chem 272, 18779-18789.

106. Berger J., Moller D. E. (2002), *The mechanisms of action of PPARs*, Annu Rev Med 53, 409-435.

107. Rangwala S. M., Lazar M. A. (2004), *Peroxisome proliferator-activated receptor gamma in diabetes and metabolism*, Trends Pharmacol Sci 25, 331-336.

108. Tontonoz P. et al. (1995), *PPAR gamma 2 regulates adipose expression of the phosphoenolpyruvate carboxykinase gene*, Mol Cell Biol 15, 351-357.

109. Guan H. P. et al. (2002), *A futile metabolic cycle activated in adipocytes by antidiabetic agents*, Nat Med 8, 1122-1128.

110. Hibuse T. et al. (2005), *Aquaporin 7 deficiency is associated with development of obesity through activation of adipose glycerol kinase*, Proc Natl Acad Sci U S A 102, 10993-10998.

111. Bensinger S. J., Tontonoz P. (2008), *Integration of metabolism and inflammation by lipid-activated nuclear receptors*, Nature 454, 470-477.

112. Pascual G. et al. (2005), *A SUMOylation-dependent pathway mediates transrepression of inflammatory response genes by PPAR-gamma*, Nature 437, 759-763.

113. Barak Y. et al. (1999), *PPAR gamma is required for placental, cardiac, and adipose tissue development*, Mol Cell 4, 585-595.

114. He W. et al. (2003), *Adipose-specific peroxisome proliferator-activated receptor gamma knockout causes insulin resistance in fat and liver but not in muscle*, Proc Natl Acad Sci U S A 100, 15712-15717.

115. Hevener A. L. et al. (2003), *Muscle-specific Pparg deletion causes insulin resistance*, Nat Med 9, 1491-1497.

116. Matsusue K. et al. (2003), *Liver-specific disruption of PPARgamma in leptin-deficient mice improves fatty liver but aggravates diabetic phenotypes*, J Clin Invest 111, 737-747.

117. Norris A. W. et al. (2003), *Muscle-specific PPARgamma-deficient mice develop increased adiposity and insulin resistance but respond to thiazolidinediones*, J Clin Invest 112, 608-618.

118. Akiyama T. E. et al. (2002), *Conditional disruption of the peroxisome proliferator-activated receptor gamma gene in mice results in lowered expression of ABCA1, ABCG1, and apoE in macrophages and reduced cholesterol efflux*, Mol Cell Biol 22, 2607-2619.

119. Kubota N. et al. (1999), *PPAR gamma mediates high-fat diet-induced adipocyte hypertrophy and insulin resistance*, Mol Cell 4, 597-609.
120. Miles P. D. et al. (2000), *Improved insulin-sensitivity in mice heterozygous for PPAR-gamma deficiency*, J Clin Invest 105, 287-292.
121. Norman R. A. et al. (1997), *Genomewide search for genes influencing percent body fat in Pima Indians: suggestive linkage at chromosome 11q21-q22. Pima Diabetes Gene Group*, Am J Hum Genet 60, 166-173.
122. Deeb S. S. et al. (1998), *A Pro12Ala substitution in PPARgamma2 associated with decreased receptor activity, lower body mass index and improved insulin sensitivity*, Nat Genet 20, 284-287.
123. Altshuler D. et al. (2000), *The common PPARgamma Pro12Ala polymorphism is associated with decreased risk of type 2 diabetes*, Nat Genet 26, 76-80.
124. Ristow M. et al. (1998), *Obesity associated with a mutation in a genetic regulator of adipocyte differentiation*, N Engl J Med 339, 953-959.
125. Kliewer S. A. et al. (1995), *A prostaglandin J2 metabolite binds peroxisome proliferator-activated receptor gamma and promotes adipocyte differentiation*, Cell 83, 813-819.
126. Nagy L. et al. (1998), *Oxidized LDL regulates macrophage gene expression through ligand activation of PPARgamma*, Cell 93, 229-240.
127. Huang J. T. et al. (1999), *Interleukin-4-dependent production of PPAR-gamma ligands in macrophages by 12/15-lipoxygenase*, Nature 400, 378-382.
128. Lehmann J. M. et al. (1995), *An antidiabetic thiazolidinedione is a high affinity ligand for peroxisome proliferator-activated receptor gamma (PPAR gamma)*, J Biol Chem 270, 12953-12956.
129. Cock T. A. et al. (2004), *Peroxisome proliferator-activated receptor-gamma: too much of a good thing causes harm*, EMBO Rep 5, 142-147.
130. Sohda T. et al. (1982), *Studies on antidiabetic agents. I. Synthesis of 5-[4-(2-methyl-2-phenylpropoxy)-benzyl]thiazolidine-2,4-dione (AL-321) and related compounds*, Chem Pharm Bull (Tokyo) 30, 3563-3573.
131. [Anon] (2010), *Regulators restrict Avandia in the US and suspend it in the EU*, Nat Rev Drug Discov 9, 828-828.
132. Rosen C. J. (2010), *Revisiting the rosiglitazone story--lessons learned*, N Engl J Med 363, 803-806.
133. Olefsky J. M., Saltiel A. R. (2000), *PPAR gamma and the treatment of insulin resistance*, Trends Endocrinol Metab 11, 362-368.
134. Brzozowski A. M. et al. (1997), *Molecular basis of agonism and antagonism in the oestrogen receptor*, Nature 389, 753-758.
135. Shang Y., Brown M. (2002), *Molecular determinants for the tissue specificity of SERMs*, Science 295, 2465-2468.

136. Gelman L. et al. (2007), *Molecular basis of selective PPARgamma modulation for the treatment of Type 2 diabetes*, Biochim Biophys Acta 1771, 1094-1107.

137. Zhang F. et al. (2007), *Selective Modulators of PPAR-gamma Activity: Molecular Aspects Related to Obesity and Side-Effects*, PPAR Res 2007, 32696.

138. Fievet C. et al. (2006), *PPARalpha and PPARgamma dual agonists for the treatment of type 2 diabetes and the metabolic syndrome*, Curr Opin Pharmacol 6, 606-614.

139. Kendall D. M. et al. (2006), *Improvement of glycemic control, triglycerides, and HDL cholesterol levels with muraglitazar, a dual (alpha/gamma) peroxisome proliferator-activated receptor activator, in patients with type 2 diabetes inadequately controlled with metformin monotherapy: A double-blind, randomized, pioglitazone-comparative study*, Diabetes Care 29, 1016-1023.

140. Henry R. R. et al. (2009), *Effect of the dual peroxisome proliferator-activated receptor-alpha/gamma agonist aleglitazar on risk of cardiovascular disease in patients with type 2 diabetes (SYNCHRONY): a phase II, randomised, dose-ranging study*, Lancet 374, 126-135.

141. Ratner R. E. et al. (2007), *Efficacy, safety and tolerability of tesaglitazar when added to the therapeutic regimen of poorly controlled insulin-treated patients with type 2 diabetes*, Diab Vasc Dis Res 4, 214-221.

142. Rubenstrunk A. et al. (2007), *Safety issues and prospects for future generations of PPAR modulators*, Biochim Biophys Acta 1771, 1065-1081.

143. Gross B., Staels B. (2007), *PPAR agonists: multimodal drugs for the treatment of type-2 diabetes*, Best Pract Res Clin Endocrinol Metab 21, 687-710.

144. Artis D. R. et al. (2009), *Scaffold-based discovery of indeglitazar, a PPAR pan-active anti-diabetic agent*, Proc Natl Acad Sci U S A 106, 262-267.

145. Brown A. D. et al. (2008), *Process Development for Sodelglitazar: A PPAR Panagonist*, Organic Process Research & Development 13, 297-302.

146. US National Institute of Health, *ClinicalTrials.gov*, (http://clinicaltrials.gov/ct2/results?term=GW677954).

147. Choi J. H. et al. (2010), *Anti-diabetic drugs inhibit obesity-linked phosphorylation of PPARgamma by Cdk5*, Nature 466, 451-456.

148. Jones D. (2010), *Potential remains for PPAR-targeted drugs*, Nat Rev Drug Discov 9, 668-669.

149. Houtkooper R. H., Auwerx J. (2010), *Obesity: New life for antidiabetic drugs*, Nature 466, 443-444.

150. Kahn B. B., McGraw T. E. (2010), *Rosiglitazone, PPARgamma, and type 2 diabetes*, N Engl J Med 363, 2667-2669.

151. Drug Topics, *Top 200 generic drugs by total prescriptions*, (http://drugtopics.modernmedicine.com/drugtopics/data/articlestandard//drugtopics/252010/674982/article.pdf).

152. International Diabetes Federation, *Global Guideline for Type 2 Diabetes. Glucose control: oral therapy*, (http://www.idf.org/webdata/docs/GGT2D%2009%20Oral%20therapy.pdf).

153. Bailey C. J., Turner R. C. (1996), *Metformin*, N Engl J Med 334, 574-579.

154. Towler M. C., Hardie D. G. (2007), *AMP-activated protein kinase in metabolic control and insulin signaling*, Circ Res 100, 328-341.

155. Krentz A. J. et al. (2008), *New drugs for type 2 diabetes mellitus: what is their place in therapy?*, Drugs 68, 2131-2162.

156. Williams G. (1994), *Management of non-insulin-dependent diabetes mellitus*, Lancet 343, 95-100.

157. US Food and Drug Administration, *FDA significantly restricts access to the diabetes drug Avandia*, (http://www.fda.gov/Drugs/DrugSafety/PostmarketDrugSafetyInformationforPatientsandProviders/ucm226956.htm).

158. US Food and Drug Administration, *Pioglitazone HCl (marketed as Actos, Actoplus Met, and Duetact) Information*, (http://www.fda.gov/Drugs/DrugSafety/PostmarketDrugSafetyInformationforPatientsandProviders/ucm109136.htm).

159. Ryan G. J. et al. (2005), *Pramlintide in the treatment of type 1 and type 2 diabetes mellitus*, Clin Ther 27, 1500-1512.

160. Barber T. M. et al. (2010), *The incretin pathway as a new therapeutic target for obesity*, Maturitas 67, 197-202.

161. Carpino P. A., Goodwin B. *Diabetes area participation analysis: a review of companies and targets described in the 2008 - 2010 patent literature*, Expert Opin Ther Pat 20, 1627-1651.

162. McCarty M. F. (2005), *Nutraceutical resources for diabetes prevention--an update*, Med Hypotheses 64, 151-158.

163. Muller M., Kersten S. (2003), *Nutrigenomics: goals and strategies*, Nat Rev Genet 4, 315-322.

164. Francis G. A. et al. (2003), *Nuclear receptors and the control of metabolism*, Annu Rev Physiol 65, 261-311.

165. Powell K. (2007), *Functional foods from biotech--an unappetizing prospect?*, Nat Biotechnol 25, 525-531.

166. Sirtori C. R. et al. (2009), *Functional foods for dyslipidaemia and cardiovascular risk prevention*, Nutr Res Rev 22, 244-261.

167. Palomer X. et al. (2008), *Role of vitamin D in the pathogenesis of type 2 diabetes mellitus*, Diabetes Obes Metab 10, 185-197.

168. Danescu L. G. et al. (2009), *Vitamin D and diabetes mellitus*, Endocrine 35, 11-17.

169. Davi G. et al. (2010), *Nutraceuticals in diabetes and metabolic syndrome*, Cardiovasc Ther 28, 216-226.

170. Buttriss J. L., Benelam B. (2010), *Nutrition and health claims: the role of food composition data*, Eur J Clin Nutr 64 Suppl 3, S8-13.

171. Li J. W., Vederas J. C. (2009), *Drug discovery and natural products: end of an era or an endless frontier?*, Science 325, 161-165.

172. Ganesan A. (2004), *Natural products as a hunting ground for combinatorial chemistry*, Curr Opin Biotechnol 15, 584-590.

173. Harvey A. L. (2008), *Natural products in drug discovery*, Drug Discov Today 13, 894-901.

174. Endo A. et al. (1976), *ML-236A, ML-236B, and ML-236C, new inhibitors of cholesterogenesis produced by Penicillium citrinium*, J Antibiot (Tokyo) 29, 1346-1348.

175. Pfizer, *Annual Review 2008*, (http://media.pfizer.com/files/annualreport/2008/annual/review2008.pdf).

176. Jeffreys D. (2005), *Aspirin: The Remarkable Story of a Wonder Drug*. (Bloomsbury, ISBN 1-58234-600-3).

177. Hayes A. N., Gilbert S. G. (2008), *Molecular, clinical and environmental toxicology*. Luch A., Ed., (Birkhäuser Basel, ISBN 3764383356).

178. Skov M. J. et al. (2007), *Nonclinical safety of ziconotide: an intrathecal analgesic of a new pharmaceutical class*, Int J Toxicol 26, 411-421.

179. Kino T. et al. (1987), *FK-506, a novel immunosuppressant isolated from a Streptomyces. I. Fermentation, isolation, and physico-chemical and biological characteristics*, J Antibiot (Tokyo) 40, 1249-1255.

180. Tribe H. T. (1998), *The discovery and development of cyclosporin*, Mycologist 12, 20-22.

181. Nobelprize.org, *Sir Alexander Fleming - Biography*, (http://nobelprize.org/nobel_prizes/medicine/laureates/1945/fleming.html).

182. Chaturvedi D. et al. (2010), *Artemisinin and its derivatives: a novel class of anti-malarial and anti-cancer agents*, Chem Soc Rev 39, 435-454.

183. Georg Gunda I. et al. (1994), *Preface, Brief History of the Discovery and Development of Taxane Anticancer Agents*, Taxane Anticancer Agents. (American Chemical Society), vol. 583, pp. ix-xiii.

184. Witters L. A. (2001), *The blooming of the French lilac*, J Clin Invest 108, 1105-1107.

185. Eng J. (1992), *Exendin peptides*, Mt Sinai J Med 59, 147-149.

186. Bohacek R. S. et al. (1996), *The art and practice of structure-based drug design: a molecular modeling perspective*, Med Res Rev 16, 3-50.

187. International Human Genome Sequencing Consortium (2004), *Finishing the euchromatic sequence of the human genome*, Nature 431, 931-945.

188. Taubes G. (2009), *Insulin resistance. Prosperity's plague*, Science 325, 256-260.

189. Shulman A. I., Mangelsdorf D. J. (2005), *Retinoid x receptor heterodimers in the metabolic syndrome*, N Engl J Med 353, 604-615.

190. Winter R., Noll F. (1998), *Methoden der Biophysikalischen Chemie*. (Teubner Verlag).

191. Zhang J. H. et al. (1999), *A Simple Statistical Parameter for Use in Evaluation and Validation of High Throughput Screening Assays*, J Biomol Screen 4, 67-73.

192. Cheng Y., Prusoff W. H. (1973), *Relationship between the inhibition constant (K1) and the concentration of inhibitor which causes 50 per cent inhibition (I50) of an enzymatic reaction*, Biochem Pharmacol 22, 3099-3108.

193. Nolte R. T. et al. (1998), *Ligand binding and co-activator assembly of the peroxisome proliferator-activated receptor-gamma*, Nature 395, 137-143.

194. Livak K. J., Schmittgen T. D. (2001), *Analysis of relative gene expression data using real-time quantitative PCR and the 2(-Delta Delta C(T)) Method*, Methods 25, 402-408.

195. Rozen S., Skaletsky H. (2000), *Primer3 on the WWW for general users and for biologist programmers*, Methods Mol Biol 132, 365-386.

196. National Center for Biotechnology Information (NCBI), *Primer-BLAST*, (http://www.ncbi.nlm.nih.gov/tools/primer-blast/).

197. Battke F. et al. (2010), *Mayday--integrative analytics for expression data*, BMC Bioinformatics 11, 121.

198. Dennis G., Jr. et al. (2003), *DAVID: Database for Annotation, Visualization, and Integrated Discovery*, Genome Biol 4, P3.

199. Huang da W. et al. (2009), *Systematic and integrative analysis of large gene lists using DAVID bioinformatics resources*, Nat Protoc 4, 44-57.

200. Subramanian A. et al. (2005), *Gene set enrichment analysis: a knowledge-based approach for interpreting genome-wide expression profiles*, Proc Natl Acad Sci U S A. 102, 15545-15550. Epub 12005 Sep 15530.

201. Ringner M. (2008), *What is principal component analysis?*, Nat Biotechnol 26, 303-304.

202. Saeed A. I. et al. (2003), *TM4: a free, open-source system for microarray data management and analysis*, Biotechniques 34, 374-378.

203. Lamb J. et al. (2006), *The Connectivity Map: using gene-expression signatures to connect small molecules, genes, and disease*, Science. 313, 1929-1935.

204. Lamb J. (2007), *The Connectivity Map: a new tool for biomedical research*, Nat Rev Cancer 7, 54-60.

205. Heikkinen S. et al. (2007), *Evaluation of glucose homeostasis*, Curr Protoc Mol Biol Chapter 29, Unit 29B 23.

206. Chen L. et al. (2006), *CCL27 is a critical factor for the development of atopic dermatitis in the keratin-14 IL-4 transgenic mouse model*, Int Immunol 18, 1233-1242.

207. Gomez-Lechon M. J. et al. (1996), *A microassay for measuring glycogen in 96-well-cultured cells*, Anal Biochem 236, 296-301.

208. Mitscher L. A. et al. (1981), *Amorfrutin A and B, bibenzyl antimicrobial agents from Amorpha fruticosa*, Phytochemistry 20, 781-785.

209. Bruning J. B. et al. (2007), *Partial agonists activate PPARgamma using a helix 12 independent mechanism*, Structure 15, 1258-1271.

210. Berger J. P. et al. (2003), *Distinct properties and advantages of a novel peroxisome proliferator-activated protein [gamma] selective modulator*, Mol Endocrinol 17, 662-676.

211. Schupp M. et al. (2005), *Molecular characterization of new selective peroxisome proliferator-activated receptor gamma modulators with angiotensin receptor blocking activity*, Diabetes 54, 3442-3452.

212. Nagaoka T. et al. (1998), *Cyclic nucleotide phosphodiesterase 3 expression in vivo: evidence for tissue-specific expression of phosphodiesterase 3A or 3B mRNA and activity in the aorta and adipose tissue of atherosclerosis-prone insulin-resistant rats*, Diabetes 47, 1135-1144.

213. Tang Y. et al. (1999), *Improvement in insulin resistance and the restoration of reduced phosphodiesterase 3B gene expression by pioglitazone in adipose tissue of obese diabetic KKAy mice*, Diabetes 48, 1830-1835.

214. Masaki T. et al. (2003), *Peripheral, but not central, administration of adiponectin reduces visceral adiposity and upregulates the expression of uncoupling protein in agouti yellow (Ay/a) obese mice*, Diabetes 52, 2266-2273.

215. Schoonjans K. et al. (1996), *PPARalpha and PPARgamma activators direct a distinct tissue-specific transcriptional response via a PPRE in the lipoprotein lipase gene*, EMBO J 15, 5336-5348.

216. Michailidou Z. et al. (2007), *Omental 11beta-hydroxysteroid dehydrogenase 1 correlates with fat cell size independently of obesity*, Obesity (Silver Spring) 15, 1155-1163.

217. Finck B. N. et al. (2006), *Lipin 1 is an inducible amplifier of the hepatic PGC-1alpha/PPARalpha regulatory pathway*, Cell Metab 4, 199-210.

218. Clemenz M. et al. (2008), *Liver-specific peroxisome proliferator-activated receptor alpha target gene regulation by the angiotensin type 1 receptor blocker telmisartan*, Diabetes 57, 1405-1413.

219. Nesto R. W. et al. (2003), *Thiazolidinedione use, fluid retention, and congestive heart failure: a consensus statement from the American Heart Association and American Diabetes Association. October 7, 2003*, Circulation 108, 2941-2948.

220. Ricote M. et al. (1998), *The peroxisome proliferator-activated receptor-gamma is a negative regulator of macrophage activation*, Nature 391, 79-82.

221. Jiang C. et al. (1998), *PPAR-gamma agonists inhibit production of monocyte inflammatory cytokines*, Nature. 391, 82-86.

222. Sizer K. M. et al. (1994), *Pioglitazone promotes insulin-induced activation of phosphoinositide 3-kinase in 3T3-L1 adipocytes by inhibiting a negative control mechanism*, Mol Cell Endocrinol 102, 119-129.

223. Mendes Sdos S. et al. (2009), *Microarray analyses of the effects of NF-kappaB or PI3K pathway inhibitors on the LPS-induced gene expression profile in RAW264.7 cells: synergistic effects of rapamycin on LPS-induced MMP9-overexpression*, Cell Signal 21, 1109-1122.

224. Harrington W. W. et al. (2007), *The Effect of PPARalpha, PPARdelta, PPARgamma, and PPARpan Agonists on Body Weight, Body Mass, and Serum Lipid Profiles in Diet-Induced Obese AKR/J Mice*, PPAR Res 2007, 97125.

225. Kuda O. et al. (2009), *Prominent role of liver in elevated plasma palmitoleate levels in response to rosiglitazone in mice fed high-fat diet*, J Physiol Pharmacol 60, 135-140.

226. Marchesini G. et al. (2001), *Nonalcoholic fatty liver disease: a feature of the metabolic syndrome*, Diabetes 50, 1844-1850.

227. Pfutzner A. et al. (2004), *Fasting intact proinsulin is a highly specific predictor of insulin resistance in type 2 diabetes*, Diabetes Care 27, 682-687.

228. Spiegelman B. M. et al. (1983), *Molecular cloning of mRNA from 3T3 adipocytes. Regulation of mRNA content for glycerophosphate dehydrogenase and other differentiation-dependent proteins during adipocyte development*, J Biol Chem 258, 10083-10089.

229. Kulozik P. et al. (2011), *Hepatic Deficiency in Transcriptional Cofactor TBL1 Promotes Liver Steatosis and Hypertriglyceridemia*, Cell Metab 13, 389-400.

230. Audie J., Scarlata S. (2007), *A novel empirical free energy function that explains and predicts protein-protein binding affinities*, Biophys Chem 129, 198-211.

231. Huang T. H. et al. (2005), *Herbal or natural medicines as modulators of peroxisome proliferator-activated receptors and related nuclear receptors for therapy of metabolic syndrome*, Basic Clin Pharmacol Toxicol 96, 3-14.

232. Goldberg R. B. et al. (2005), *A comparison of lipid and glycemic effects of pioglitazone and rosiglitazone in patients with type 2 diabetes and dyslipidemia*, Diabetes Care 28, 1547-1554.

233. Winterstein A. G. (2011), *Rosiglitazone and the risk of adverse cardiovascular outcomes*, Clin Pharmacol Ther 89, 776-778.

234. Ferrannini E. et al. (2011), *HDL-cholesterol and not HbA1c was directly related to Cardiovascular Outcome in PROactive*, Diabetes Obes Metab.

235. Krebs E. G., Fischer E. H. (1964), *Phosphorylase and Related Enzymes of Glycogen Metabolism*, Vitam Horm 22, 399-410.

236. Röhm J. K., Koolman J. (2002), *Taschenatlas der Biochemie* (Thieme, Stuttgart).

237. Angel J. F. (1980), *Gluconeogenesis in meal-fed, vitamin B-6-deficient rats*, J Nutr 110, 262-269.

238. Sethi R., Haque W. (2001), Patent no. WO 01/03682 A2.

239. Hagiwara S. et al. (2009), *Effects of pyridoxamine (K-163) on glucose intolerance and obesity in high-fat diet C57BL/6J mice*, Metabolism 58, 934-945.

240. Wishart D. S. et al. (2009), *HMDB: a knowledgebase for the human metabolome*, Nucleic Acids Res 37, D603-610.

241. Schneider G. et al. (1999), *"Scaffold-Hopping" by Topological Pharmacophore Search: A Contribution to Virtual Screening*, Angew Chem Int Ed Engl 38, 2894-2896.

242. Schneider G. et al. (2000), *Virtual Screening for Bioactive Molecules by Evolutionary De Novo Design Special thanks to Neil R. Taylor for his help in preparation of the manuscript*, Angew Chem Int Ed Engl 39, 4130-4133.

243. Kliewer S. A. et al. (1997), *Fatty acids and eicosanoids regulate gene expression through direct interactions with peroxisome proliferator-activated receptors α and γ*, Proceedings of the National Academy of Sciences 94, 4318-4323.

244. Berger J., Moller D. E. (2002), *The Mechanisms of action of PPARs*, Annu Rev Med 53, 409-435.

245. Buckle D. R. et al. (1996), *Non thiazolidinedione antihyperglycaemic agents. 2: [alpha]-Carbon substituted [beta]-phenylpropanoic acids1*, Bioorg Med Chem Lett 6, 2127-2130.

246. Lipinski C. A. et al. (2001), *Experimental and computational approaches to estimate solubility and permeability in drug discovery and development settings*, Adv Drug Deliv Rev 46, 3-26.

247. Ertl P. et al. (2000), *Fast calculation of molecular polar surface area as a sum of fragment-based contributions and its application to the prediction of drug transport properties*, J Med Chem 43, 3714-3717.

248. Ertl P. (2007), *Polar Surface Area*, Molecular Drug Properties, Mannhold R., Ed., (Wiley-VCH).

249. Feher M., Schmidt J. M. (2003), *Property distributions: differences between drugs, natural products, and molecules from combinatorial chemistry*, J Chem Inf Comput Sci 43, 218-227.

250. Savkur R. S., Burris T. P. (2004), *The coactivator LXXLL nuclear receptor recognition motif*, J Pept Res 63, 207-212.

251. Feige J. N., Auwerx J. (2007), *Transcriptional coregulators in the control of energy homeostasis*, Trends Cell Biol 17, 292-301.

252. Perissi V., Rosenfeld M. G. (2005), *Controlling nuclear receptors: the circular logic of cofactor cycles*, Nat Rev Mol Cell Biol 6, 542-554.

253. Mukherjee R. et al. (2002), *Ligand and coactivator recruitment preferences of peroxisome proliferator activated receptor alpha*, J Steroid Biochem Mol Biol 81, 217-225.

254. Zhou G. et al. (1998), *Nuclear receptors have distinct affinities for coactivators: characterization by fluorescence resonance energy transfer*, Mol Endocrinol 12, 1594-1604.

255. Kremoser C. et al. (2007), *Panning for SNuRMs: using cofactor profiling for the rational discovery of selective nuclear receptor modulators*, Drug Discov Today 12, 860-869.

256. Iannone M. A. et al. (2001), *Multiplexed molecular interactions of nuclear receptors using fluorescent microspheres*, Cytometry 44, 326-337.

257. Cosma M. P. (2002), *Ordered recruitment: gene-specific mechanism of transcription activation*, Mol Cell 10, 227-236.

258. Farnham P. J. (2009), *Insights from genomic profiling of transcription factors*, Nat Rev Genet 10, 605-616.

259. Feige J. N. et al. (2007), *The endocrine disruptor monoethyl-hexyl-phthalate is a selective peroxisome proliferator-activated receptor gamma modulator that promotes adipogenesis*, J Biol Chem 282, 19152-19166.

260. Valouev A. et al. (2008), *Genome-wide analysis of transcription factor binding sites based on ChIP-Seq data*, Nat Methods.

261. Koster H. et al. (2007), *Capture compound mass spectrometry: a technology for the investigation of small molecule protein interactions*, Assay Drug Dev Technol 5, 381-390.

262. Lu M. et al. (2011), *Brain PPAR-gamma promotes obesity and is required for the insulin-sensitizing effect of thiazolidinediones*, Nat Med 17, 618-622.

263. Ryan K. K. et al. (2011), *A role for central nervous system PPAR-gamma in the regulation of energy balance*, Nat Med 17, 623-626.

264. Juge-Aubry C. E. et al. (1995), *Peroxisome proliferator-activated receptor mediates cross-talk with thyroid hormone receptor by competition for retinoid X receptor. Possible role of a leucine zipper-like heptad repeat*, J Biol Chem 270, 18117-18122.

265. Kouidhi S. et al. (2010), *Peroxisome proliferator-activated receptor-gamma (PPARgamma) modulates hypothalamic Trh regulation in vivo*, Mol Cell Endocrinol 317, 44-52.

266. Larsen P. J. et al. (2003), *Differential influences of peroxisome proliferator-activated receptors gamma and -alpha on food intake and energy homeostasis*, Diabetes 52, 2249-2259.

267. Myers M. G., Jr., Burant C. F. (2011), *PPAR-gamma action: it's all in your head*, Nat Med 17, 544-545.

268. Vazquez M. et al. (2001), *Bezafibrate induces acyl-CoA oxidase mRNA levels and fatty acid peroxisomal beta-oxidation in rat white adipose tissue*, Mol Cell Biochem 216, 71-78.

269. Cabrero A. et al. (1999), *Uncoupling protein-3 mRNA levels are increased in white adipose tissue and skeletal muscle of bezafibrate-treated rats*, Biochem Biophys Res Commun 260, 547-556.

270. Mori Y. et al. (2004), *Bezafibrate-induced changes over time in the expression of uncoupling protein (UCP) mRNA in the tissues: a study in spontaneously type 2 diabetic rats with visceral obesity*, J Atheroscler Thromb 11, 224-231.

271. Matias I., Di Marzo V. (2007), *Endocannabinoids and the control of energy balance*, Trends Endocrinol Metab 18, 27-37.

272. Di Marzo V. et al. (2001), *Leptin-regulated endocannabinoids are involved in maintaining food intake*, Nature 410, 822-825.

273. Lenman A., Fowler C. J. (2007), *Interaction of ligands for the peroxisome proliferator-activated receptor gamma with the endocannabinoid system*, Br J Pharmacol 151, 1343-1351.

274. Ong S. E., Mann M. (2006), *A practical recipe for stable isotope labeling by amino acids in cell culture (SILAC)*, Nat Protoc 1, 2650-2660.

275. Kruger M. et al. (2008), *SILAC mouse for quantitative proteomics uncovers kindlin-3 as an essential factor for red blood cell function*, Cell 134, 353-364.

276. Rizzo G., Fiorucci S. (2006), *PPARs and other nuclear receptors in inflammation*, Curr Opin Pharmacol 6, 421-427.

277. Straus D. S., Glass C. K. (2007), *Anti-inflammatory actions of PPAR ligands: new insights on cellular and molecular mechanisms*, Trends Immunol 28, 551-558.

278. Lehmann J. M. et al. (1997), *Peroxisome proliferator-activated receptors alpha and gamma are activated by indomethacin and other non-steroidal anti-inflammatory drugs*, J Biol Chem 272, 3406-3410.

279. Heneka M. T., Landreth G. E. (2007), *PPARs in the brain*, Biochim Biophys Acta 1771, 1031-1045.

280. Cuzzocrea S. et al. (2004), *Rosiglitazone, a ligand of the peroxisome proliferator-activated receptor-gamma, reduces acute inflammation*, Eur J Pharmacol 483, 79-93.

281. Giaginis C. et al. (2009), *Peroxisome proliferator-activated receptor-gamma (PPAR-gamma) ligands as potential therapeutic agents to treat arthritis*, Pharmacol Res 60, 160-169.

282. Shiojiri T. et al. (2002), *PPAR gamma ligands inhibit nitrotyrosine formation and inflammatory mediator expressions in adjuvant-induced rheumatoid arthritis mice*, Eur J Pharmacol 448, 231-238.

283. Ricote M. et al. (1998), *Expression of the peroxisome proliferator-activated receptor gamma (PPARgamma) in human atherosclerosis and regulation in macrophages by colony stimulating factors and oxidized low density lipoprotein*, Proc Natl Acad Sci U S A. 95, 7614-7619.

284. Rousseaux C. et al. (2005), *Intestinal antiinflammatory effect of 5-aminosalicylic acid is dependent on peroxisome proliferator-activated receptor-gamma*, J Exp Med 201, 1205-1215.

285. Dubuquoy L. et al. (2006), *PPARgamma as a new therapeutic target in inflammatory bowel diseases*, Gut 55, 1341-1349.

286. Raederstorff D. (2007), Patent no. WO 2007/093387.

287. Sertznig P. et al. (2008), *Peroxisome proliferator-activated receptors (PPARs) and the human skin: importance of PPARs in skin physiology and dermatologic diseases*, Am J Clin Dermatol 9, 15-31.

288. Staumont-Salle D. et al. (2008), *Peroxisome proliferator-activated receptor alpha regulates skin inflammation and humoral response in atopic dermatitis*, J Allergy Clin Immunol 121, 962-968 e966.

289. Schoepe S. et al. (2006), *Glucocorticoid therapy-induced skin atrophy*, Exp Dermatol 15, 406-420.

290. Guttman-Yassky E. (2007), *Atopic dermatitis*, Curr Probl Dermatol 35, 154-172.

291. Chaturvedi R. K., Beal M. F. (2008), *PPAR: a therapeutic target in Parkinson's disease*, J Neurochem 106, 506-518.

292. Afman L., Muller M. (2006), *Nutrigenomics: from molecular nutrition to prevention of disease*, J Am Diet Assoc 106, 569-576.

293. Roberts S. C. (2007), *Production and engineering of terpenoids in plant cell culture*, Nat Chem Biol 3, 387-395.

8 Abbreviations

Abbreviation/Symbol	Full name/Meaning
11β-HSD1 (HSD11B1)	Hydroxysteroid (11-β) dehydrogenase 1
A1	Amorfrutin 1
ACOX1	Acyl-Coenzyme A oxidase 1
ACS	Acyl- Coenzyme A synthetase
Adipoq	Adiponectin
ADMET	Absorption, Distribution, Metabolism, Excretion, Toxicity
AF	Activation function
ALT	Alanine transaminase
ANOVA	Analysis of variance
AP-1	Activating protein-1
Arg	Arginine
ATF6	Activating transcription factor-6
ATP	Adenosine triphosphate
AUC	Area under the curve
AUC_i	Inverse area under the curve
BMI	Body mass index
BSA	Bovine serum albumin
CATS	Chemically Advanced Template Search
CBP	CREB-binding protein
CREB	cAMP response element-binding protein
cDNA	Complementary DNA
CNS	Central nervous system
CPT	Carnitine palmitoyltransferase
cRNA	Complementary RNA
CRP	C-reactive protein
DAG	Diacylglycerol
DAVID	Database for Annotation, Visualization and Integrated Discovery
DBD	DNA-binding domain

DIO	Diet-induced obesity
DMEM	Dulbecco's modified Eagle's medium
DMSO	Dimethyl sulfoxide
DNA	Deoxyribonucleic acid
DPP-4	Dipeptidyl peptidase-4
EC50	Effective concentration (at 50%)
EDTA	Ethylenediaminetetraacetic acid
EGTA	Ethyleneglycoltetraacetic acid
ELISA	Enzyme-linked immunosorbent assay
ER	Endoplasmatic reticulum
FABP	Fatty acid binding protein
FATP	Fatty acid transport protein
FBS	Fetal bovine serum
FDR	False discovery rate
FFA	Free fatty acids
FRET	Fluorescence resonance energy transfer
GDM	Gene distance matrix
GLP-1	Glucagon-like peptide 1
GLUT4	Glucose transporter 4
GSEA	Gene Set Enrichment Analysis
GST	Glutathione S-transferase
GyK	Glycerol kinase
HDL	High-density lipoprotein
HFD	High-fat diet
HOMA	Homeostatic model assessment
HPLC	High performance liquid chromatography
HPT axis	Hypothalamic-pituitary-thyroid axis
IBMX	3-isobutyl-1-methylxanthine
IC50	Inhibitory concentration (at 50%)
IgG-HRP	Immunoglobin G – horseradish peroxidase
IKK	Inhibitor kappa B kinase
IL-1	Interleukin 1

IL-6	interleukin 6
IPIST	Intraperitoneal insulin sensitivity test
IR	Insulin Resistance
IRE1	Inositol requiring enzyme 1
IRS-1	Insulin receptor substrate 1
JNK	JUN N-terminal kinase
K_i	Affinity constant
LBD	Ligand-binding domain
LDL	Low-density lipoprotein
LFD	Low-fat diet
LPL	Lipoprotein lipase
LPS	Lipopolysaccharides
LXR	Liver X receptor
MCP-1	Monocyte chemotactic protein-1
MIAME	Minimum Information About a Microarray Experiment
mTOR	Mammalian target of rapamycin
NCOR	Nuclear receptor corepressor 2
NF-κB	Nuclear factor of kappa light polypeptide gene enhancer in B-cells
NMR	Nuclear magnetic resonance
NR	Nuclear receptor
OGTT	Oral glucose tolerance test
P	P value
PAI-1	Plasminogen activator inhibitor-1
PAMPA	Parallel artificial membrane permeability assay
PBS	Phosphate buffered saline
PCA	Principal component analysis
PCR	Polymerase chain reaction
PEPCK	Phosphoenolpyruvate carboxykinase
PERK	PKR-like eukaryotic initiation factor 2α kinase
PGC1α	PPARγ coactivator 1α
PI3K	Phosphoinositide 3-kinase

PKC	Protein kinase C
PKR	Double-stranded RNA-activated protein kinase
PLTP	Phospholipid transfer protein
PPAR	Peroxisome proliferator-activated receptor
PSA	Polar surface area
qPCR	Quantitative PCR
RNA	Ribonucleic acid
ROS	Reactive oxygen species
Ros, R	Rosiglitazone
RXR	Retinoid X receptor
s.d.	Standard deviation
s.e.m.	Standard error of mean
SDS	Sodium dodecyl sulfate
Ser	Serine
shRNA	Small hairpin RNA
siRNA	Small interfering RNA
SPPARM	Selective PPAR modulator
SRC	Steroid receptor coactivator
TBL1	Transducin beta-like 1
TLR	Toll-like receptor
TNFα	Tumor necrosis factor α
TR-FRET	Time-resolved fluorescence resonance energy transfer
TZD	Thiazolidinedione
UAS	Upstream Activation Sequence
UCP	Uncoupling protein
UPR	Unfolded protein response
Veh	Vehicle
vWAT	Visceral white adipose tissue
WAT	White adipose tissue

9 Supplementary Data

9.1 Supplementary Figures

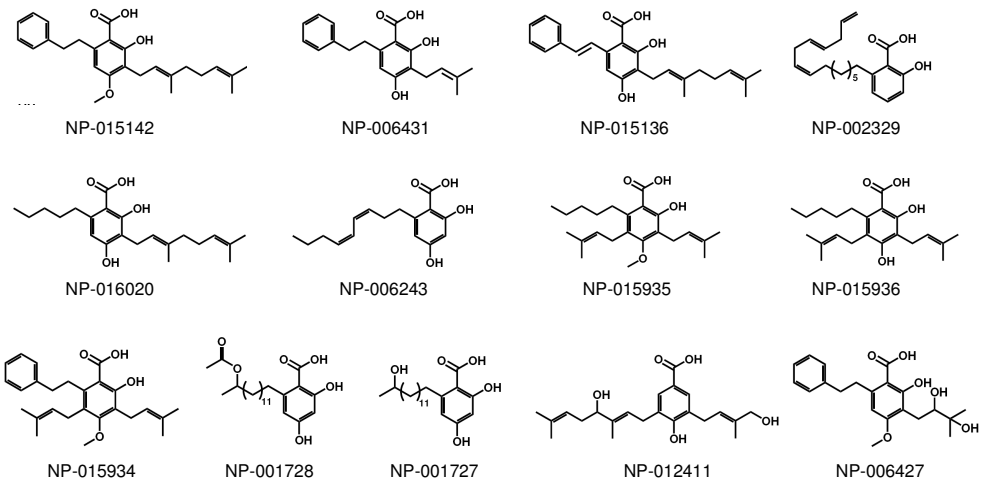

Figure S1. Structures of further amorfrutins.

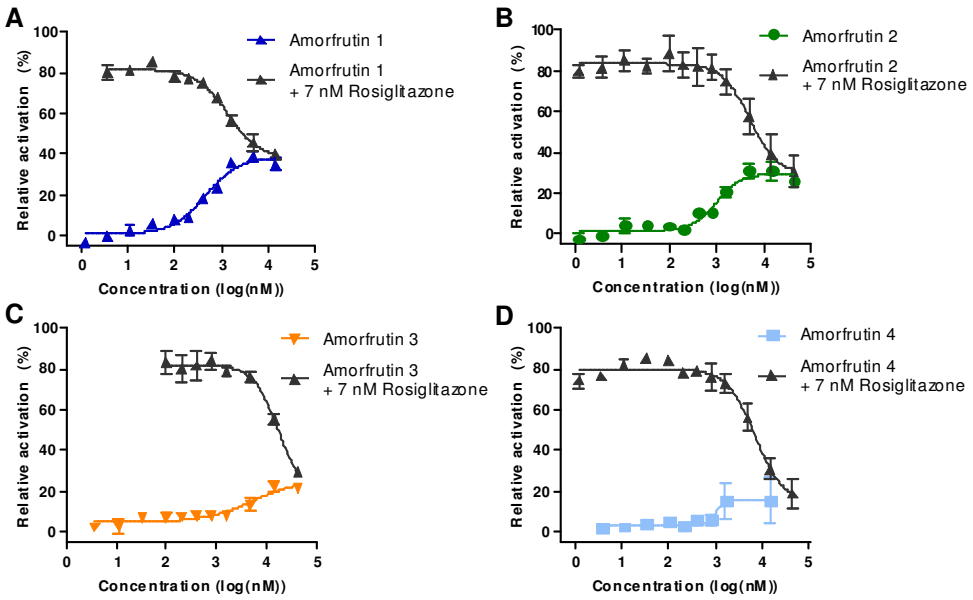

Figure S2. Cellular activation of PPARγ by amorfrutins determined in a competitive reporter gene assay. To accurately determine EC50 and efficacy values, the reporter cells were additionally treated with the indicated concentrations of amorfrutins in presence of 7 nM rosiglitazone. Data are expressed as mean ± s.d. (n=3).

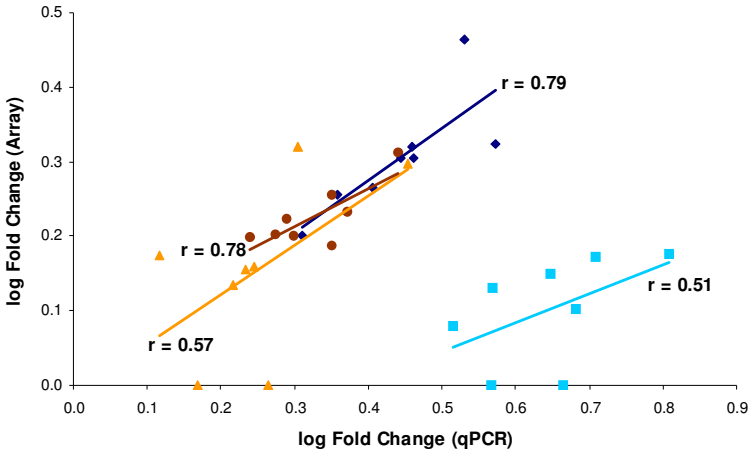

Figure S3. Correlation of gene expression regulation obtained by Illumina Bead Array and qPCR. Four genes were arbitrary chosen and displayed as follows: ADIPOQ (blue diamonds), NR1H3 (red circles), HSD11B1 (orange triangles), FABP4 (light blue squares). Pearson product-moment correlation coefficients are indicated for each gene.

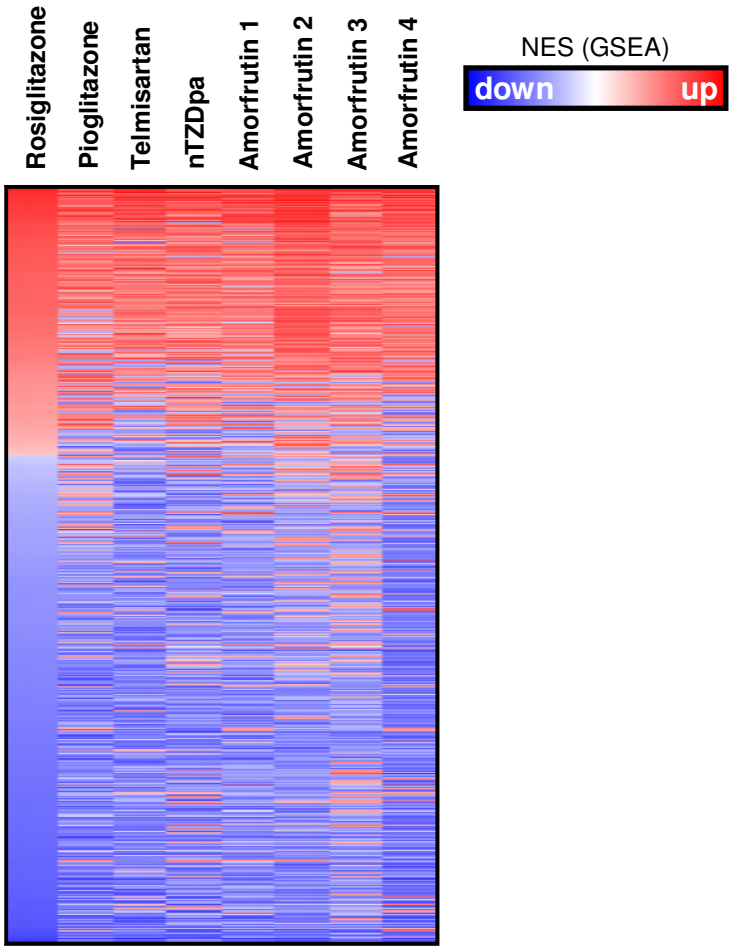

Figure S4. Gene Set Enrichment Analysis (GSEA) of expression profiles using the MsigDB C2 gene sets including KEGG pathways and data from chemical and genetic perturbation experiments. Normalized enrichment scores are shown for gene sets with FDR≤0.25 for at least one compound. Gene sets were either up-regulated (red) or down-regulated (blue) in the compound expression profiles.

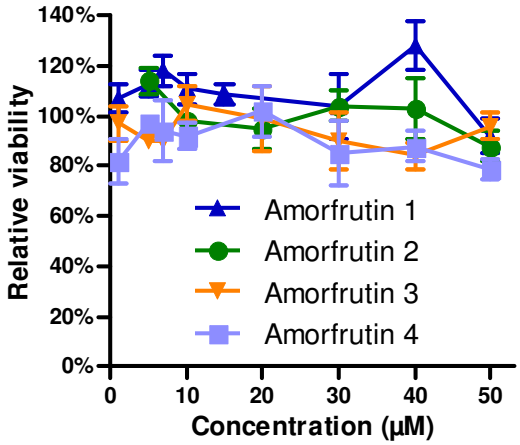

Figure S5. Viability of HepG2 cells treated for 24 h with amorfrutins was assessed with the WST-1 reagent. Data are expressed relative to vehicle control and shown as mean ± s.e.m. (n=3).

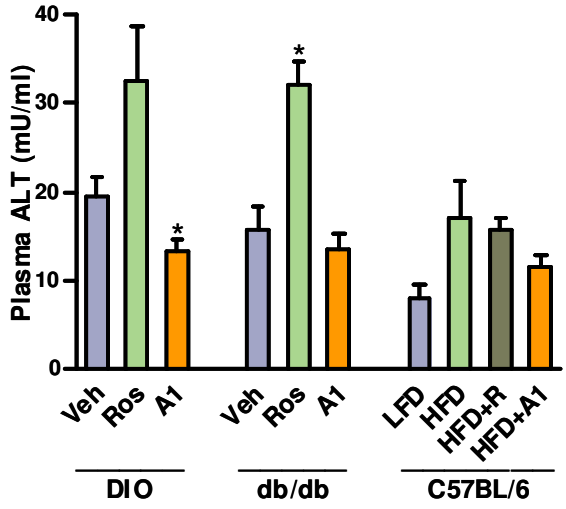

Figure S6. Effect of treatment on plasma alanine transaminase (ALT) in DIO mice (n=13, 3 weeks), db/db mice (n=13, 3 weeks) and C57BL/6 mice (n=12, 15 weeks). Data are expressed as mean ± s.e.m. *, P≤0.05 vs. vehicle only.

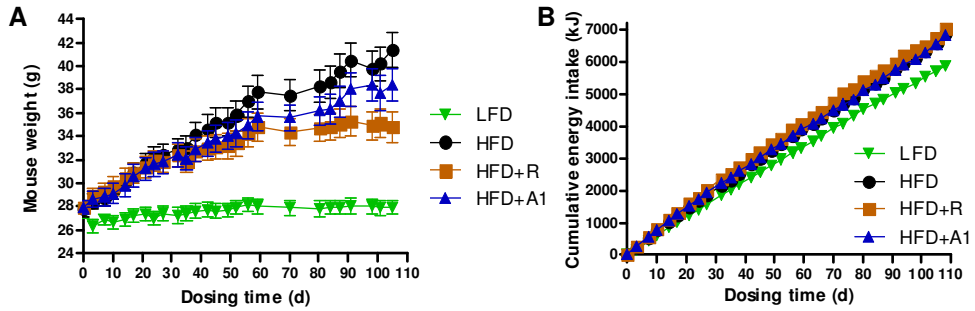

Figure S7. Effects of low-fat diet (LFD) or high-fat diet (HFD) without or with rosiglitazone (HFD+R) or amorfrutin 1 (HFD+A1) on body weight **(A)** and cumulative energy intake **(B)** in C57BL/6 mice. Data are expressed as mean ± s.e.m.

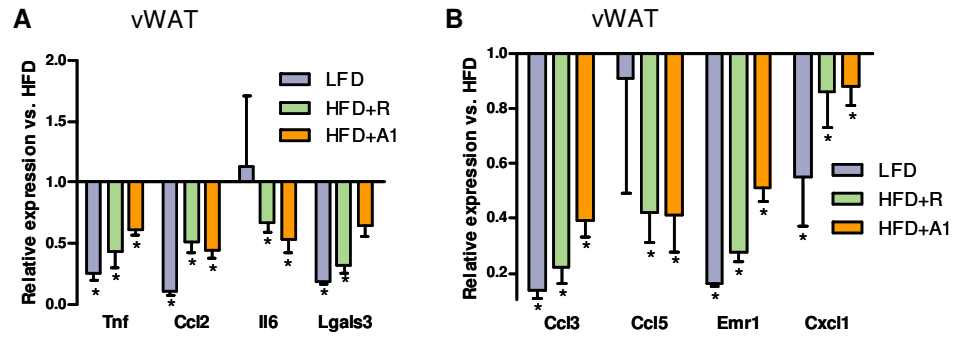

Figure S8. Regulation of gene expression in visceral white adipose tissue (vWAT) after feeding of low-fat diet (LFD) or high-fat diet (HFD) without or with rosiglitazone (HFD+R) or amorfrutin 1 (HFD+A1) over 15 weeks in C57BL/6 mice (n=12). Expression of genes involved in inflammatory processes **(A)** and presence of macrophage-specific markers **(B)** were analyzed by qPCR. Gene expression of HFD-fed mice is set to 1. Data are expressed as mean ± s.e.m. *, P≤0.05 vs. HFD.

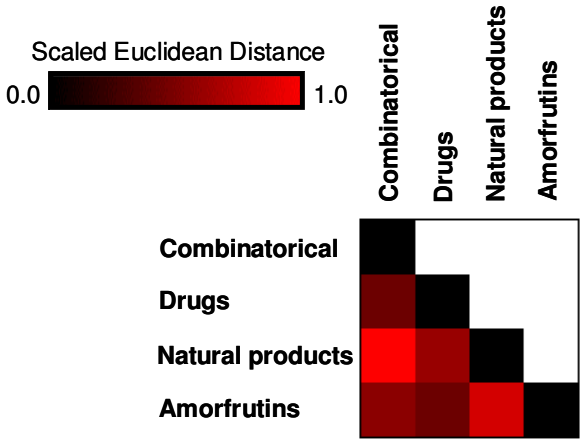

Figure S9. Distance matrix of ten chemical properties specific for compounds from combinatorial libraries, drug databases, natural product collections and amorfrutin class. Squares show the similarity in Euclidean space, ranging from the same properties (black) to completely different (red). Chemical properties were number of chiral centers, rotatable bonds, C-N bonds, C-O bonds, C-halogen bonds, C-S bonds, hydrogen bond acceptors and donors, the ratio of aromatic atoms to ring atoms, and the ring fusion degree in a solvated environment. Data were taken from ref (*249*).

9.2 Supplementary table

Table S1. Binding affinity constants (Ki) and sources of amorfrutins. Selectivity is the ratio of the binding constants.

Compound	Ki [µM]			Selectivity for PPARγ vs.		Biological sources
	PPARγ	PPARα	PPARβ/δ	PPARα	PPARβ/δ	
NP-003520 (Amorfrutin 1)	0.236	27	27	114	114	*Glycyrrhiza foetida*, *Amorpha fruticosa*
NP-003521 (Amorfrutin 2)	0.287	25	17	87	59	*Glycyrrhiza foetida*, *Amorpha fruticosa*
NP-006430 (Amorfrutin 3)	0.352	115	68	327	193	*Glycyrrhiza foetida*, *Amorpha fruticosa*
NP-009525 (Amorfrutin 4)	0.278	8.0	6.0	29	22	*Glycyrrhiza foetida*, *Amorpha fruticosa*
NP-015142	0.019	2.6	1.8	137	95	*Amorpha fruticosa*
NP-006431	0.093	7.8	2.3	84	25	*Glycyrrhiza foetida*
NP-015136	0.134	5.0	1.4	37	10	*Amorpha fruticosa*
NP-002329	0.264	2.8	2.2	11	8	*Anacardium occidentale*
NP-016020	0.280	7.0	2.7	25	10	*Cannabis sativa*
NP-006243	0.305	12	3.8	39	12	fermented fungi (species undetermined)
NP-015935	0.524	8.2	5.8	16	11	*Glycyrrhiza foetida*
NP-015936	0.613	4.4	7.0	7	11	*Glycyrrhiza foetida*
NP-015934	0.508	11	4.5	22	9	*Glycyrrhiza foetida*
NP-001728	0.860	9.6	n.d.	11	n.d.	*Picris altissima*
NP-001727	1.3	38	38	29	29	*Picris altissima*
NP-012411	1.6	128	40	80	25	*Eriodictyon glutinosum*
NP-006427	3.2	n.d.	n.d.	n.d.	n.d.	*Glycyrrhiza foetida*

n.d., not determined.

Table S2. Effective (EC50) or inhibitory (IC50) concentrations of different compounds and efficacy of their recruitment of cofactor peptides to PPARγ. For the coactivators, efficacy is the maximum recruitment relative to the rosiglitazone-induced activation of PPARγ. For corepressor NCOR2, efficacy is the minimal binding observed relative to the rosiglitazone-induced inhibition.

Cofactor	CBP-1		PGC1a		TRAP220/DRIP-2		PRIP/RAP250		NCOR2	
Compound	EC50	Efficacy	EC50	Efficacy	EC50	Efficacy	EC50	Efficacy	IC50	Efficacy
Rosiglitazone	18 nM	100%	17 nM	100%	11 nM	100%	94 nM	100%	64 nM	0%
Pioglitazone	1.6 µM	87%	1.0 µM	75%	3.1 µM	93%	7.6 µM	84%	6.0 µM	19%
nTZDpa	7.0 µM	15%	3.0 µM	33%	4.8 µM	15%	12 µM	72%	17 nM	27%
Telmisartan	9.6 µM	32%	3.8 µM	118%	5.8 µM	67%	11 µM	147%	5.8 µM	26%
Amorfrutin 1	12 µM	13%	10 µM	24%	45 µM	21%	158 µM	119%	51 nM	25%
Amorfrutin 2	77 µM	24%	41 µM	21%	61 µM	33%	201 µM	153%	318 nM	15%
Amorfrutin 3	110 nM	6%	484 nM	14%	3.0 µM	9%	7.2 µM	10%	2.8 µM	8%
Amorfrutin 4	188 nM	13%	859 nM	37%	27 µM	27%	217 nM	10%	335 nM	22%

Table S3. Results of Gene Set Enrichment Analysis (GSEA) after treatment of human adipocytes with different compounds. Data for fatty acid metabolism (top) and pro-inflammatory (down) gene sets are shown.

NAME	Rosiglitazone		Pioglitazone		Telmisartan		nTZDpa		Amorfrutin 1		Amorfrutin 2		Amorfrutin 3		Amorfrutin 4	
	NES	FDR	NES	FDR	NES	FDR	NES	FDR	NES	FDR	NES	FDR	NES	FDR	NES	FDR
FATTY_ACID_METABOLISM	2.05	0.005	1.69	0.163	1.93	0.018	1.89	0.044	2.04	0.016	2.01	0.007	1.60	0.338	1.89	0.029
HSA00100_BIOSYNTHESIS_OF_STEROIDS	2.05	0.005	1.85	0.062	2.31	0.000	2.30	0.001	1.99	0.015	2.18	0.001	1.76	0.157	2.24	0.000
FATTY_ACID_DEGRADATION	1.98	0.010	1.90	0.038	1.80	0.071	1.65	0.227	1.83	0.062	2.03	0.005	1.58	0.334	1.63	0.227
HSA00062_FATTY_ACID_ELONGATION_IN_MITOCHONDRIA	1.80	0.054	1.64	0.193	1.96	0.013	1.46	0.411	1.62	0.303	1.74	0.081	1.78	0.146	1.96	0.016
MITOCHONDRIAL_FATTY_ACID_BETAOXIDATION	1.79	0.057	1.74	0.147	1.74	0.103	1.35	0.519	1.80	0.082	2.01	0.007	1.45	0.473	1.71	0.129
HSA00071_FATTY_ACID_METABOLISM	1.79	0.060	1.29	0.565	1.68	0.164	1.54	0.311	1.46	0.451	1.54	0.231	1.18	0.713	1.27	0.617
FATTY_ACID_BIOSYNTHESIS_PATH_2	1.56	0.231	1.27	0.582	1.73	0.104	1.15	0.693	1.26	0.625	1.54	0.227	1.68	0.231	1.71	0.127
HSA01040_POLYUNSATURATED_FATTY_ACID_BIOSYNTHESIS	1.09	0.749	1.05	0.743	1.14	0.775	0.99	0.868	1.43	0.480	1.69	0.100	1.32	0.599	1.65	0.213
HSA04060_CYTOKINE_CYTOKINE_RECEPTOR_INTERACTION	-1.84	0.066	-1.77	0.082	-1.82	0.087	-0.78	0.910	-2.04	0.019	-1.36	0.470	-1.96	0.121	-2.20	0.000
IFN_ALPHA_UP	-1.80	0.074	-1.40	0.395	-1.06	0.638	-1.27	0.492	-1.32	0.465	-1.55	0.392	-1.29	0.697	-1.78	0.064
IFNA_HCMV_6HRS_UP	-1.71	0.103	-1.27	0.500	-1.74	0.120	-1.80	0.076	-1.46	0.367	-1.92	0.106	-1.68	0.336	-1.94	0.022
IFNALPHA_NL_UP	-1.70	0.112	-1.44	0.351	-1.29	0.429	-1.56	0.230	-1.05	0.737	-1.31	0.529	-1.68	0.324	-1.77	0.063
SANA_IFNG_ENDOTHELIAL_UP	-1.67	0.129	-1.68	0.138	-1.07	0.642	-1.61	0.208	-1.25	0.535	-1.71	0.289	-1.34	0.657	-1.94	0.023
PASSERINI_INFLAMMATION	-1.62	0.152	-1.04	0.732	-1.30	0.425	-1.28	0.485	-0.96	0.809	-1.49	0.408	-1.63	0.388	-1.64	0.114
IFN_ALL_UP	-1.62	0.154	-0.71	0.977	-1.06	0.640	-0.84	0.875	-0.80	0.909	-1.42	0.421	-1.24	0.730	-1.82	0.053
SANA_TNFA_ENDOTHELIAL_UP	-1.61	0.154	-1.65	0.158	-1.79	0.099	-2.00	0.017	-1.92	0.068	-1.87	0.116	-1.59	0.354	-2.05	0.007
CCR5PATHWAY	-1.48	0.270	-1.83	0.056	-1.41	0.338	-0.84	0.874	-1.70	0.163	-1.36	0.465	-1.56	0.438	-1.60	0.132
IFNA_UV-CMV_COMMON_HCMV_6HRS_UP	-1.47	0.268	-1.37	0.425	-1.72	0.133	-2.06	0.012	-1.77	0.124	-1.89	0.110	-1.83	0.160	-1.62	0.125
TNFALPHA_TGZ_ADIP_UP	-1.41	0.323	-1.39	0.398	-1.55	0.244	-1.00	0.744	-0.85	0.887	-1.14	0.645	-0.87	0.933	-1.64	0.116
NI2_MOUSE_UP	-1.39	0.343	-1.62	0.181	-1.40	0.341	-1.16	0.615	-1.66	0.217	-1.50	0.426	-0.82	0.971	-1.63	0.123
TNFALPHA_ADIP_UP	-1.37	0.349	-1.53	0.277	-1.53	0.249	-0.99	0.747	-0.83	0.892	-1.15	0.641	-0.97	0.898	-1.75	0.063
IL6_FIBRO_UP	-1.35	0.361	-1.29	0.475	-1.69	0.143	0.76	1.000	-0.98	0.792	-0.84	0.954	-1.17	0.757	-1.67	0.097
ST_INTERFERON_GAMMA_PATHWAY	-1.32	0.389	-1.03	0.756	-1.37	0.368	-0.42	0.999	-0.94	0.821	-1.21	0.575	-0.39	1.000	-1.70	0.082
IFNGPATHWAY	-1.26	0.437	-0.74	0.968	-1.32	0.405	0.72	0.999	-0.86	0.885	-1.32	0.512	0.55	0.996	-1.43	0.244
IFN_BETA_UP	-1.23	0.450	-0.71	0.975	-1.18	0.517	-1.07	0.711	-0.83	0.893	-1.26	0.553	-0.79	0.981	-1.50	0.200
IFNALPHA_NL_HCC_UP	-1.19	0.495	-0.75	0.969	0.76	1.000	-0.92	0.814	0.59	1.000	-1.15	0.639	-1.13	0.776	-1.46	0.222
IFNALPHA_HCC_UP	-1.05	0.621	-0.47	1.000	-0.84	0.866	-1.18	0.599	0.68	1.000	-1.19	0.599	-1.12	0.792	-1.47	0.218
HSA04350_TGF_BETA_SIGNALING_PATHWAY	-1.01	0.659	-1.36	0.430	-1.04	0.659	-0.79	0.909	-1.00	0.772	-0.73	0.962	-1.15	0.765	-1.53	0.178
IL1_CORNEA_UP	-0.95	0.735	-0.89	0.874	-1.51	0.265	-1.64	0.181	-1.82	0.097	-1.39	0.447	-1.18	0.752	-1.62	0.124
HSA04620_TOLL_LIKE_RECEPTOR_SIGNALING_PANG_PATHWAY	-0.89	0.796	-0.74	0.969	-1.64	0.163	-1.51	0.263	-1.48	0.354	-1.51	0.423	-1.11	0.803	-1.63	0.125

Normalized enrichment scores (NES) for each gene set was calculated with compound-specific expression profiles by use of GSEA. Gene sets were filtered with FDR≤0.25 for at least one compound.

Table S4. Validation of the gene expression signature for rosiglitazone using the Connectivity Map. Obtained gene lists were compared to other small molecule experiments in different human cell lines. Eleven of the 13 most significantly correlated compounds are well-known PPARγ ligands including rosiglitazone (4 connections).

rank	batch	cmap name	dose	cell	score	up	down	instance_id
1	603	rosiglitazone	10 µM	PC3	1.000	0.235	-0.175	1233
2	1005	pioglitazone	10 µM	PC3	0.997	0.268	-0.140	5930
3	603	15-delta prostaglandin J2	10 µM	PC3	0.907	0.212	-0.160	1231
4	1075	pioglitazone	10 µM	PC3	0.887	0.259	-0.104	7088
5	1089	pioglitazone	10 µM	PC3	0.887	0.222	-0.141	7528
6	60	15-delta prostaglandin J2	10 µM	PC3	0.869	0.191	-0.165	446
7	1015	pioglitazone	10 µM	PC3	0.853	0.245	-0.104	5977
8	727	rosiglitazone	10 µM	PC3	0.829	0.250	-0.089	4457
10	603	troglitazone	10 µM	PC3	0.798	0.259	-0.068	1232
11	55	rosiglitazone	10 µM	PC3	0.773	0.181	-0.135	430
13	602	rosiglitazone	10 µM	HL60	0.741	0.164	-0.139	1174

Table S5. Gene Set Enrichment Analysis (GSEA) of liver from DIO mice treated for 23 days with 4mg/kg/d rosiglitazone, 100 mg/kg/d amorfrutin 1 or vehicle only. Normalized enrichment scores (NES) and false discovery rates (FDR q-val) are shown for toxicity related pathways adopted from the PAMM-003A RT² Profiler™ PCR Array Mouse Stress & Toxicity PathwayFinder (SABiosciences, MD, USA). None of these gene sets was enriched within the gene expression profiles.

NAME	SIZE	Rosiglitazone		Amorfrutin 1	
		NES	FDR q-val	NES	FDR q-val
HEATSHOCK	10	1.19	0.517	-0.98	0.609
APOPTOSIS SIGNALING	8	0.56	0.964	-1.44	0.195
DNA DAMAGE AND REPAIR	11	-0.61	0.933	1.03	0.856
PROLIFERATION AND CARCINOGENESIS	6	-0.96	0.637	-1.66	0.100
OXIDATIVE OR METABOLIC STRESS	27	-1.05	0.655	-0.90	0.604
INFLAMMATION	14	-1.08	0.889	0.87	0.631
GROWTH ARREST AND SENESCENCE	6	-1.14	1.000	-1.05	0.681

Table S6. Metabolic parameters of DIO mice under fed conditions. Mice were treated with 4mg/kg/d rosiglitazone, 100 mg/kg/d amorfrutin 1 or vehicle only. Samples were collected after 17 days of dosing.

Parameter	23 days dosing		
	Vehicle	Rosiglitazone	Amorfrutin
Insulin (ng/ml)	3.1 ± 1.6	1.0 ± 0.3[a]	1.7 ± 0.3[a]
Glucose (mM)	6.6 ± 1.1	6.1 ± 0.5	7.3 ± 0.9
Free fatty acids (mM)	0.6 ± 0.11	0.32 ± 0.10[a]	0.49 ± 0.10[a]
Triglycerides (mM)	1.93 ± 0.32	1.30 ± 0.25[a]	1.38 ± 0.38[a]

Values are expressed as mean ± s.e.m. (n = 9-13). a, $P \leq 0.05$ vs. vehicle.

Table S7. Metabolic parameters of DIO mice under fasted conditions. Mice were treated with 4mg/kg/d rosiglitazone, 100 mg/kg/d amorfrutin1 or vehicle only. Samples were collected after 17 and 23 days of dosing.

Parameter	17 days dosing			23 days dosing		
	Vehicle	Rosiglitazone	Amorfrutin	Vehicle	Rosiglitazone	Amorfrutin
Insulin (ng/ml)	2.8 ± 1.4	1.1 ± 0.4[a]	1.3 ± 0.7[a]	1.5 ± 0.2	0.6 ± 0.1[a]	1.1 ± 0.4[a]
Glucose (mM)	9.5 ± 1.2	7.5 ± 1.2[a]	8.5 ± 0.9[a]	7.4 ± 1.2	6.5 ± 1.0	7.6 ± 1.4
Free fatty acids (mM)	0.67 ± 0.15	0.31 ± 0.07[a]	0.54 ± 0.16[a]	0.55 ± 0.11	0.32 ± 0.06[a]	0.43 ± 0.10[a]
Triglycerides (mM)	1.48 ± 0.43	0.86 ± 0.11[a]	0.92 ± 0.29[a]	1.81 ± 0.30	1.35 ± 0.15[a]	1.24 ± 0.23[a]

Values are expressed as mean ± s.e.m. (n = 9-13). a, $P \leq 0.05$ vs. vehicle.

Table S8. Metabolic parameters of C57BL/6 mice under fed conditions. Mice were fed with LFD or HFD with 4mg/kg/d rosiglitazone, 37 mg/kg/d amorfrutin 1 or vehicle only. Samples were collected after 13 weeks of dosing.

Parameter	13 weeks dosing		
	HFD	HFD+R	HFD+A1
Insulin (ng/ml)	2.84 ± 0.41	1.61 ± 0.42[a]	1.96 ± 0.47[a]
Glucose (mM)	9.86 ± 0.98	9.05 ± 0.68[a]	9.74 ± 0.94
Free fatty acids (mM)	5.30 ± 2.20	1.90 ± 0.40[a]	2.70 ± 0.80[a]
Triglycerides (mM)	3.10 ± 0.95	2.15 ± 0.37[a]	2.38 ± 0.65[a]

Values are expressed as mean ± s.e.m. (n = 6-12). a, P ≤ 0.05 vs. HFD.

Table S9. Metabolic parameters of C57BL/6 mice under fasted conditions. Mice were fed with LFD or HFD with 4mg/kg/d rosiglitazone, 37 mg/kg/d amorfrutin 1 or vehicle only. Samples were collected after 8 weeks or 15 weeks of dosing.

Parameter	8 weeks dosing				15 weeks dosing			
	LFD	HFD	HFD+R	HFD+A1	LFD	HFD	HFD+R	HFD+A1
Insulin (ng/ml)	0.35 ± 0.08	1.40 ± 0.32	0.61 ± 0.15[a]	1.04 ± 0.16[a]	0.59 ± 0.37	1.75 ± 1.37	0.63 ± 0.38[a]	1.44 ± 0.69
Glucose (mM)	6.41 ± 1.52	10.30 ± 3.17	9.21 ± 2.3	10.02 ± 2.76	7.3 ± 2.2	7.4 ± 1.9	6.2 ± 1.1	7.7 ± 1.4
Free fatty acids (mM)	1.21 ± 0.12	1.53 ± 0.09	0.98 ± 0.07[a]	1.39 ± 0.08[a]	0.88 ± 0.2	1.23 ± 0.46	0.78 ± 0.17[a]	0.84 ± 0.42[a]
Triglycerides (mM)	0.51 ± 0.22	1.57 ± 0.20	1.11 ± 0.3[a]	1.14 ± 0.45[a]	0.42 ± 0.23	1.04 ± 0.27	0.72 ± 0.14[a]	0.82 ± 0.22[a]

Values are expressed as mean ± s.e.m. (n = 6-12). a, P ≤ 0.05 vs. HFD.

Table S10. Metabolic parameters of db/db mice under fed conditions. Mice were treated with 4mg/kg/d rosiglitazone, 100 mg/kg/d amorfrutin 1 or vehicle only. Samples were collected after 17 days of dosing.

Parameter	17 days		
	Vehicle	Rosiglitazone	Amorfrutin
Insulin (ng/ml)	8.4 ± 2.0	9.7 ± 2.2	6.1 ± 1.3[a]
Glucose (mM)	48.8 ± 17.6	13.3 ± 5.7[a]	34.6 ± 6.3[a]
Free fatty acids (mM)	0.95 ± 0.17	0.28 ± 0.04[a]	0.73 ± 0.09[a]
Triglycerides (mM)	1.9 ± 0.78	0.82 ± 0.19[a]	1.34 ± 0.48[a]

Values are expressed as mean ± s.e.m. (n = 6-13). a, P ≤ 0.05 vs. vehicle.

Table S11. Metabolic parameters of db/db mice under fasted conditions. Mice were treated with 4mg/kg/d rosiglitazone, 100 mg/kg/d amorfrutin1 or vehicle only. Samples were collected after 17 and 23 days of dosing.

Parameter	17 days dosing			23 days dosing		
	Vehicle	Rosiglitazone	Amorfrutin	Vehicle	Rosiglitazone	Amorfrutin
Insulin (ng/ml)	4.6 ± 1.8	3.8 ± 0.9	3.2 ± 1.3[a]	4.6 ± 1.0	3.7 ± 0.8	2.9 ± 0.8[a]
Glucose (mM)	30.5 ± 5.2	19.6 ± 6.9[a]	30.9 ± 6.6	59.7 ± 8.5	19.8 ± 8.3[a]	48.2 ± 14.4[a]
Free fatty acids (mM)	1.39 ± 0.62	0.62 ± 0.21[a]	1.25 ± 0.62	2.03 ± 0.53	0.72 ± 0.31[a]	1.28 ± 0.57[a]
Triglycerides (mM)	1.58 ± 0.66	0.87 ± 0.14[a]	1.13 ± 0.34[a]	2.23 ± 0.4	1.07 ± 0.19[a]	1.71 ± 0.63[a]
Pancreas insulin (µg/tissue)	n.d.	n.d.	n.d.	147 ± 78	1102 ± 253[a]	304 ± 153[a]

Values are expressed as mean ± s.e.m. (n = 6-13). a, P ≤ 0.05 vs. vehicle.